Posiva SKB Report 11
June 2021

Discrete fracture network simulations in support of hydraulic rejection criteria for deposition holes

Pete Appleyard

POSIVA OY

Olkiluoto
FI-27160 Eurajoki, Finland
Phone +358 2 8372 31
posiva.fi

SVENSK KÄRNBRÄNSLEHANTERING AB

SWEDISH NUCLEAR FUEL
AND WASTE MANAGEMENT CO

Box 3091, SE-169 03 Solna
Phone +46 8 459 84 00
skb.se

ISSN 2489-2742
Posiva SKB Report 11
SKB ID 1913805
Posiva ID RDOC-105020
June 2021

Discrete fracture network simulations in support of hydraulic rejection criteria for deposition holes

Pete Appleyard, Jacobs Clean Energy Limited

This report concerns a study which was conducted for Svensk Kärnbränslehantering AB (SKB) and Posiva Oy. The conclusions and viewpoints presented in the report are those of the author. SKB or Posiva may draw modified conclusions, based on additional literature sources and/or expert opinions.

This report is published on www.skb.se and www.posiva.fi.

Abstract

During the construction of a nuclear waste facility, it is important to gain an understanding of likely flow conditions after the repository is closed. The post-closure flows in the vicinity of specific constructed openings, such as deposition holes, are important for repository performance. However, these quantities cannot be directly determined in the field, so they must be inferred from measurable quantities such as the inflow to a pilot borehole that precedes a deposition hole, data calculated from hydraulic testing in that pilot borehole, and inflows to the deposition hole itself.

In this report, these quantities are determined using a hydrogeological model of the Forsmark site, in which the positions of 6 916 deposition holes have been simulated. The model is initially run purely stochastically. It is then run with fractures conditioned on the fracture traces observed in the tunnels and pilot boreholes of a synthetic reality, which is a separate realisation of the same DFN.

Quantities simulated in each of the pilot boreholes for the deposition holes (inflow and specific capacity calculated from hydraulic testing) are correlated with simulated inflows to the corresponding deposition holes in open-repository conditions. These measurable quantities are then correlated with corresponding simulated post-closure performance measures U_0 (flow rate per unit length in the fractures intersecting a hole) and F (flow-related transport resistance). In conditioned models, calculated flow measures for each deposition hole position are also correlated with flow measures in the synthetic reality for the same position.

These correlations are used to determine the success of predictions of deposition hole inflow from pilot borehole hydraulic measurements, and the success of predictions of post-closure performance measures from measurable quantities. The correlations presented are then used to propose new rejection criteria based on specific capacity and deposition hole inflows. Based on this model, these new rejection criteria result in the rejection of 2.1 % of all deposition hole positions, including 91.5 % of the positions whose post-closure U_0 and F would make them unsuitable for use.

Sammanfattning

Under byggandet av en kärnavfallsanläggning är det viktigt att få en förståelse för sannolika flödesförhållanden efter att förvaret stängs. Flödena efter förslutning i närheten av specifika konstruerade underjordsöppningar såsom deponeringshål är viktiga för förvarets prestanda. Dessa flöden kan dock inte bestämmas direkt i fält, utan måste härledas från mätbara storheter såsom flödet till ett pilotborrhål som föregår ett deponeringshål, från data från hydrauliska tester i pilotborrhålet, eller från inflöden till själva deponeringshålet.

I denna rapport bestäms dessa kvantiteter med hjälp av en hydrogeologisk modell av Forsmark, där positionerna för 6 916 deponeringshål har simulerats. Modellen körs initialt rent stokastiskt. Den körs sedan med sprickor konditionerade på de spricksår som observerats i tunnlarna och i pilotborrhål i en syntetisk verklighet; denna syntetiska verklighet är en separat realisering av samma DFN.

Storheterna simulerade i vart och ett av pilotborrhålen för deponeringshålen (inflöde och specifik kapacitet beräknad från hydraulisk testning) är korrelerade mot simulerade inflöden till motsvarande deponeringshål under öppna förvarförhållanden. Dessa mätbara kvantiteter korreleras sedan mot motsvarande simulerade prestandamått för slutna förhållanden såsom U0 (flöde per längdenhet för sprickor som skär ett hål) och F (flödesrelaterat transportmotstånd). I konditionerade modeller korreleras också beräknade flödesmått för varje deponeringshålsposition med flödesmått i den syntetiska verkligheten för samma position.

Dessa korrelationer används sedan för att undersöka hur väl prediktionerna fungerar för att bestämma inflöden i deponeringshål baserat på hydrauliska mätningar i pilotborrhål, och hur väl prediktioner av prestandamått för slutna förhållanden kan göras utifrån mätbara kvantiteter. De presenterade korrelationerna används sedan för att föreslå nya hydrauliska acceptanskriterier baserat på specifik kapacitet och inflöden i deponeringshål. Baserat på denna modell resulterar dessa nya acceptanskriterier i att 2,1 % av alla deponeringshålspositioner förkastas, inklusive 91,5 % av positionerna vars U0 och F vid slutna förhållanden skulle göra dem olämpliga för användning.

Tiivistelmä

Ydinjätteiden loppusijoitustilan rakentamisen tueksi on tärkeää arvioida pohjaveden virtaustilannetta tilojen sulkemisen jälkeen. Loppusijoitustilan toimintakyky riippuu tilojen sulkemisen jälkeisistä virtauksista louhituissa rakenteissa, mm. sijoitusrei'issä. Näitä ominaisuuksia ei kuitenkaan ole mahdollista määrittää suoraan, vaan ne pitää tulkita loppusijoitustiloista mitatuista suureista kuten vuotovesimääristä sijoitusreikien pilottireikiin, pilottirei'issä tehtyjen hydraulisten kokeiden tuloksista ja vuotovesimääristä avarrettuihin sijoitusreikiin.

Loppusijoitusreiän ympäristöön liittyviä virtausominaisuuksia tarkastellaan tässä raportissa mallintamalla 6916 loppusijoitusreiän ympäristöt Forsmarkin dataan perustuvalla hydrogeologisella mallilla. Sijoitusreikien ympäristöt on mallinnettu sekä stokastisesti, että ehdollistamalla rakoilu loppusijoitusreiän pinnalla havaittuun rakoiluun. Havaittu rakoilu loppusijoitusreikien pinnalla perustuu mallinnuksessa synteettiseen todellisuuteen. Rakohavainnot sijoitusreikien ympäristössä on muodostettu yhdestä DFN mallin realisaatiosta.

Sijoitusreikien pilottirei'istä on simuloitu vuotovesimäärät ja hydrauliseen testaamiseen liittyvä ominaiskapasiteetti (specific capacity). Sen jälkeen pilottireikiin simuloidut hydraulisia ominaisuuksia on verrattu laskettuun vuotovesimäärään pilottireikiä vastaavissa paikoissa sijaitseviin avoimiin sijoitusreikiin. Lasketut suureet ovat todellisessa loppusijoitustilassa mitattavissa olevia ominaisuuksia. Näitä on verrattu vastaaviin laskennallisiin loppusijoitustilan sulkemisen jälkeisiin toimintakykytavoitteisiin U0 (loppusijoitusreikää leikkaavan raon virtaama raon leveys metriä kohti) ja F (virtauksesta riippuva kulkeutumisvastus). Ehdollistetussa mallissa lasketut sijoitusreikäkohtaiset virtaamia on verrattu vastaaviin virtauksiin samoissa paikoissa synteettisen todellisuuden mallissa.

Laskettujen tulosten perusteella on arvioitu kuinka hyvin loppusijoitusreiän pilottireikä ennustaa vuotovesimäärää sijoitusreikään, sekä kuinka hyvin mitattavien hydraulisten suureiden perusteella on sulkemisen jälkeisiä toimintakykyominaisuuksia. Tulosten perusteella on ehdotettu hydraulisen kokeen ominaiskapasiteettiin ja loppusijoitusreiän vuotovesimäärään perustuvaa kriteeriä, jonka perusteella loppusijoitusreikäpaikka voidaan hyväksyä tai hylätä. Tässä raportissa esitetty kriteeri johtaa 2,1 % loppusijoitusrei'istä hylkäämiseen. Pitkäaikaisturvallisuuden toimintakykytavoitteiden U0 ja F osalta kriteeri poistaa 91,5 % epäsopivista arvoista.

Contents

1 Introduction

During the construction of a spent nuclear fuel repository, such as the one proposed at Forsmark, it will be necessary to determine which deposition hole positions are suitable for emplacement of canisters. The suitability of a deposition hole position will rest on several factors, including the local properties of the fractured rock around the position and hence the flow conditions that will prevail in the repository after it is closed. As these post-closure flow conditions cannot be measured directly, they will need to be inferred based on measurable quantities associated with constructed engineered openings (such as pilot boreholes and deposition holes).

The objective of this work is to find methods for predicting whether the flow and transport characteristics of a given deposition hole position are suitable for the emplacement of spent nuclear fuel. These predictions are based on correlations between quantities that can be measured directly in open repository conditions and quantities that cannot be measured directly. Quantities that can be measured directly include inflow, and the results of hydraulic tests. Quantities that cannot be measured directly are the flow rate per unit length in the fractures intersecting the deposition hole (called U_0) and the flow-related transport resistance (F).

From these correlations, limiting values are inferred that allow a prediction of whether the flow characteristics of a given deposition hole position meet the requirements of a given performance target. These predictions are then assessed to determine their accuracy.

Correlations are calculated initially using unconditioned models, and then using models where the fracture networks are conditioned to match the fracture traces found in engineered openings in a synthetic reality. The aim of using conditioning is first to see whether this improves the correlation, and second to see whether alternative correlations can be found based on the comparison between the calculated flow characteristics of each deposition hole position and the flow characteristics of the corresponding deposition hole position in the synthetic reality.

It would be possible to condition the model using measured flow in pilot boreholes, in addition to the geometric trace data. However, the additional computing cost required to complete this conditioning is prohibitive.

In previous work, attempts have been made to correlate hydraulic injection test data with deposition hole inflow data and post-closure performance measures, with a model based on Forsmark (Joyce et al. 2013) and as part of the Olkiluoto Demonstration Tunnel 2 (DT2) modelling (Baxter et al. 2018). However, in the DT2 model only six deposition holes were tested. For the previous Forsmark modelling, only a subset of deposition holes was considered (3 per deposition tunnel) and hydraulic tests were performed on multiple pilot boreholes simultaneously, meaning that they may potentially have interfered with one another.

In Appleyard et al. (2018), a method was presented to create conditioned simulations based on the observed characteristics of the fractures that intersect the tunnels and pilot boreholes. This method uses a library to create an empirical distribution of fractures that might potentially intersect a tunnel, borehole, deposition hole or pilot borehole. These are then used to modify realisations of fracture networks to approximately match local observations. While it was demonstrated that a conditioned model more accurately predicts flows to specific deposition holes than a model in which no conditioned data is taken into account, it is not necessarily clear from that work whether the conditioning predicts flow more accurately than a prediction generated by inferring a flow from a known pilot borehole inflow or specific capacity.

In this work, the approach used in DT2 modelling is applied to the deposition hole positions in the Forsmark layout used for the SR-Site safety assessment (Joyce et al. 2010). Of the 6 916 deposition holes found in this layout, about 25 % are intersected by fractures carrying flow, which gives a reasonable statistical sample of approximately 1 700 deposition holes per realisation of fractures. As ten realisations of fractures will be used (based on ten realisations of fractures that were generated during the SR-Site safety assessment), there will be approximately 17 000 modelled deposition holes that are intersected by flow-carrying fractures for each measure calculated.

Correlations between simulated pilot borehole inflow or hydraulic test data and simulated deposition hole inflows are examined and the number of incorrect predictions (those that falsely predict acceptance and those that falsely predict rejection based on measurements in the same realisation or in the synthetic reality) that are inferred is determined. Similar correlations are then examined between simulated hydraulic test data and simulated post-closure performance measures (i.e. U_0 and F).

2 Methodology

2.1 Calculation methods

Five principal flow-related quantities that are useful for determining post-closure safety are calculated in this project. Three of these could be measured in the field. These are the inflow to pilot boreholes in open conditions, the inflow to deposition holes in open conditions, and the specific capacity of the fractures intersecting each pilot borehole calculated from a hydraulic test (which may be an injection test where water is pumped into the pilot borehole, or a PFL test where water is pumped out of the pilot borehole (Follin et al. 2011)). The remaining two flow-related quantities are for post-closure conditions, and thus cannot be measured in the field. These are the flow rate per unit length in the fractures intersecting each deposition hole (U_0) and the flow-related transport resistance for particles released at the deposition hole (F).

The five measures are calculated for 10 realisations of the discrete fracture network (DFN) model for Forsmark. These realisations are the same as were used in SR-Site (Joyce et al. 2010), with the exception that the fractures representing the excavation damaged zone (EDZ) are removed. As there are 6916 deposition holes in the layout, this gives a total of 69160 deposition holes over the 10 realisations whose flows could be calculated.

The models described in Joyce et al. (2010) are available at three scales. The regional-scale model is implemented as an upscaled equivalent continuous porous medium (ECPM) covering a wide region around the Forsmark site. The site-scale model contains more detail and an embedded DFN representation around the repository. The repository-scale model has the most detailed representation of the openings in the repository and the surrounding fractures. The repository-scale model is divided into three blocks as shown in Figure 2-1.

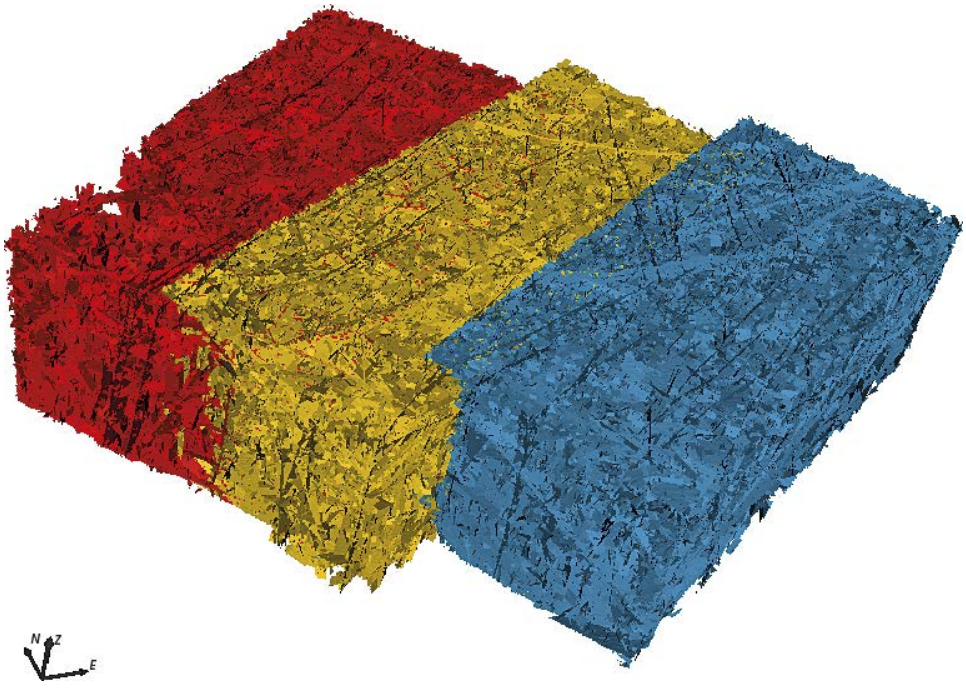

Figure 2-1. *Image of the fractures in the three blocks for the repository-scale model. The red model is block 1, the yellow model is block 2 and the blue model is block 3. Note that the blocks overlap in some areas.*

Models generated for the current work use definitions from SR-Site, including the model geometries, repository layout and boundary conditions (imported from the regional-scale model) for the site- and repository-scale models. However, unlike the SR-Site models, the models used in this work do not include an excavation-damaged zone (EDZ) and they assume a constant water density of 999.923 kg/m^3 (consistent with freshwater). Each repository-scale block is a cuboid that extends from −800 metres to −20 metres elevation, and each has a different horizontal extent, deposition hole count and number of fractures, as given in Table 2-1.

While models in Joyce et al. (2010) were generated using ConnectFlow version 9.6 (Jacobs 2008), for this work the fractures are imported into ConnectFlow version 12.0 (Jacobs 2018a) to allow access to software features added to ConnectFlow between versions 9.6 and 12.0.

There would be advantages to combining the three repository-scale blocks into a single repository-scale model of approximately 3 million sub-fractures that would not be too large to simulate using modern computers. However, no attempt has been made in this project to achieve this. As noted in Subsection 3.1.2, this means that fractures representing tunnels connecting the blocks are excluded from the models to ensure that there are no non-physical fast pathways from the surface of the block to the meshed openings in the repository within the block.

Table 2-1. Details of repository-scale block model dimensions, numbers of fractures and numbers of deposition holes in the models used for this work. A sub-fracture is a small part of a larger physical fracture, used to improve model discretisation in ConnectFlow.

Block	Number of deposition holes	Approximate horizontal dimensions	Approximate number of fractures	Approximate number of sub-fractures
1	1994	2095 m × 1295 m	170000–185000	1000000–1200000
2	2769	2355 m × 995 m	180000–195000	1000000–1150000
3	2153	2195 m × 1005 m	160000–170000	950000–1050000

All models used for this work assume a repository block in which all deposition tunnels are excavated, and all deposition holes are at the same stage of construction (i.e. all are either identical pilot boreholes or deposition holes). This does not realistically reflect the actual construction methodology to be used in the real repository. In a real repository, the first deposition holes will be excavated, used for storage, and backfilled long before the work begins on some of the later deposition tunnels. As a result, the information used in this work will not all be available to a modeller during construction. There will also be an effect on the flow field in the model. Nonetheless, the conclusions drawn remain useful in demonstrating the basic correlations between flow measures in a repository context.

Calculation of inflows to pilot boreholes and deposition holes is performed as a single calculation for each repository-scale block model using tools created for Appleyard et al. (2018). Flows are simulated using open repository conditions. This means that external boundary conditions are imported from regional-scale data, and a head of −470 metres (corresponding to the approximate repository elevation and chosen for simplicity) is applied in all tunnels, deposition holes and pilot boreholes.

The calculated inflows are compared against the existing criterion that the inflow to a deposition hole should not exceed 0.1 l/min. This rejection criterion is in place so that the backfill material performance is not impaired by inflow of water. It is not related to post-closure flow conditions (SKB 2010).

Another possible method of obtaining hydraulic data is through hydraulic injection testing, as performed in Hjerne et al. (2016). In injection testing, water is pumped into a pilot borehole to create a given overpressure, and the flow required to maintain this pressure is measured. An alternative method, PFL testing, involves pumping water out of a pilot borehole to a given underpressure and measuring the flow required to maintain this pressure.

To calculate hydraulic test results, the pilot boreholes are assumed to be packed off 35 centimetres below the deposition tunnels. This distance is chosen to avoid intersecting an excavation damaged zone (EDZ), assumed to extend 30 centimetres from the bottom of the deposition tunnel, as described in Joyce et al. (2010). For injection testing, a fixed overpressure of 200 kPa (2 bar) is maintained and the outflow from the pilot borehole is calculated. For PFL testing, the fixed underpressure in this work is based on a head difference of 10 metres, equivalent (given the assumed gravitational acceleration and water density) to 98.0924 kPa. This is larger than the head difference that will actually be used, but for reasons described below, this discrepancy should not affect results.

The hydraulic simulations are used to calculate the specific capacity of the fractures intersecting the pilot borehole, which is the outflow (or inflow) rate from the pilot borehole per metre of difference of head in the pilot borehole relative to the case where there is no pumping. The specific capacity is useful because it scales with fracture transmissivity and connectivity. It is assumed during hydraulic testing that the inflows to an open tunnel will have a negligible effect on the results of the injection testing, meaning that, instead of calculating the overpressure based on the results from the inflow calculations, it is sufficient to set al. other pressure boundary conditions (on external surfaces and deposition tunnels) to zero head and set the residual pressure in the tested pilot borehole to 200 kPa. To ensure the validity of this approximation, it is tested in Subsection 3.1.1.

A separate hydraulic test is calculated for each pilot borehole, so that the hydraulic tests do not interfere with one another. They are not run on those pilot boreholes that are not hydraulically connected (via the fracture network) to the external surfaces of the model, or to the deposition tunnels, through the modelled fracture network. If a pilot borehole is not connected to a fracture, or is connected to an isolated cluster of fractures, it is clear without need for calculation that the test will give zero flow at steady state.

In more difficult-to-calculate cases, it is necessary to take care to confirm successful numerical convergence by the solver. If the solution does not converge successfully, strange numerical results can occur (including, for example, flow travelling in the wrong direction). The pilot boreholes likely to fail to converge are generally those that are connected through a local cluster of fractures to another pilot borehole or tunnel, but not to the wider fracture network. Where convergence is not achieved, the best course of action is to exclude the pilot borehole from later calculations involving specific capacity even if the result appears plausible. In practice, this problem is not widespread and does not significantly affect the results found in this report. During the operational phase, it is anticipated that the specific capacity will be measured in the pilot borehole, not simulated. As such, problems in numerical convergence will not arise.

Tests performed as part of this project, and shown in Figure 2-2, demonstrate that, when calculated on a pilot borehole by pilot borehole basis, the specific capacities generated through PFL and injection testing are equal for well-converged solutions. The specific capacity does not depend on the head difference chosen (provided that it is not zero). It is thus possible to calculate specific capacity using one of the two measures and assume that the specific capacity calculated using the other measure will be the same. In this work, injection testing was performed in models both with and without conditional simulation, but PFL tests were only performed for conditioned models. However, the fact that they give the same result means that specific capacities from PFL tests can be used to replace those from injection tests in conditioned models where they are more numerically stable.

Results from (injection-style) PSS tests and PFL tests in a real-world setting are compared in Follin et al. (2011). While the results from these tests are closely correlated, they are not generally identical in the real world as they are in this model. Follin et al. (2011) conclude that the discrepancy in the real world likely arises because PFL measurements are performed on boreholes (and pilot boreholes) that have already been pumped for several days, but PSS tests are performed soon after pumping begins. In calculating specific capacity in this work, all injection tests and PFL tests are assumed to run to a steady state. It is thus unsurprising that the discrepancy reported in Follin et al. (2011) does not arise here.

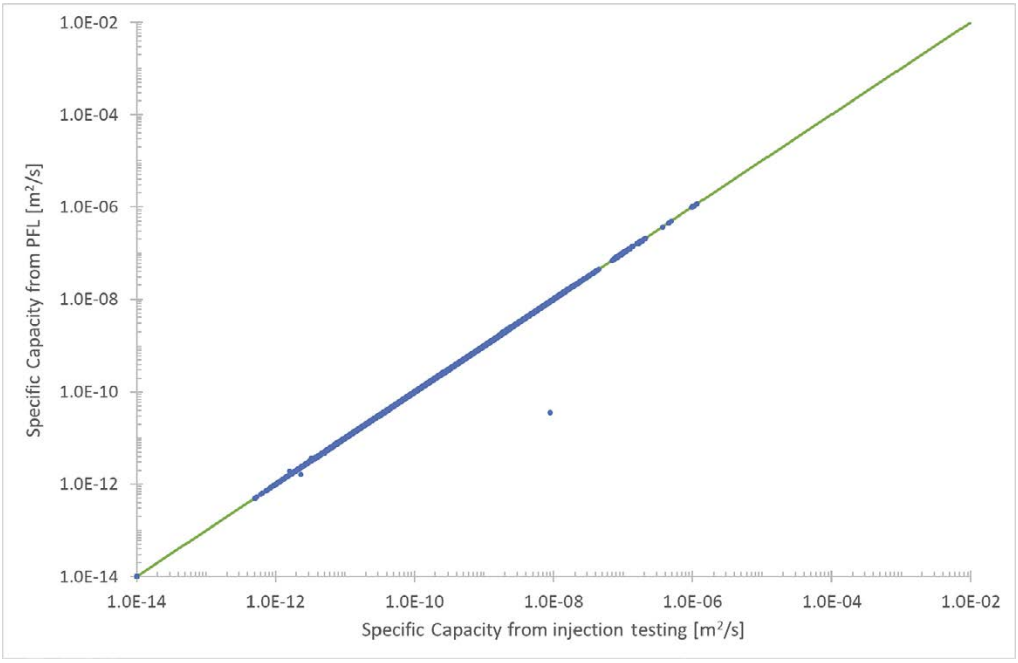

Figure 2-2. *Comparison between specific capacity calculated from PFL results (y-axis) and calculated from injection test results (x-axis). For clarity, the line (y = x), where the two are the same, is shown in green. The single point that is obviously anomalous was found to result from a poorly converged injection test calculation.*

Post-closure performance measures are calculated in a model in which the tunnels and deposition holes are backfilled with a low permeability material (represented as a continuous porous medium, CPM). Two measures are defined: the flow rate per unit length in fractures intersecting the deposition hole (U_0) and the flow-related transport resistance (F).

U_0 is, more specifically, the average tangential flow rate per unit length in the fractures connected to a deposition hole. This is therefore the sum of the flow rates per unit length associated with each fracture, which are calculated using the Cordes-Kinzelbach mass-conserving method (Cordes and Kinzelbach 1992, Jacobs 2018b), as described in Subsection 2.8.7 of Appleyard et al. (2018). To illustrate this, Figure 2-14 from Appleyard et al. is reproduced here as Figure 2-3.

F is the sum of the transport resistances calculated for the fractures crossed by a particle released at a deposition hole, as described in Joyce et al. (2010). These transport resistances are determined based on the modelled release of particles from the deposition holes. The particles are tracked through the repository-scale block models, and then continued through the site-scale model to determine a value for F that takes account of flow routes available for the entire site-scale domain. Once calculated, values of U_0 are to be compared against a post-closure performance target, which is 1 l/(yr·m) (equivalent to 10^{-3} m^2/yr). Values of F are compared against a post-closure performance target of 10^4 yr/m.

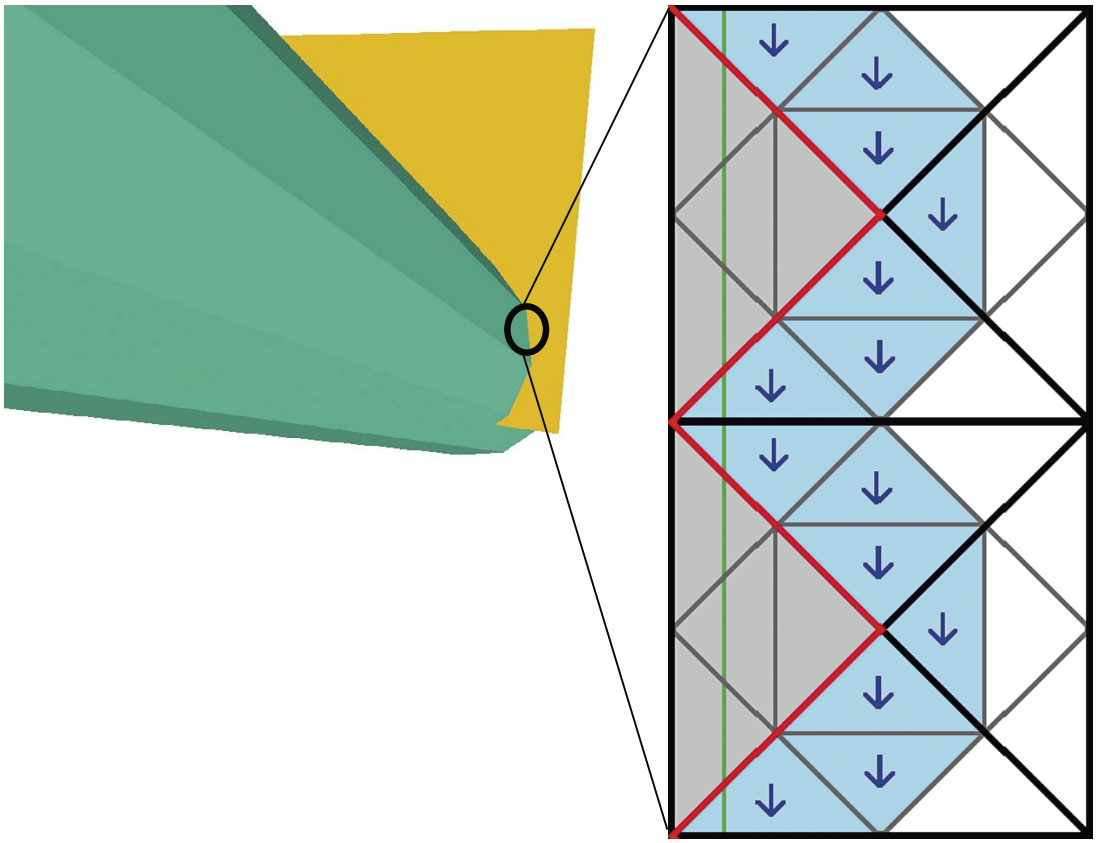

Figure 2-3. *Depiction of the measurement of U based on the flow in a small section of the intersection between a fracture and deposition hole. Left: a fracture (yellow) intersects a deposition hole (green). Right: the fracture is discretised as a regular array of rectangular blocks, each is divided into four triangular finite elements for the flow solve (bounded by black and red lines), and each of them is then subdivided into four sub-triangles for calculating the flow field and particle tracking (bounded by dark grey lines). Two rectangular blocks are depicted here. The green line indicates the physical intersection between the finite elements and the deposition hole, the red line indicates how it is mapped to the finite element edges. Grey areas are areas of the fracture that are ignored because they are within the deposition hole. Blue arrows show the tangential component of the flow vectors used to calculate U (tangential to the original intersection, not to the mapped intersection) in the blue triangles.*

2.2 Conditional simulation

Conditional simulation, or conditioning, for fractures in a DFN is a process that aims to reproduce the fractures observed on the surfaces of real-world engineered openings (such as tunnels and deposition holes).

Realisations of most DFN models are purely stochastic in nature. This means that, while they respect the broad fracture property distributions determined to be appropriate for a given site, the fractures that intersect any specific pilot borehole, deposition hole or deposition tunnel will only match the fractures observed in a repository in a statistical sense. The aim of conditioning is to alter the fracture network so that it includes fractures that match (at least approximately) the fractures observed on the surfaces of the engineered openings, while continuing to respect the property distributions for the entire DFN.

As described in Appleyard et al. (2018), the method for generating conditional simulations in ConnectFlow relies on the creation of a large fracture library from many thousands of realisations of the DFN model. The library contains the location of each fracture that intersects any of the engineered openings of interest in any realisation, and the information necessary to regenerate that fracture. The intended result is an empirical distribution of fractures that could be generated in the DFN. Fractures from this empirical distribution that approximately match observed site data can thus be added to a separate realisation of the same model without adversely affecting the statistical distributions of the fractures.

The data in the library may also include information associated with the flow within each fracture (according to the realisation of the DFN in which it was generated). This measure of flow is dependent on boundary conditions chosen by the user, based on the source of flow data that is available from observations. However, in this project, it was judged that for a model of the required size, library generation including flow would take too long to be practically viable, particularly if the flows were derived from hydraulic testing.

Large fractures are likely to be more important than small fractures for creating flow connections, and are likely to be less common than small fractures given that the relationship between size and frequency in most models approximates an inverse power law. Large fractures that intersect the repository are also likely to intersect it in many different places, meaning that it is likely to be harder to find a match for a larger fracture when conditioning. The fact that an intersection exists or does not exist between a fracture and a given pilot borehole or tunnel may put significant constraints on the size and orientation of the fracture. These constraints must be respected by the conditioning process.

ConnectFlow therefore allows the user to create additional libraries that only include larger fractures in the model. This increases the range of large fractures in the model, without the run time requirements for libraries with the full range of fracture sizes. When selecting fractures to be included, ConnectFlow will weight the probability for each fracture based on the number of realisations that it could have arisen from. This means that the relationship between fracture size and intensity is maintained.

Even with this larger number of available fractures in the library, however, accurately matching large fractures in conditioning is difficult and computationally expensive. It is thus highly desirable for large fractures to be modelled deterministically where practicable.

It is clearly also necessary for there to be a set of observed fractures that the conditioning is attempting to match. While ideally real observed data from a repository would be used, this is not possible for this study because the engineered openings have not been yet been constructed. Instead, for conditioned calculations, one additional realisation of the model was used to provide the observed fracture data. This realisation is called the synthetic reality, and the ten realisations used for unconditioned calculations were conditioned to match it. For obvious reasons, the synthetic reality could not be the same as one of the unconditioned realisations or as one of the realisations in the conditioning library.

The intersections from the synthetic reality used for conditioning in this work are those found on the surfaces of main tunnels and deposition tunnels, and intersections detected in pilot boreholes for deposition holes. It is assumed that all tunnels and pilot boreholes are included simultaneously in the model and that all intersections in pilot boreholes are mapped, but that only fractures creating an intersection more than 50 centimetres long are mapped in tunnels.

The method for generating a conditioned realisation of a fracture network is initially the same as for an unconditioned realisation, in that fractures are created stochastically based on the general property distributions specified by the user. This stochastic realisation is called the “background” realisation, and it remains important because it is likely that all flow to and from the engineered openings will have to traverse these fractures.

Fractures that intersect the engineered openings are removed and replaced with fractures chosen from the library. The choice of fractures is made randomly from a list of fractures found in a similar environment to the observed fracture, weighted by a “closeness-of-fit” function, and by the number of realisations of the model that could have created a given fracture. The “closeness-of-fit” function measures the degree of similarity between the observed fracture intersection with a surface and the fracture intersection found in the library. Thus, it is based only on information that could be measured, and not based on (for example) the fracture size.

To increase the number of library fractures that might be used, a library fracture may be shifted along a tunnel, or between tunnels, so that it matches an observed fracture. However, fractures cannot be rotated and cannot be moved in a way that will significantly alter the fracture distributions.

Full details of the methodology are described in Appleyard et al. (2018).

3 Calculation with no conditional simulation

The first phase of this work is to determine correlations between flow and transport metrics without conditioning.

After some initial tests to verify some aspects of the model to be used, correlations are explored for quantities measured in open repository conditions between:

- pilot borehole inflows and specific capacities, and
- specific capacities and deposition hole inflows.

After this, correlations are found between these quantities and post-closure performance metrics. These are correlations between:

- specific capacities and post-closure U_0 and F, and
- deposition hole inflows and post-closure U_0 and F.

As there is no conditional simulation in this phase of work, the correlations do not make specific predictions for individual deposition holes, but instead may be used to predict results for an ensemble of deposition holes.

3.1 Initial tests

3.1.1 Background head in hydraulic testing

In principle, when calculating results of hydraulic tests, the overpressure or underpressure in each pilot borehole should be relative to the pressure that would exist in the pilot borehole under open repository conditions with no hydraulic test being run. As all the pilot boreholes are packed off, each internal pressure will not necessarily be the same as the nearby tunnels or neighbouring pilot boreholes. It would thus be necessary to calculate a separate over- or underpressure in each pilot borehole individually.

In practice, given that there are over 69 000 pilot boreholes whose internal pressures would need to be calculated, this would be time-consuming. A simplification is to assume that the entire model is at a constant head (e.g. 0 metres), allowing a change to be made to that head that would be the same for every pilot borehole, i.e. the response to a relative change in pressure is calculated. Such an assumption was made for injection test simulations in Baxter et al. (2018), but its validity is tested here.

To test the assumption, 12 pilot boreholes are chosen at random from the 375 that are intersected by fractures in the first realisation of the repository-scale block 1 model. An overpressure in each case is calculated based on an inflow calculation using packed-off pilot boreholes and open repository conditions in the deposition tunnels, and injection tests are simulated on each pilot borehole. Equivalent simulations for the same 12 pilot boreholes are also performed using a constant head on all boundaries and an overpressure for each individual pilot borehole in turn. Figure 3-1 shows that the flow from a pilot borehole using a uniform background head is essentially the same as that using the calculated background head.

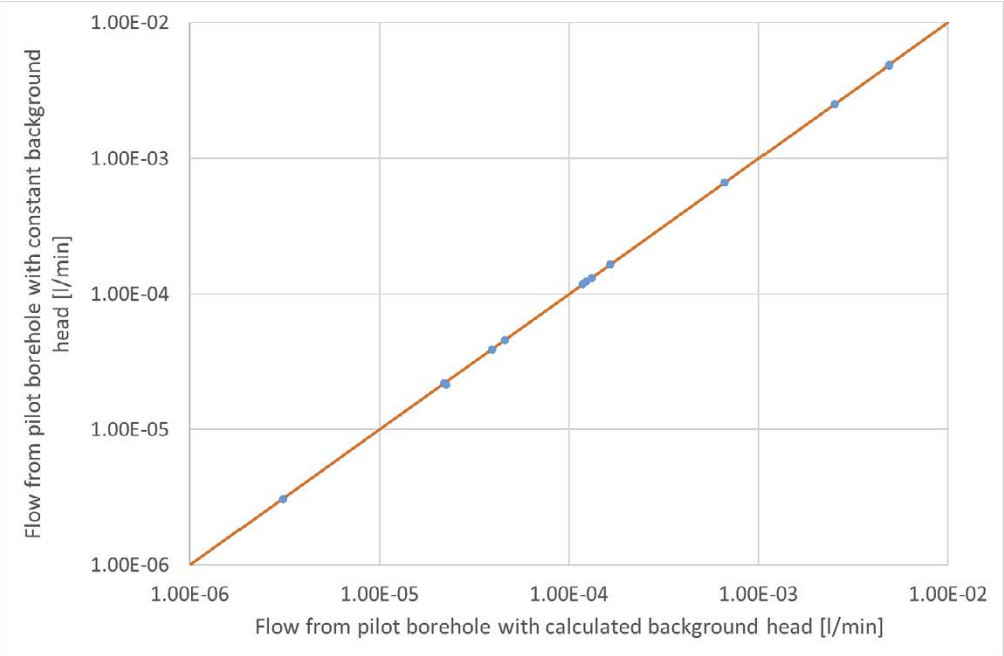

Figure 3-1. *Comparison between flow from twelve pilot boreholes in calculated injection tests using a constant background head (y-axis) and using a calculated background head (x-axis). For clarity, the line (y = x), where the two are the same, is shown in orange.*

3.1.2 Fast pathways from the boundary to the fractures

The repository-scale DFN model for each block contains various repository openings in addition to the deposition tunnels, pilot boreholes and deposition holes that are associated with the block. These include access tunnels and shafts, and deposition tunnels associated with other blocks that protrude into the block being modelled, all represented as implicit fracture zones (IFZs). These provide high conductivity connections between the model boundary and the deposition tunnels, creating the possibility of short-cuts, or fast pathways, from the edge of the model (which provides a supply of water) to the repository.

These fast pathways would not exist if the model region included the entire repository and may cause unrealistically high flows in pilot boreholes and deposition holes. It is thus necessary to investigate whether fast pathways exist in the model, and if so, what measures need to be put in place (i.e. which repository openings need to be removed from the model) in order to prevent them from biasing the simulations.

To do this, calculations of the flow field are first performed in models using open repository conditions for each of the three blocks. These calculations demonstrate that there are very high flows to the deposition tunnels if all openings are left in. A second set of models are generated, where tunnels linking the blocks are removed but other openings are left in. It is found that removing the access tunnels linking the blocks substantially reduces the number of points where there is high inflow, and where relatively high inflows remain, they are significantly reduced. The difference is shown in Figure 3-2. This change means that the issue of fast pathways is much reduced, and as such this model was accepted and used for later calculations. However, a better solution would be to combine all three blocks into a single model, although that is beyond the scope of the current work.

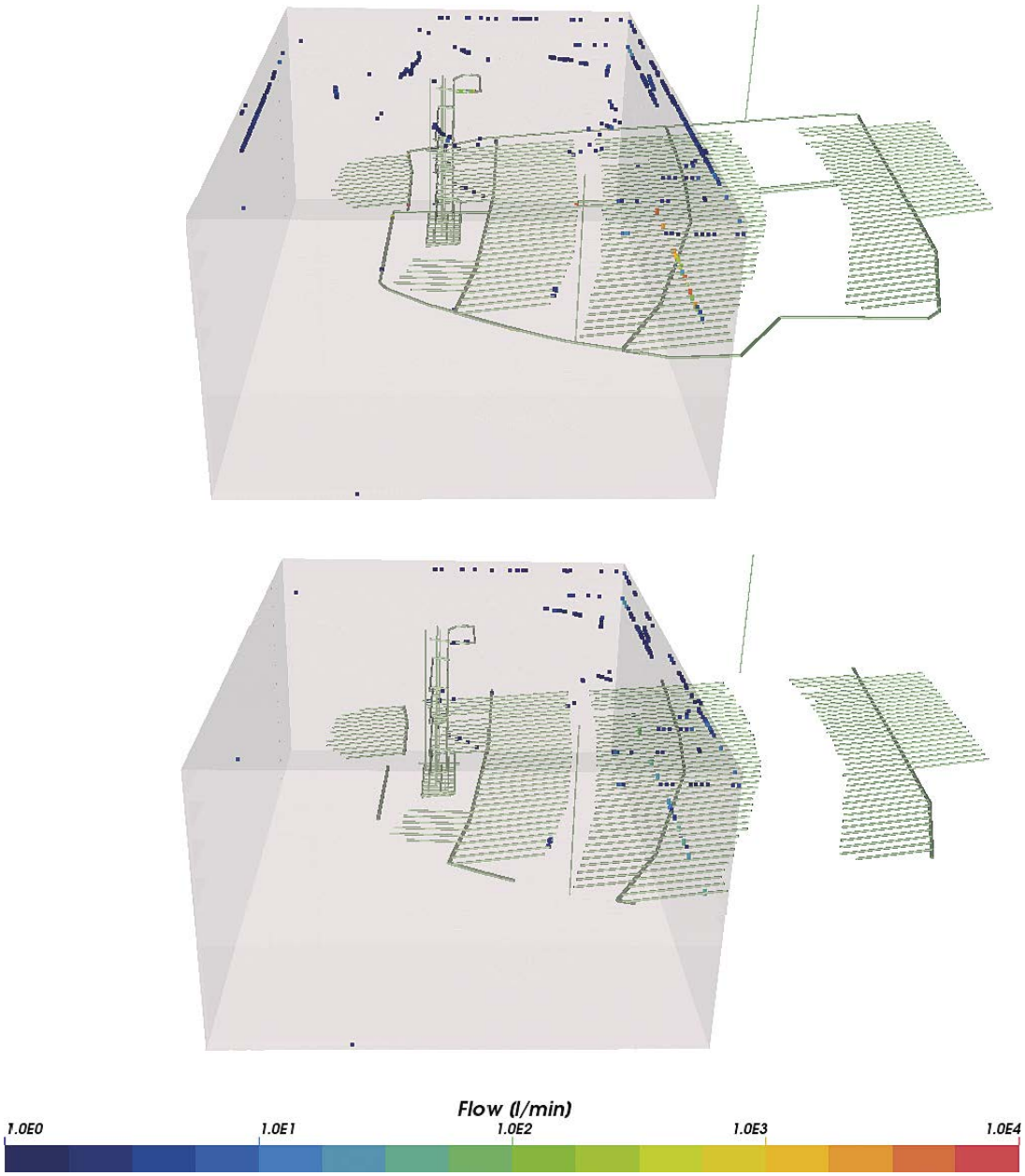

Figure 3-2. *Comparison between high-flow surfaces in block 1 with (top) and without (bottom) access tunnels between repository blocks. The green lines show repository openings. The coloured dots highlight points of high flow; orange and red dots show higher flows than green and blue ones. Flows less than 1 l/min are not shown. There are several points in the top image where high flows reach the deposition tunnels that are no longer present in the bottom image.*

3.2 Open repository conditions

3.2.1 Inflow testing

As part of repository construction, it is helpful to understand how measurable quantities (inflow into pilot boreholes, inflow into deposition holes and results from hydraulic testing) correlate, and hence how well one method can predict another. These correlations can inform decisions of deposition hole suitability prior to full construction of each deposition hole.

As shown in Figure 3-3, the inflows to pilot boreholes and deposition holes are generally well-correlated with each other. Deposition hole inflows are generally greater than or approximately equal to pilot borehole inflows. In simple fracture geometries this is as would be expected. A fracture that intersects a pilot borehole will also intersect the corresponding deposition hole. In most cases, if a fracture carries flow to the pilot borehole, it will also carry that flow to the deposition hole.

A small proportion (2 305 out of 61 795, or 3.7 %) of those pilot boreholes where no inflow is detected are associated with deposition holes where inflow is detected. In addition, a number of those pilot boreholes where inflow is detected are associated with deposition holes where the detected inflow is significantly larger. Both scenarios are likely to be caused by flow-bearing fractures that intersect a deposition hole but that do not reach the deposition hole centre line (and hence the pilot borehole). Of the 407 deposition holes with inflow greater than 0.1 l/min, 183 (45.0 %) are associated with pilot boreholes whose inflow is greater than 0.1 l/min. Conversely, all pilot boreholes with inflow greater than 0.1 l/min are associated with deposition holes with inflow greater than 0.1 l/min.

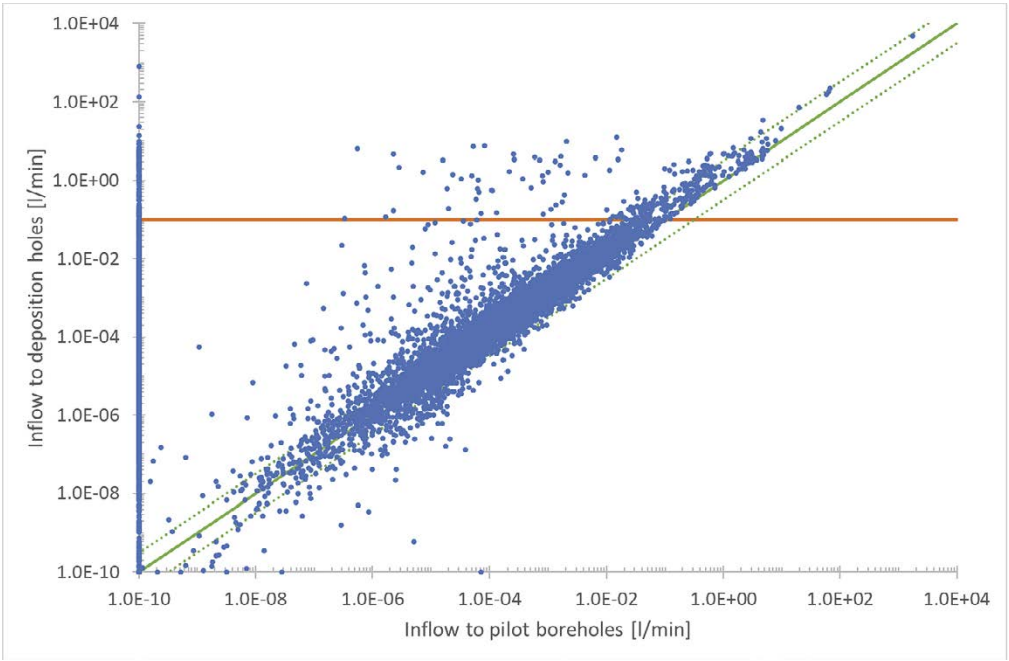

Figure 3-3. *Comparison between inflows into deposition holes and inflows to pilot boreholes over 10 unconditioned realisations (blue dots). Negligible flows are represented as 10^{-10} l/min. The orange line indicates the existing rejection criterion for flow into deposition holes (0.1 l/min). The solid green line is where the inflow is equivalent in the two cases, and the dotted green lines are where the inflows are different by half an order of magnitude.*

There are also a smaller number of cases where the pilot borehole inflow is significantly higher than the deposition hole inflow, including five positions where the pilot borehole receives significant inflow but the associated deposition hole does not. This is likely due to the precise details of the fracture geometry and connectivity. For example, it can occur if the pilot borehole intersects a fracture whose outlet to the wider fracture network will be severed when the deposition holes are excavated. This is illustrated in Figure 3-5, which shows the flow route to one of the pilot boreholes. The only available flow path to the pilot borehole passes through a fracture intersection that lies entirely within a neighbouring deposition hole. The flow path is thus cut off when the deposition hole is excavated.

Typically, the difference between pilot borehole inflow and deposition hole inflow is small. A total of 7 360 deposition hole positions have both non-negligible deposition hole inflow and non-negligible pilot borehole inflow. Of these, the median difference between deposition hole inflow and corresponding pilot borehole inflow is a factor of 1.51. Most of these holes (4 574, or 62.1 %) have a deposition hole inflow that is greater than the corresponding pilot borehole inflow by less than half an order of magnitude. Another 1 488 deposition hole positions (20.2 %) have a deposition hole inflow that is less than the corresponding pilot borehole inflow by less than half an order of magnitude.

Of the remaining deposition hole positions, 1 083 (14.7 %) have a deposition hole inflow that is significantly greater than the corresponding pilot borehole inflow (i.e. by more than half an order of magnitude). The remaining 215 deposition hole positions (2.9 % of the total) have a deposition hole inflow significantly less than the corresponding pilot borehole inflow. A plot of the cumulative distribution of these differences is given in Figure 3-4.

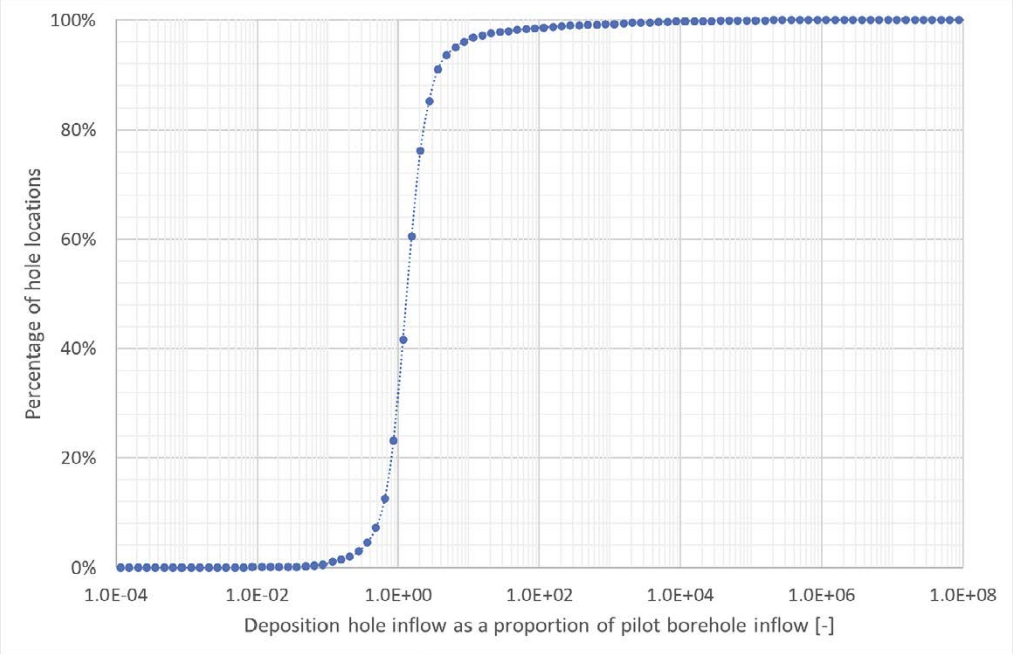

Figure 3-4. *Cumulative distribution of ratios of deposition hole inflow to pilot borehole inflow across deposition hole positions that have inflow in 10 unconditioned realisations. Holes with negligible deposition hole inflow or negligible pilot borehole inflow (or both) are not included.*

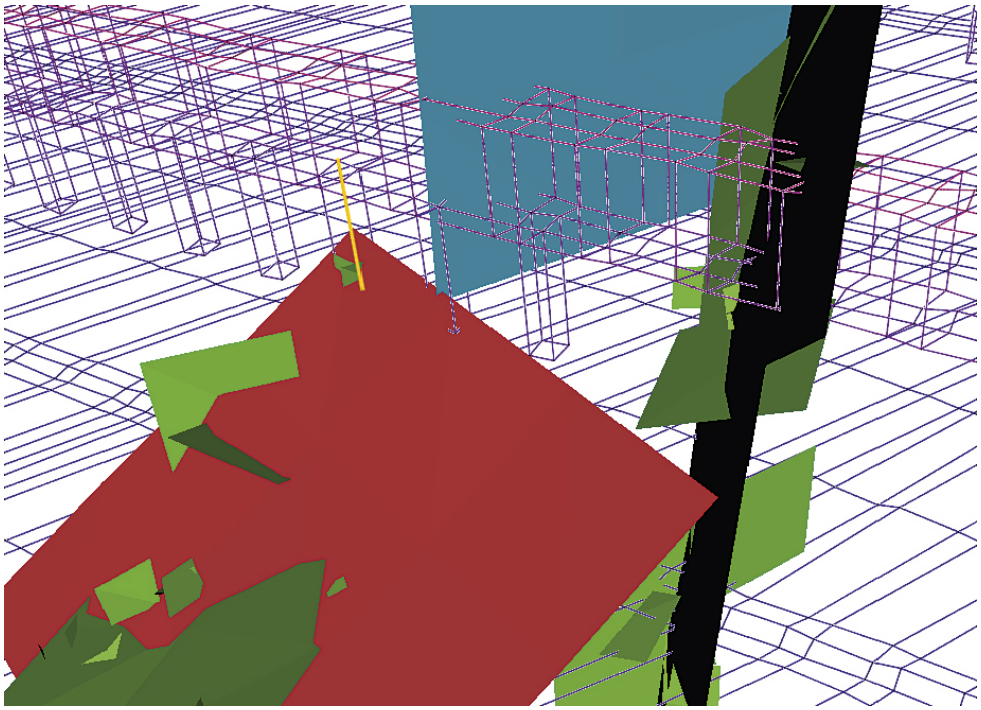

Figure 3-5. *The only flow path to the yellow pilot borehole is through the intersection between the red and blue fractures, which is within the volume of the neighbouring deposition hole. Once the deposition hole is excavated, this intersection no longer exists, and the flow path to the yellow pilot borehole is severed.*

The calculations in this section assume that flows less than 10^{10} l/min are insignificant and thus treated as being equivalent to zero. This limit is chosen as it allows almost all modelled flows to be analysed. However, it is equivalent to 1 millilitre of inflow every 19 years and is thus far lower than the detection limit for any instrument that might realistically be used to measure the flows in a repository.

Overall, 86.0 % of deposition holes do not have inflow or have negligible inflow. Another 13.4 % of deposition holes have non-negligible inflow that is lower than the existing hydraulic rejection criterion of 0.1 l/min, and a total of 407 out of 69 160 (0.6 %) deposition holes have inflows that exceed 0.1 l/min. These values are given in Table 3-1.

Two deposition holes, from the 69 160, recorded significant net outflows, probably due to peculiarities in the fracture geometry. These are excluded from results.

The equivalent data for pilot boreholes is given in Table 3-2. The table has an additional band for flows between 10^{-2} l/min and 10^{-1} l/min, values that were chosen to be the same as, and one order of magnitude lower than, the existing rejection criterion for deposition hole inflows. The number of pilot boreholes for each inflow band that are associated with deposition holes whose inflows exceed 0.1 l/min is also given. Unsurprisingly, the proportion of deposition holes whose inflows exceed 0.1 l/min is substantially larger when considering only those associated with pilot boreholes that have high flows.

Table 3-1. Number of deposition holes found to have negligible inflow (i.e. flow less than 10^{-10} l/min), found to have inflow at a rate less than the existing hydraulic rejection criterion (0.1 l/min) and found to have inflow at a rate greater than the existing hydraulic rejection criterion.

Deposition hole inflow rate	Number of deposition holes	Percentage
Negligible inflow	59 495	86.0 %
Inflow rate less than 0.1 l/min	9 256	13.4 %
Inflow rate less than 0.1 l/min	407	0.588 %
Excluded	2	0.003 %
All	69 160	100 %

Table 3-2. Number of pilot boreholes by inflow rate, and the number in each inflow band that have associated deposition hole inflows that exceed the existing hydraulic rejection criterion (0.1 l/min). Flows less than 10^{-10} l/min are assumed to be negligible.

Pilot borehole flow rate	Number of pilot boreholes	Percentage of total	Number of deposition holes whose inflows exceed 0.1 l/min	Percentage of pilot boreholes rejected
Less than 10^{-10} l/min	61 794	89.4 %	100	0.162 %
10^{-10} l/min to 10^{-2} l/min	6 751	9.76 %	45	0.667 %
10^{-2} l/min to 10^{-1} l/min	430	0.622 %	79	18.4 %
More than 10^{-1} l/min	183	0.265 %	183	100 %
All	69 158	100 %	407	0.588 %

3.2.2 Hydraulic testing

The correlation between specific capacity and deposition hole inflow is shown in Figure 3-6. It is clear from the figure that specific capacities and deposition hole inflows are not as well-correlated as between the two inflow tests. It is also notable that deposition hole inflow may be significantly higher or lower than might be predicted from a simple correlation between inflow and specific capacity; by contrast there are few points where the deposition hole inflow was significantly lower than the pilot borehole inflow.

The plot includes a total of 2 553 deposition hole positions where the specific capacity is negligible, but deposition hole flow is non-negligible. This means that 4.3 % of those points where specific capacity is negligible are associated with deposition holes that have non-negligible inflow. Most of these probably arise for similar reasons as found in the case with pilot borehole inflows: not all intersections between the deposition hole and the fracture network will be found in the pilot borehole used for hydraulic testing. These results are significant because they represent deposition hole positions where the flow will be difficult to predict from measurements in pilot boreholes.

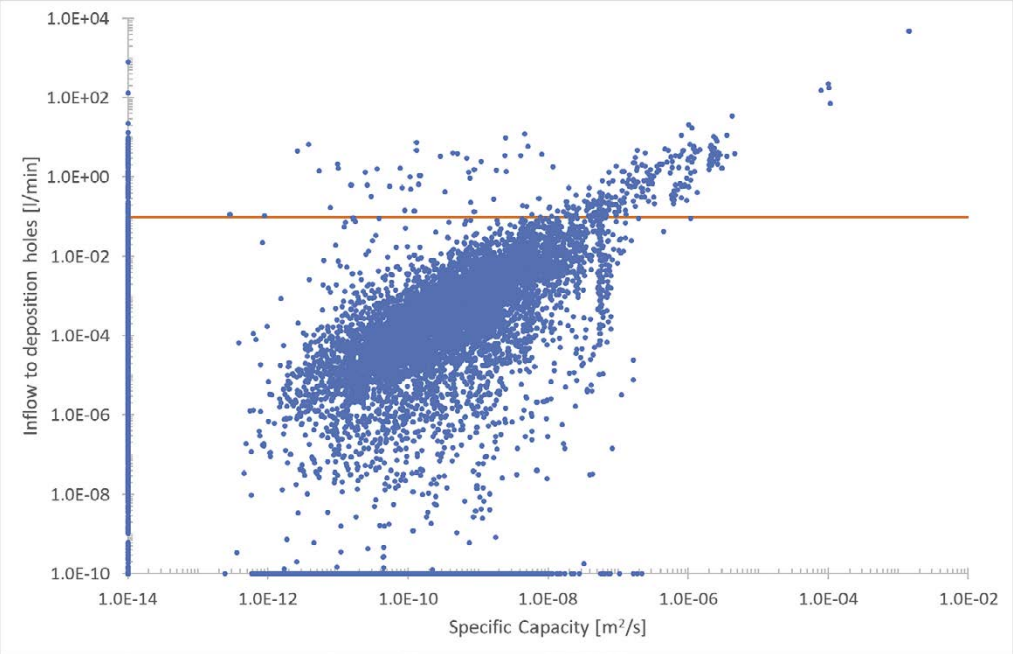

Figure 3-6. *Comparison between inflow into deposition holes and specific capacity from injection tests in pilot boreholes over 10 unconditioned realisations (blue dots). Negligible inflows are represented as 10^{-10} l/min, and negligible specific capacities are represented as 10^{-14} m^2/s. The orange line indicates the existing hydraulic rejection criterion for flow into deposition holes (0.1 l/min).*

There are also 3 523 pilot boreholes with non-negligible specific capacity that are associated with deposition holes with no significant inflow. This is 33.1 % of the 10 633 pilot boreholes with non-negligible specific capacity. It is likely that in these cases the pilot borehole has a simple hydraulic connection to the deposition tunnel but not to the wider fracture network.

Modified versions of both scenarios – such as where some but not all fractures intersecting the deposition hole intersect the pilot borehole, or where the pilot borehole is connected to the wider fracture network but only by a more tortuous route – may account for cases where the deposition hole inflow is non-negligible but smaller than anticipated.

As when comparing inflow tests, the calculations in this section assume that inflows less than 10^{-10} l/min are insignificant and thus treated as being equivalent to zero (this value is significantly lower than any realistic detection limit). Similarly, for hydraulic tests, the lower limit for specific capacity is set to be 10^{-14} m^2/s (equivalent to 6×10^{-10} l/(min·m)).

Four of the 69 160 calculations did not converge successfully after multiple attempts. As discussed in Section 2.1, these four results are excluded from results presented involving specific capacity, leaving 69 156 data points.

3.3 Correlations with post-closure performance measures

3.3.1 Hydraulic testing

Comparing correlations between measurable quantities may allow a prediction of whether a given deposition hole will have flow that exceeds a given hydraulic rejection criterion. However, a key factor in repository safety is the behaviour of the groundwater once the repository is closed. In this case, the post-closure behaviour is characterised for each deposition hole based on the flow rate per unit length in the fractures intersecting the deposition hole (U_0) and flow-related transport resistance (F) encountered by particles released from backfilled deposition holes after the repository is closed.

U_0 is considered negligible in this work if it is less than 10^{-9} l/(yr·m) for a given deposition hole. By this standard, of the 69 160 deposition holes simulated, a total of 19 287 (27.9 %) have some flow. Of these 567 (2.9 % of deposition holes with flows) are associated with values of U_0 that exceed the post-closure performance target of 1 l/(yr·m).

The correlation between specific capacities and U_0 for corresponding deposition holes in a closed repository is given by Figure 3-7. The figure shows that high specific capacities are correlated with high U_0. For lower specific capacities, while there is a general trend in the same direction, the correlation is weaker and hence the predictive power of the specific capacity is likely to be poorer.

Slightly over half (9 907 out of 19 285, or 51.4 %) of the total number of deposition hole positions where U_0 is non-negligible are associated with pilot boreholes with negligible specific capacity. This result implies that a prediction based on specific capacity alone will likely fail to find many of the positions where U_0 will exceed the post-closure performance target. However, among pilot boreholes where there is non-negligible specific capacity, most (9 378 out of 10 633, or 88.1 %) are associated with non-negligible U_0.

All deposition holes considered have an associated value of F, but in a large majority of cases this value is very high (indicating a high resistance to transport). There are 134 deposition holes, or 0.2 % of the total, that have a value for F that is less than the post-closure performance target of 10^4 yr/m. This value is significantly smaller than the equivalent number for U_0.

The correlation between specific capacities and F is given by Figure 3-8. A similar pattern exists here as for U_0. There is a better (inverse) correlation for higher specific capacity. However, the correlation is weaker than with U_0. This is because F is also accumulated by particles in fractures that are distant from the starting deposition hole and so it is less sensitive to conditions around the deposition hole.

Correlation lines drawn on these plots can be used to infer specific capacity limits that may be useful in predicting which deposition holes are likely to have unacceptable values of U_0 and F. Predicted specific capacity limits based on these plots are given in Section 3.4.

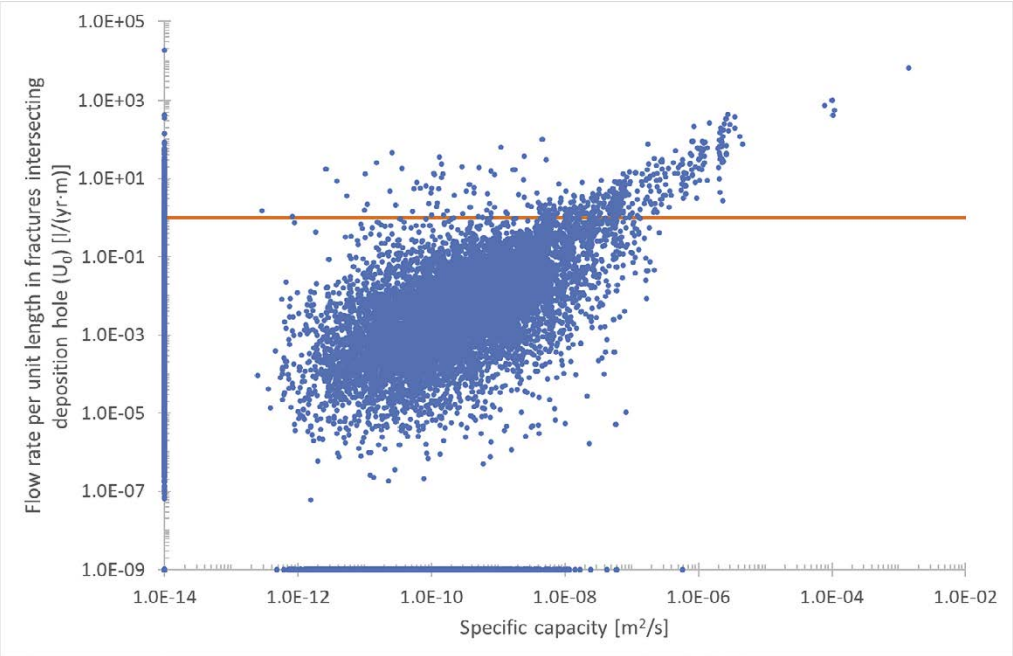

Figure 3-7. *Comparison between pilot borehole specific capacity and U_0 over 10 unconditioned realisations (blue dots). Negligible values of U_0 are included as 10^{-9} l/(yr·m), and negligible specific capacities are represented as 10^{-14} m²/s. The orange line indicates the post-closure performance target for U_0 of 1 l/(yr·m).*

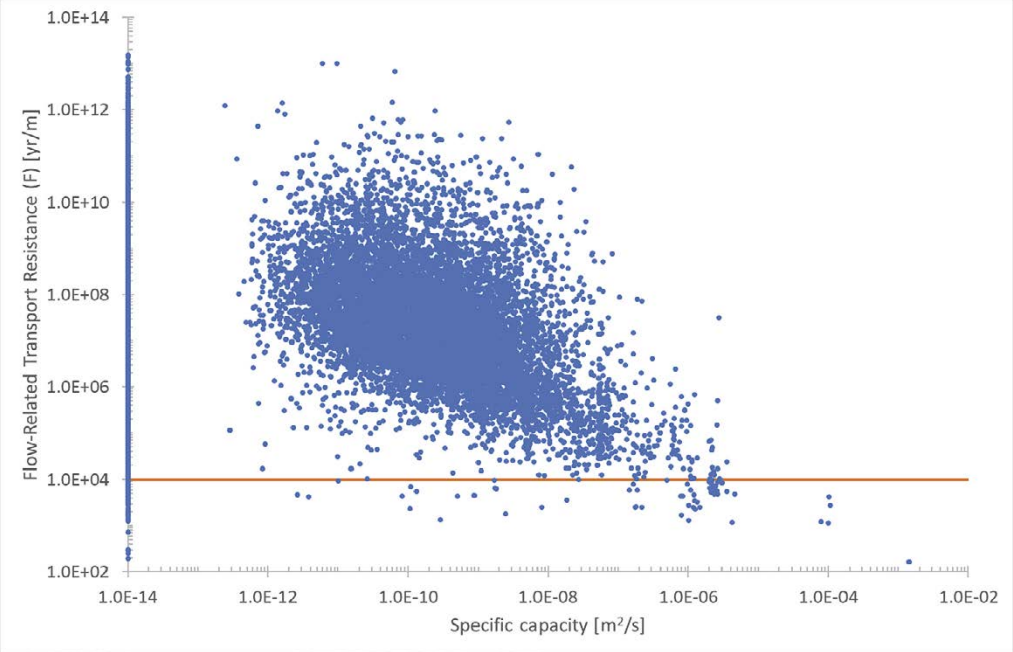

Figure 3-8. *Comparison between pilot borehole specific capacity and F over 10 unconditioned realisations (blue dots). Negligible specific capacities are represented as 10^{-14} m²/s. The orange line indicates the post-closure performance target for F of 10^4 yr/m.*

3.3.2 Deposition hole inflows

Comparing U_0 with deposition hole inflows instead of hydraulic test data, as in Figure 3-9, gives a somewhat better correlation. The correlation is particularly strong where the deposition hole inflow and U_0 are relatively high, which implies that deposition hole inflow may be a more reliable predictor of U_0 than specific capacity.

The existence of inflow to the deposition hole is about as good a predictor of non-negligible U_0 as the specific capacity of the corresponding pilot borehole. For deposition hole inflow, 10 193 out of 19 285 (52.9 %) positions where U_0 is non-negligible are associated with deposition holes with negligible inflow. The equivalent number for specific capacity was 9 907. However, of deposition holes that have non-negligible inflow, almost all (9 092 out of 9 663, or 94.1 %) also have non-negligible U_0.

The post-closure performance measures for U_0 and F, based on projections of post-closure behaviour, are independent of the hydraulic rejection criterion for deposition holes, based on the properties of the backfill. However, it is useful to see how well a limiting deposition hole inflow of 0.1 l/min predicts those deposition holes with U_0 greater than the post-closure performance target for U_0.

In total, 327 out of 567 (57.7 %) deposition holes where U_0 is greater than the performance target also have inflows greater than 0.1 l/min. There are an additional 80 deposition holes that will be rejected due to high inflow, but that do not have a U_0 greater than the performance target. The details of these figures are given in Table 3-3.

The correlation between deposition hole inflow and F, shown in Figure 3-10, is similarly better than between specific capacity and F. The correlation is generally better for high inflow (and low F). It is also noticeable that deposition holes with inflows at or around 0.1 l/min are generally associated with values of F significantly greater than the post-closure performance target of 10^4 yr/m.

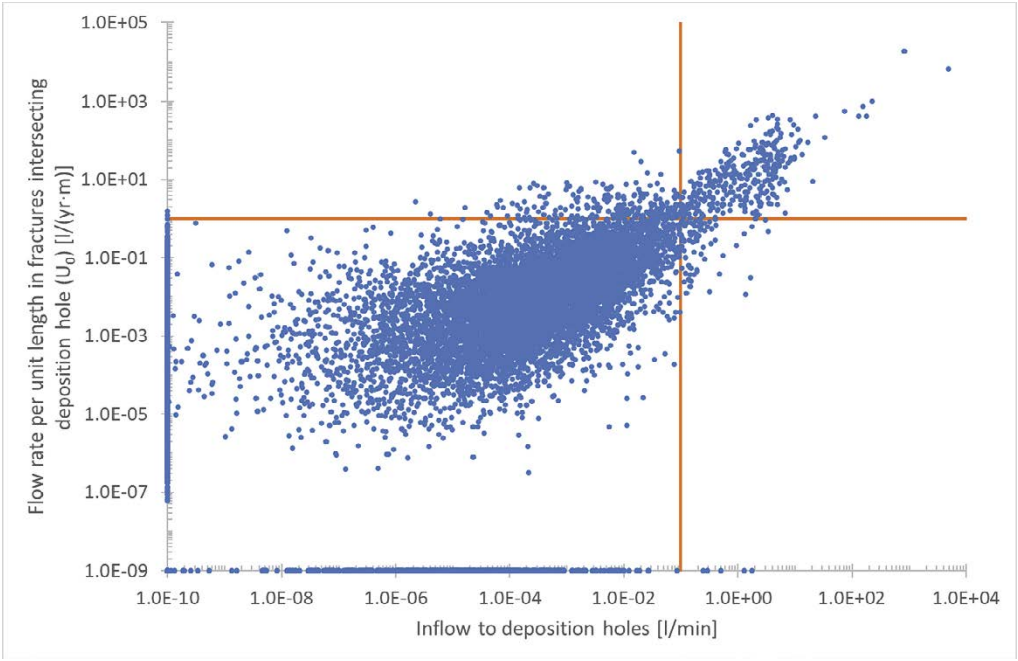

Figure 3-9. *Comparison between deposition hole inflow and U_0 over 10 unconditioned realisations (blue dots). Negligible values of U_0 are represented as 10^{-9} l/(yr·m), and negligible inflows are represented as 10^{-10} l/min. The horizontal orange line indicates the post-closure performance target of 1 l/(yr·m); the vertical orange line indicates the existing hydraulic rejection criterion of inflow 0.1 l/min.*

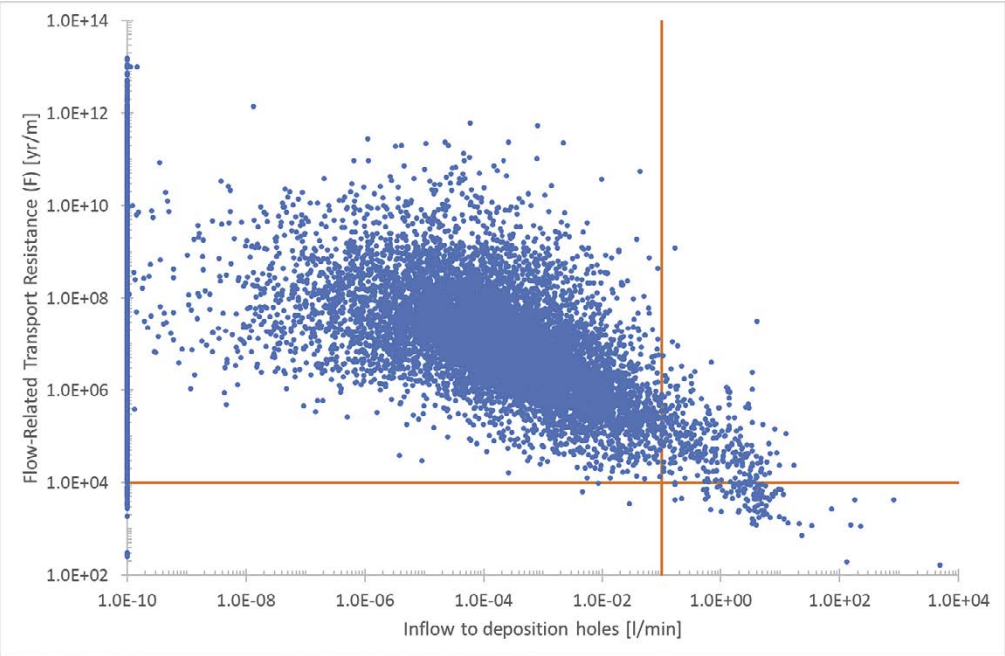

Figure 3-10. *Comparison between deposition hole inflow and F over 10 unconditioned realisations (blue dots). Negligible inflows are included as 10^{-10} l/min. The horizontal orange line indicates the post-closure performance target of 10^4 yr/m; the vertical orange line indicates the existing hydraulic rejection criterion of inflow 0.1 l/min.*

This conclusion is borne out by the numbers. Of the 134 positions with F less than the post-closure performance target, 100 (74.6 %) are associated with deposition hole inflows that are greater than 0.1 l/min. However, there are also 307 deposition holes with inflow greater than 0.1 l/min whose F is greater than the performance target. That is equivalent to 75.4 % of all deposition holes with inflow greater than the rejection criterion. The details of these figures are given in Table 3-4. Although this does not seem very useful, it is important to consider that the U_0 in many of those 307 deposition holes will still exceed the performance target for U_0. A more useful conclusion may be that it is more conservative to use limits inferred from the performance target for U_0, rather than that for F.

Table 3-3. Number of deposition holes with U_0 that exceeds the post-closure performance target of 1 l/(yr·m) for U_0. Categories have been chosen based on the existing deposition hole hydraulic rejection criterion of 0.1 l/min.

Deposition hole inflow rate	Number of deposition holes	Percentage of total	Number of deposition holes that exceed performance target for U_0	Percentage of deposition holes that exceed performance target for U_0
Less than 10^{-10} l/min	59495	86.0 %	3	0.005 %
10^{-10} l/min to 10^{-1} l/min	9256	13.4 %	237	2.56 %
More than 10^{-1} l/min	407	0.588 %	327	80.3 %
All	69158	100 %	567	0.820 %

Table 3-4. Number of deposition holes with F less than the post-closure performance target of 10^4 yr/m. Categories have been chosen based on the existing deposition hole hydraulic rejection criterion of 0.1 l/min.

Deposition hole inflow rate	Number of deposition holes	Percentage of total	Number of deposition holes with F less than performance target	Percentage of deposition holes with F less than performance target
Less than 10^{-10} l/min	59495	86.0 %	31	0.052 %
10^{-10} l/min to 10^{-1} l/min	9256	13.4 %	3	0.032 %
More than 10^{-1} l/min	407	0.588 %	100	24.6 %
All	69158	100 %	134	0.194 %

3.4 Limits inferred from correlations with post-closure performance measures

It is clear from Sections 3.2 and 3.3 that the principal flow measures calculated are correlated with one another. This section proceeds to infer limiting values for specific capacity and deposition hole inflow based on the post-closure performance targets for U_0 and F. These limiting values could be used as updated hydraulic rejection criteria during the construction of a repository.

These inferences are based on simple straight correlation lines drawn on to each plot. New limits are determined by calculating the value of (for example) specific capacity that corresponds to a given post-closure performance target on the line drawn. As all plots presented in this report use logarithmic scales on both axes, the equation of each correlation line has the form $y = ax^b$. The equations for the lines presented are given in Appendix. Conclusions and recommendations based on the limits found are provided in Chapters 5 and 6.

The correlation lines drawn are not the only ones that could be drawn and are chosen by eye rather than by mathematical methods. They do not take account of data points where one or both variables give a negligible result, but will take some account of cases where one result is smaller than anticipated for geometrical reasons (e.g. a deposition hole intersected by two flow-bearing fractures, of which only one intersects the pilot borehole).

Despite these approximations, it is useful to generate equivalent limits based on these approximate correlation lines as they give an idea of the sorts of measurable values that are implied to be equivalent to the post-closure performance target.

3.4.1 Comparing U_0 with F

One limit that may be inferred is an equivalent post-closure performance target for flow-related transport resistance (F) based on that already available for U_0. This inferred target will not supplant the existing performance target of 10^4 yr/m. However, it is still interesting as it can be compared with a result obtained in Baxter et al. (2018), and because this analysis can give an indication of whether one target is more conservative than the other.

Appendix A of Baxter et al. (2018) calculates a limit for F of 2×10^5 yr/m algebraically, based on an approximate typical transport length of 200 metres. The comparable result from this work is the limit inferred from Figure 3-11, which is 2.26×10^5 yr/m, very similar to that algebraic value. This limit is clearly significantly greater than the post-closure performance target for F (10^4 yr/m).

It is also useful to understand the relationship between U_0 and F in terms of the number of deposition holes that exceed the U_0 target but that are greater than the F target (i.e. where F is acceptable), and the number that are less than the F target (i.e. where F is unacceptable) but do not exceed the U_0 target. There are 600 deposition holes that are unacceptable in terms of either U_0 or F. Of those deposition holes that are unacceptable in terms of F, most (101 out of 134) exceed the performance target for U_0. However, of those deposition holes that are unacceptable due to high U_0, only a small proportion (101 out of 567) are unacceptable due to low F. It is reasonable to conclude from these results that a target suitable for predicting which deposition holes have U_0 greater than the target is likely to also successfully predict which deposition holes have F less than the target, but the converse is unlikely to be true.

3.4.2 Specific capacity limits

New rejection criteria for specific capacity can inferred using the lines of correlation on Figure 3-12 and Figure 3-13. The key advantage of using a rejection criterion based on specific capacity would be that it can be evaluated without the expense of excavating the deposition hole. It may also be more accurate than the pilot borehole inflow because the flows involved are likely to be larger.

The limiting specific capacity inferred from Figure 3-12 for U_0 is 4.10×10^{-8} m^2/s. The equivalent limit inferred from U_0 by a similar method in Baxter et al. (2018) was 1.5×10^{-8} m^2/s, which is broadly consistent with the value inferred here. However, the current work benefits from a larger number of points spread over a larger number of deposition holes, enabling more accurate correlation lines.

Of the 567 deposition hole positions where U_0 exceeds 1 l/(yr·m), 260 are associated with pilot boreholes that would be rejected based on this criterion. There are also another 93 pilot boreholes with higher specific capacities that would be rejected even though their U_0 does not exceed 1 l/(yr·m).

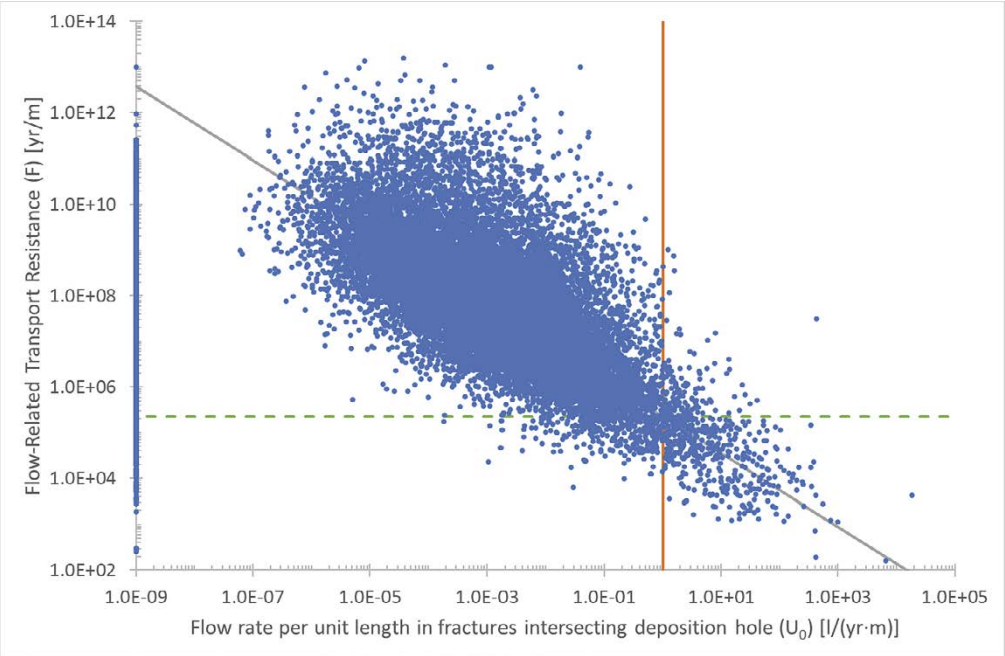

Figure 3-11. *Comparison between U_0 and F over 10 unconditioned realisations (blue dots). Negligible values of U_0 are represented as 10^{-9} l/(yr·m). The orange line indicates the post-closure performance target of 1 l/(yr·m) for U_0, the grey line is an approximate correlation line, and the green dashed line where they meet gives the inferred limit in F.*

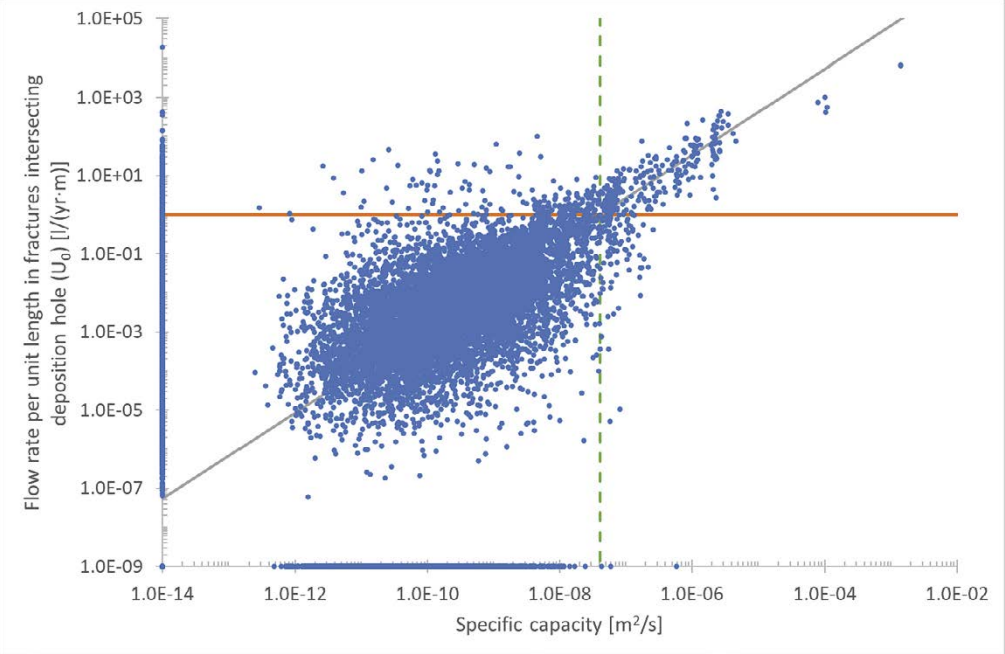

Figure 3-12. *Comparison between U_0 and the specific capacity from injection testing over 10 unconditioned realisations (blue dots). Negligible values of U_0 are represented as 10^{-9} l/(yr·m) and negligible specific capacities are represented as 10^{-14} m^2/s. The orange line shows the performance target of 1 l/(yr·m), the grey line is a correlation line, and the green dashed line where they meet gives the inferred specific capacity limit.*

There are also 134 deposition hole positions where F is less than 10^4 yr/m. Of these, 46 are rejected based on this specific capacity limit. Another 307 deposition hole positions would be rejected where F is greater than 10^4 yr/m, but many of these would have a U_0 that exceeds 1 l/(yr·m).

The limit for specific capacity based on F, inferred from Figure 3-13, is 4.77×10^{-6} m^2/s – obviously considerably higher than the limit inferred from U_0. Using this limit, only five deposition hole positions would be rejected, all of which have both U_0 greater than the performance target and F less than the performance target. There remain 595 deposition hole positions not found using this limit, that either have U_0 greater than the performance target or F less than the performance target, or both.

While a single limit may be useful, there is clearly a considerable degree of spread around the correlation line in the plot. It would certainly be possible to draw different correlation lines, and therefore to infer different specific capacity rejection criteria, for both U_0 and F. The ranges of alternative rejection criteria are shown in Figure 3-14 (for U_0) and Figure 3-15 (for F). Specifically, these give the proportion of pilot boreholes with a given specific capacity (or greater) that are associated with deposition holes where U_0 exceeds the performance target or where F is less than the performance target. The aim is thus to give an idea of the consequence of changing the limit in each case.

Obviously, reducing the limit will generally increase the number of deposition hole positions that are rejected, whether correctly or incorrectly. Figure 3-14 demonstrates that the proportion of deposition hole positions where U_0 exceeds the performance target increases rapidly with the specific capacity limit chosen.

Of those deposition hole positions rejected using a criterion of 10^{-8} m^2/s, 43.0 % have U_0 greater than the performance target (334 out of 777). If a criterion of 10^{-7} m^2/s is used, 85.5 % of rejected deposition hole positions have U_0 greater than the performance target (153 out of 179). However, there are 181 deposition hole positions with U_0 greater than the performance target that are rejected with the lower criterion but not with the higher criterion.

Figure 3-15 demonstrates a similar result, though the proportions of deposition hole positions with F less than the performance target are generally lower for the same specific capacity limits.

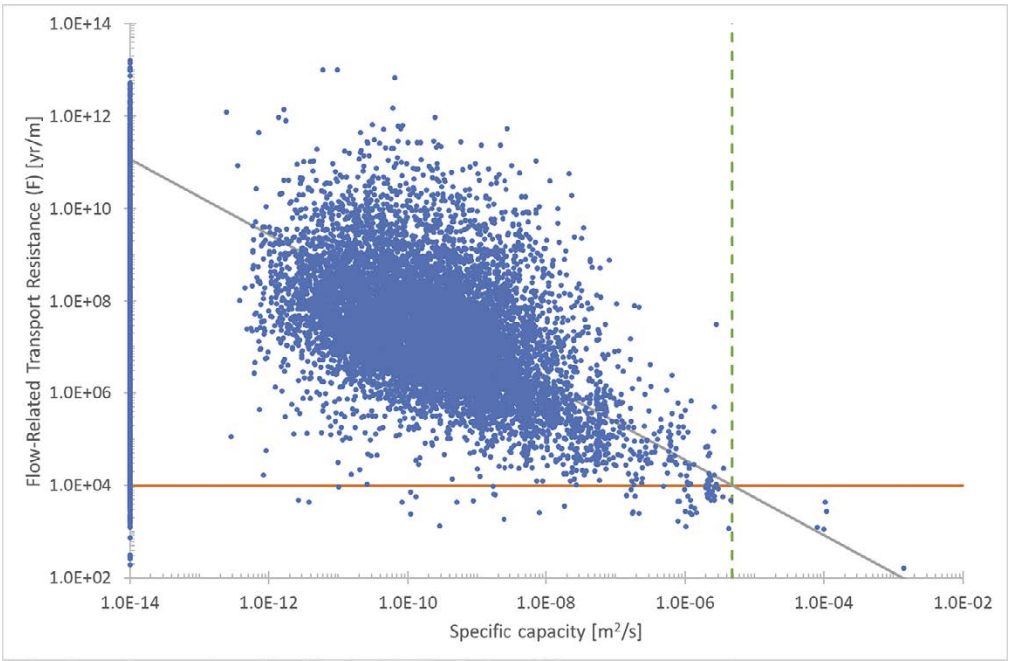

Figure 3-13. *Comparison between F and the specific capacity from injection testing over 10 unconditioned realisations (blue dots). Negligible specific capacities are represented as 10^{-14} m^2/s. The orange line shows the inferred performance target for F, the grey line is an approximate correlation line, and the green dashed line where they meet gives the inferred specific capacity limit.*

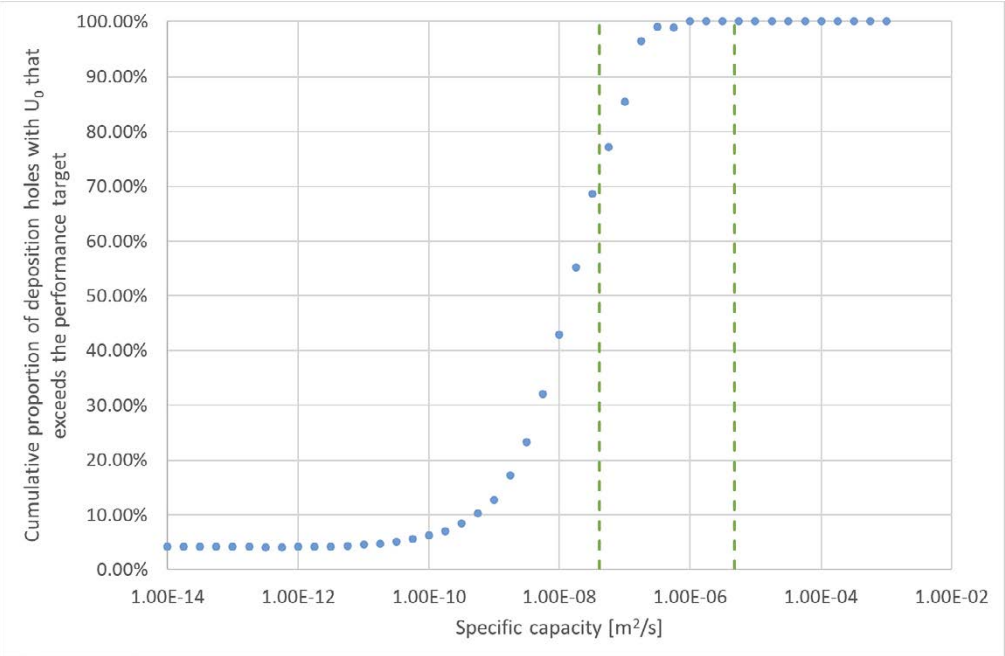

Figure 3-14. *Cumulative proportion of pilot boreholes with a given specific capacity that are associated with deposition hole positions where U_0 exceeds the post-closure performance target of 1 l/(yr·m). The vertical green dotted lines give the inferred rejection criteria for specific capacity based on U_0 (left) and F (right).*

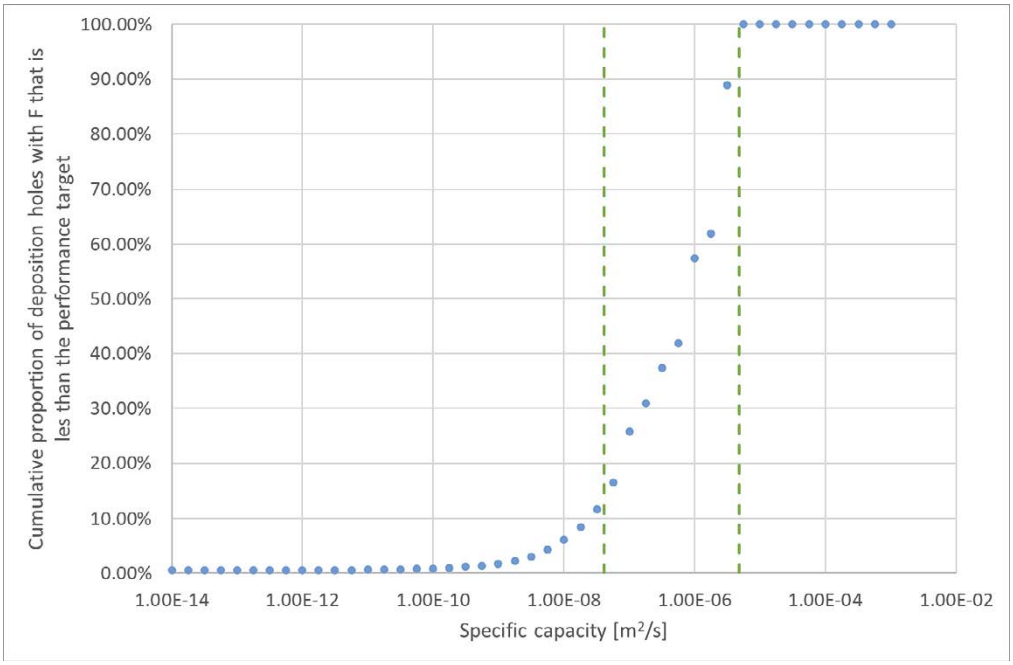

Figure 3-15. *Cumulative proportion of pilot boreholes with a given specific capacity that are associated with deposition hole positions where F is less than the post-closure performance target of 10^4 yr/m. The vertical green dotted lines give the inferred rejection criteria for specific capacity based on U_0 (left) and F (right).*

3.4.3 Inferring deposition hole inflow limits from specific capacity

Using the specific capacity limits inferred in Subsection 3.4.2, it is possible to create limits for deposition hole inflow as shown in Figure 3-16. This allows a more direct comparison between the newly inferred rejection criteria based on specific capacity and the existing rejection criterion for deposition holes. There are two new limits for specific capacity (4.10×10^{-8} m^2/s based on U_0, and 4.77×10^{-6} m^2/s based on F), so there are two new limits for deposition hole inflow.

The deposition hole inflow limit inferred from the specific capacity limit based on U_0 is 0.118 l/min. This is very similar to the existing hydraulic rejection criterion of 0.1 l/min and, as would be expected, predictions based on this limit have a similar success rate. The number of deposition holes that are rejected by this new criterion where U_0 exceeds the performance target is 318 instead of 327. The number of deposition holes rejected where U_0 does not exceed the performance target is 65 instead of 80. When considering F, instead of rejecting 307 deposition holes where F is greater than the performance target, the new rejection criterion rejects 283. All these results are in reasonable agreement with the results using 0.1 l/min.

The deposition hole inflow limit inferred from the specific capacity limit based on F is 26.54 l/min. This value is too high to be useful. The result is that only 8 pilot boreholes are rejected, and all of them are associated with deposition holes where U_0 exceeds the performance target and F is less than the performance target. However, a large majority of holes that should be rejected are not found.

Both inferred limits are greater than the existing deposition hole hydraulic rejection criterion of 0.1 l/min. It is undesirable to use limits greater than this because there is little value in excavating a deposition hole that is likely to have too much inflow. There is thus some benefit in calculating a limit for specific capacity equivalent to a deposition hole inflow of 0.1 l/min according to this method. The limit calculated from this correlation line is 3.54×10^{-8} m^2/s.

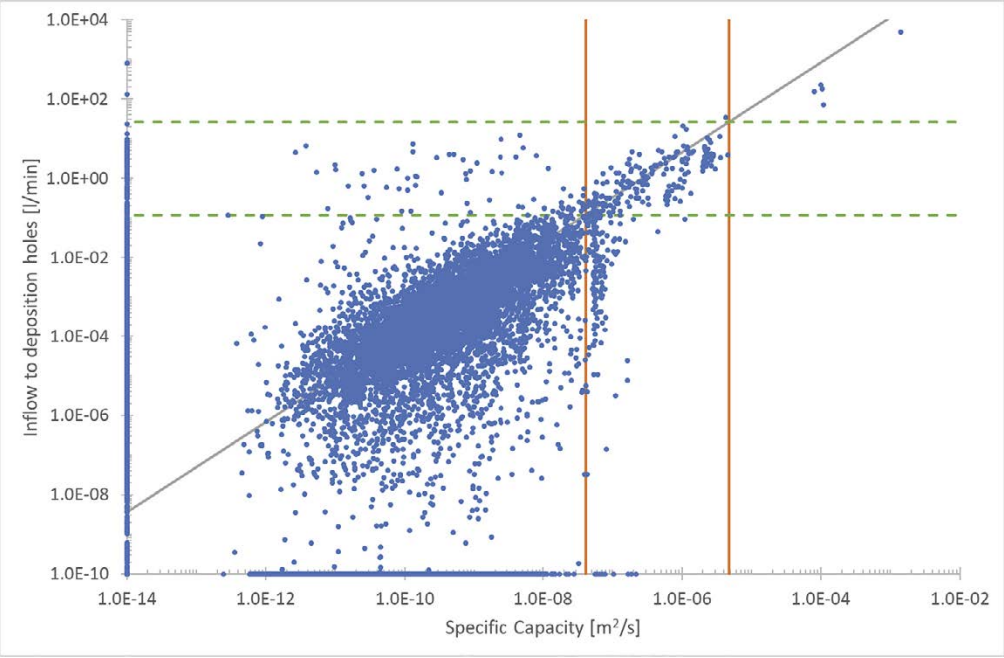

Figure 3-16. *Comparison between inflow into deposition holes and specific capacity from injection tests in pilot boreholes over 10 unconditioned realisations (blue dots). Negligible inflows are represented as 10^{-10} l/min, and negligible specific capacities are represented as 10^{-14} m^2/s. The grey line indicates the correlation, the orange lines indicate the inferred limits for specific capacity from Subsection 3.4.2 and the green dashed lines where they meet to give the inferred deposition hole inflow limits.*

3.4.4 Deposition hole inflow limits

It is possible to generate limits for deposition hole inflow directly from the correlations between deposition hole inflow and the post-closure performance measures in the same way as is done for specific capacity in Subsection 3.4.2.

If the final target measure is deposition hole inflow, then a direct inference from post-closure performance measures to deposition hole inflow limits is likely to be more useful than an indirect inference via the specific capacity. This is because the correlations between both post-closure performance measures and deposition hole inflow are better than those between the post-closure performance measures and specific capacity, and because an indirect limit requires that values be inferred twice.

The deposition hole inflow can obviously only be measured once the deposition hole has been excavated. However, the fractures intersecting a deposition hole may be different to those intersecting the associated pilot borehole. It is thus perhaps useful to apply a new set of hydraulic rejection criteria to the excavated deposition holes to further reduce the risk that inappropriate deposition holes will be used.

The new rejection criterion inferred from Figure 3-17, the correlation between deposition hole inflow and U_0, is 7.36×10^{-2} l/min. As with the calculated inflow from Subsection 3.4.3, this value is similar to the existing hydraulic rejection criterion for deposition hole inflow of 0.1 l/min. Of the 567 deposition holes where U_0 exceeds 1 l/(yr·m), 351 are rejected based on this limit, and an additional 114 deposition holes are rejected despite a U_0 less than 1 l/(yr·m).

The limit inferred from the correlation between deposition hole inflow and F in Figure 3-18 is 9.79 l/min. While somewhat lower than the calculated inflow in Subsection 3.4.3, this is still a very large number and as a result only 16 out of a total of 600 problematic deposition holes (for U_0 or F) are rejected. However, as this limit far exceeds the existing hydraulic rejection criterion for deposition hole inflow, the results that arise from it are largely academic.

As with the specific capacity limits in Subsection 3.4.2, it is useful to recognise that the limits specified here are not the only limits that could be chosen, and that the spread around the correlation lines could allow different limits. Thus the effects of the range of alternative criteria are shown in Figure 3-19 (for U_0) and Figure 3-20 (for F). These show the proportion of deposition holes with a given inflow where the U_0 exceeds the performance target, or the F is less than the performance target.

If, for example, a limit of 1×10^{-2} l/min is chosen, 444 out of 567 deposition holes where U_0 exceeds 1 l/(yr·m) are rejected, but an additional 690 deposition holes are rejected where U_0 is less than 1 l/(yr·m). In addition, 101 out of 134 deposition holes where F is less than 10^4 yr/m are rejected, as are 1 033 other deposition holes. Thus 39.2 % of deposition holes rejected have U_0 greater than the performance target and 8.9 % of deposition holes rejected have F less than the performance target.

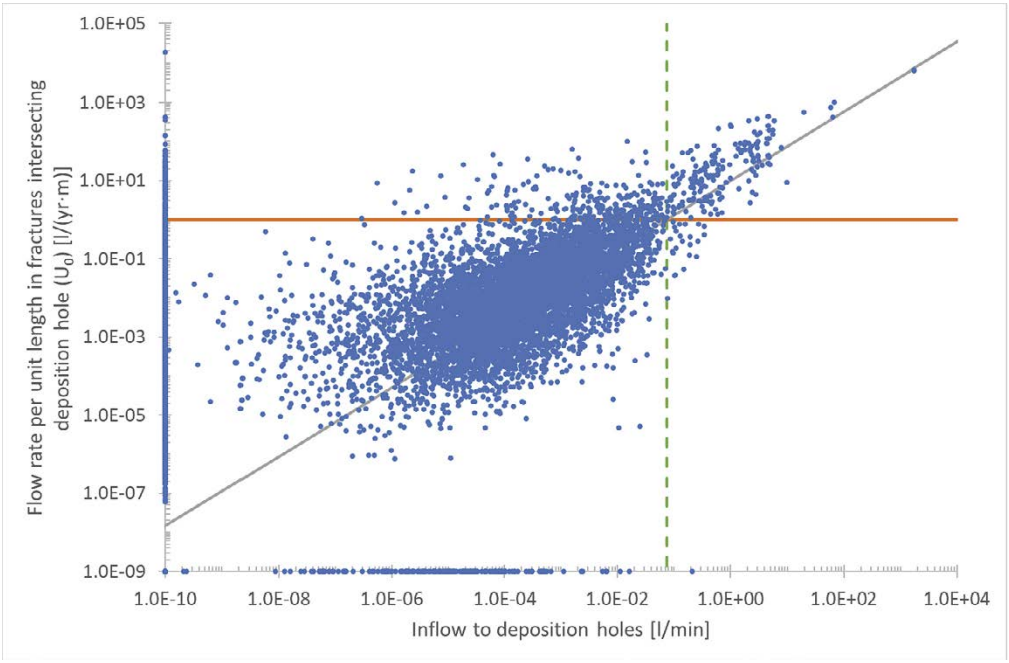

Figure 3-17. *Comparison between U_0 and inflow to deposition holes over 10 unconditioned realisations (blue dots). Negligible values of U_0 are represented as 10^{-9} l/(yr·m) and negligible inflows are represented as 10^{-10} l/min. The orange line shows the performance target of 1 l/(yr·m), the grey line is a correlation line, and the green dashed line where they meet gives the inferred deposition hole inflow limit.*

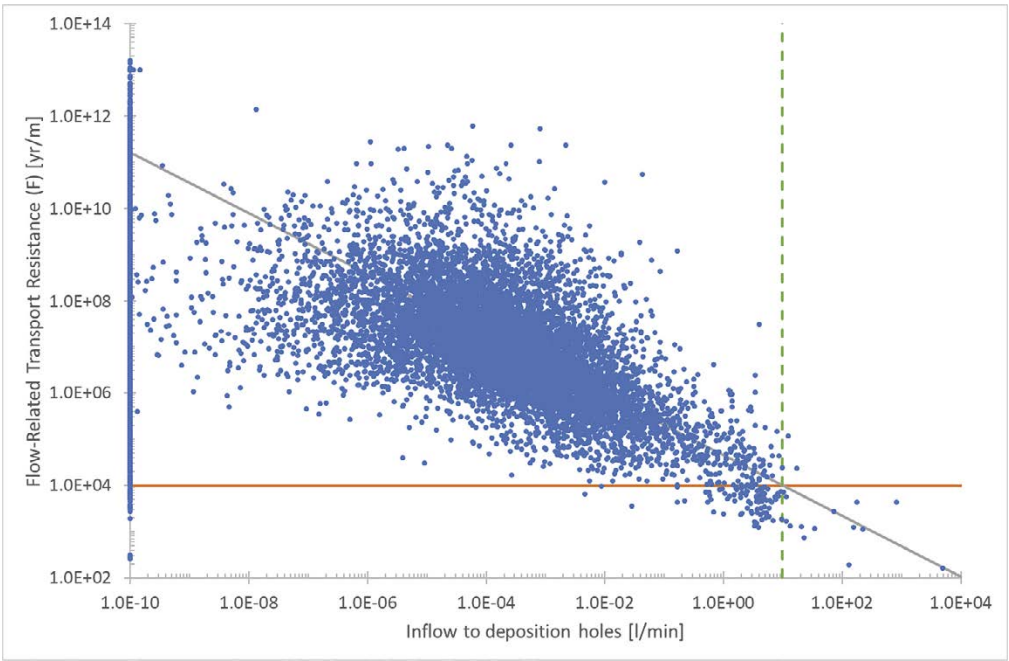

Figure 3-18. *Comparison between F and deposition hole inflows over 10 unconditioned realisations (blue dots). Negligible inflows are represented as 10^{-10} l/min. The orange line shows the inferred performance target for F, the grey line is an approximate correlation line, and the green dashed line where they meet gives the inferred inflow limit.*

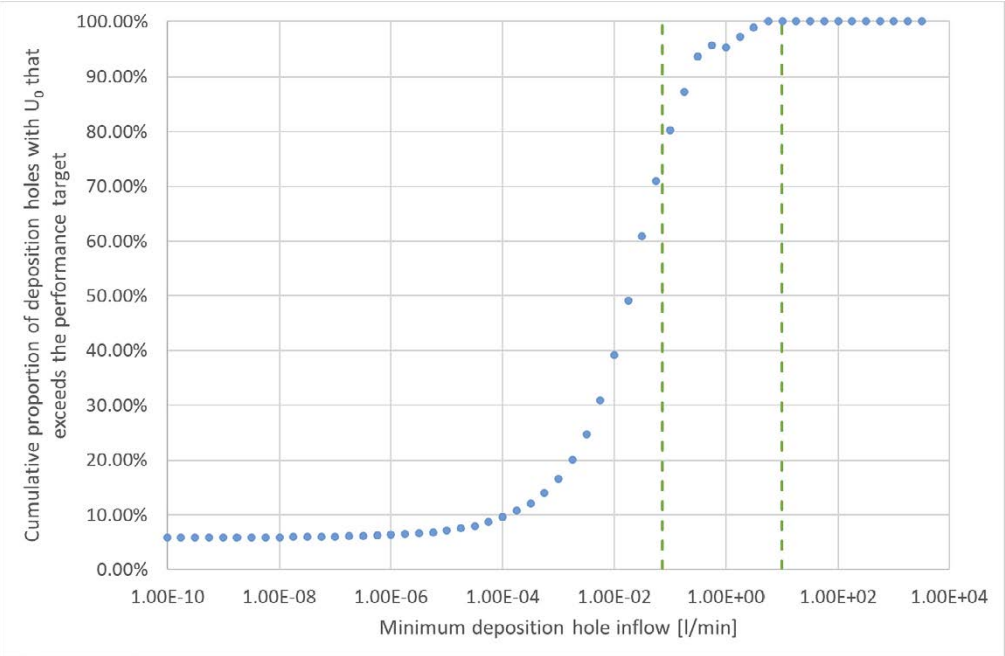

Figure 3-19. *Cumulative proportion of deposition holes with a given inflow that are associated with deposition hole positions where U_0 exceeds the post-closure performance target of 1 l/(yr·m). The vertical green dotted lines give the inferred rejection criteria for specific capacity based on U_0 (left) and F (right).*

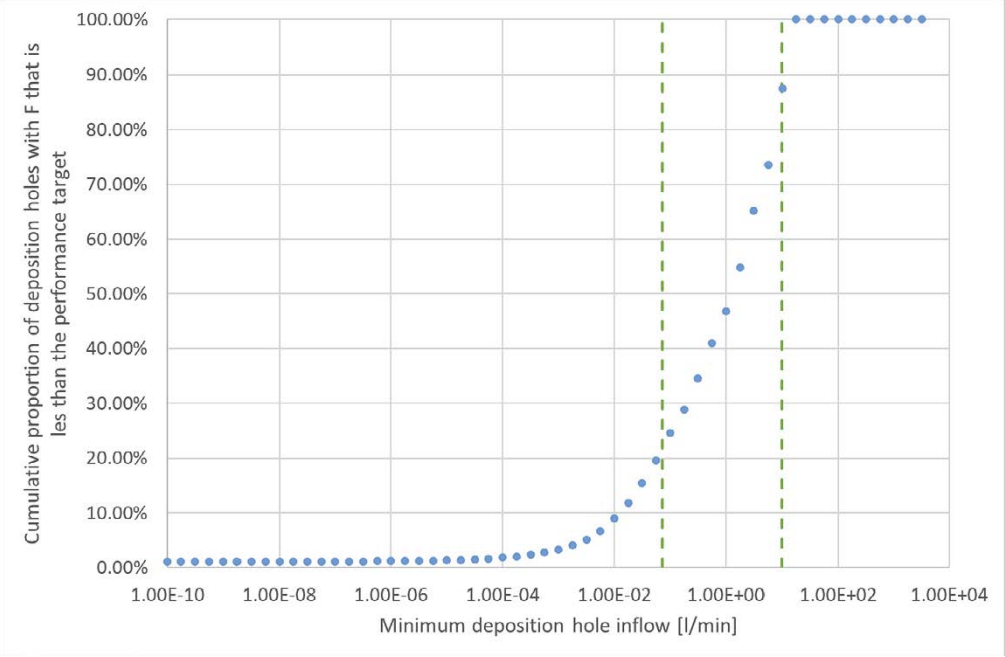

Figure 3-20. *Cumulative proportion of deposition holes with a given inflow that are associated with deposition hole positions where F is less than the post-closure performance target of 10^4 yr/m. The vertical green dotted lines give the inferred rejection criteria for specific capacity based on U_0 (left) and F (right).*

4 Calculation with conditional simulation

The second phase of work is to determine similar correlations to those found in Chapter 3, but for models where fractures have been conditioned to a synthetic reality, i.e. a separate realisation of the same DFN. As these models are conditioned, predictions for a given deposition hole position may be also compared with the results for the same deposition hole position in the synthetic reality. This is useful because it means that post-closure flow in a deposition hole can be predicted from the geometry of the fractures observed within the associated pilot borehole, without any measurement of the flow to the pilot borehole.

It was found in Appleyard et al. (2018) that adding flow measures to the conditioning process provides some improvement in predictive power, as discussed in Subsection 4.1.1. However, this is offset by the large amount of time required to calculate the flow in every realisation in the library, particularly if the flow measure required is based on hydraulic testing. For a model of this size, conditioning using flow measurements does not currently justify the considerable computational cost.

The synthetic reality used here is an eleventh realisation of the DFN used for the work described in Chapter 3.

4.1 Conditioning the model

The conditioning calculations were carried out with an emphasis on ensuring that correct fracture connections between pilot boreholes are represented. This connectivity is prioritised over the precise details of the geometry of the fracture intersection, such as its angle and the location of its intersection with the pilot borehole (though the connectivity may in practice imply some of those details). It is considered particularly important for the connections between pilot boreholes made by large fractures to be correct, especially where they intersect many tunnels and pilot boreholes, because these are likely to be the fractures that are most important in distributing flow through the model. However, these are also the fractures that are hardest to match, partly because larger fractures are statistically rarer and partly because the large number of intersections places limits on the size and orientation of the fracture. These constraints would not exist for smaller fractures or fractures with few intersections with the repository openings.

To infer these large fractures, it is assumed that connections between intersections on neighbouring openings can be reliably inferred, but that other fracture-specific information on size or transmissivity is not generally available. It is also assumed that fracture intersections with excavated tunnels will not have been measured where they are less than 50 centimetres long, but that all intersections with pilot boreholes will have been mapped.

In a real scenario, fracture size is an important consideration in the siting of the repository. The repository openings must not intersect certain critical fracture structures or critical volumes, defined by factors including the fracture size and flow. These are described in Posiva SKB (2017). This may reduce the impact of large fracture structures in an application of this method during a construction phase.

The mechanisms for getting the correct connectivity for the large fractures included creating “large-fracture libraries”, containing only fractures larger than a given size. As described in Section 2.2, a large-fracture library contains only the larger fractures in the model, excluding the smaller ones. These libraries can be generated more quickly and are smaller per realisation than libraries containing all fractures.

It is necessary, though, to take account of the different number of realisations used to create fractures of different sizes to avoid biasing the selection. If large-fracture libraries are used, the overall size distribution of fractures in the library will be biased toward the large fractures, and the probability of choosing the larger fractures must be reduced to compensate. This probability will be based on the number of realisations of fractures generated for each range of fracture sizes, and these are given in Table 4-1.

Table 4-1. Total number of realisations of fractures generated for the library in each range of fracture sizes.

Fracture effective radius range	Number of realisations
0.28 m – 5.64 m	6000
5.64 m – 56.4 m	24000
56.4 m – 564 m	74000

Secondly, the closeness-of-fit function mentioned in Section 2.2 and described in detail in Appendix B of Appleyard et al. (2018) was deliberately set up in a way that allows fractures that are relatively dissimilar to those implied by the observation. This helps because a fracture that has the correct connectivity would be disallowed if it does not match sufficiently in terms of closeness-of-fit. Loosening the closeness-of-fit requirements means that if a fracture exists that has the correct connectivity, it should be chosen.

Finally, one fracture was found in the synthetic reality for block 3 that had an effective radius of 523.5 metres and created a total of 82 intersections to be matched on 17 tunnels and 60 pilot boreholes in the repository layout. This fracture is shown in Figure 4-1.

This fracture creates a problem because it is large enough to be in the end of the tail of the size distribution and because the large number of intersections put significant limits on the sizes and orientations of fractures from the library that could be used to match it. The fracture's size means that it is likely to be very important to the flow characteristics of this part of the repository, but it is unrealistic to expect a suitable match to be found in conditioning without making the library substantially larger. However, a fracture of this size and significance is likely to be detected in a real repository and would probably be treated deterministically in modelling. For this reason, the fracture was removed from the conditioning and added as a deterministic feature in the relevant models.

In this model, this is the only fracture that was added deterministically, because it was the only fracture of this size and significance that intersected the tunnels and pilot boreholes whose intersections were mapped. The fact that the fracture intersects the side of the model region is not ideal, and the fact that such fractures exist in this model would suggest that it would be of benefit to extend the model regions used for repository-scale models (particularly by combining the three blocks).

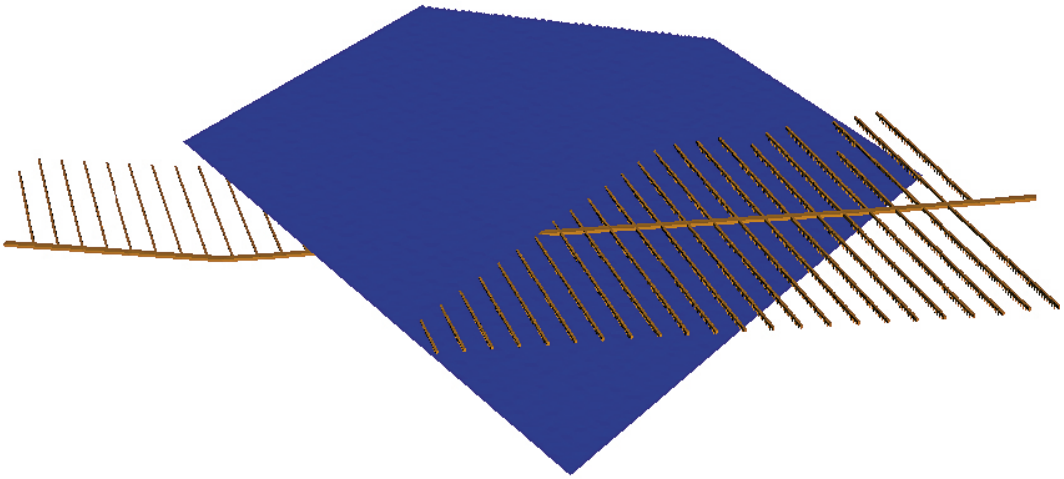

Figure 4-1. *A fracture of radius 523.5 metres (equivalent side length 928 metres) found in the synthetic reality, shown with the repository layout for block 3. The fracture intersects 77 separate tunnels and pilot boreholes. It appears to have a corner cut off because it also intersects the edge of the model region.*

4.1.1 Flow-based conditioning

It is useful to take a moment to discuss the choice not to use flow-based conditioning for this work. As described in Appleyard et al. (2018), the conditioning methodology in ConnectFlow can take account of flow metrics. However, this element of the conditioning process was not used in this work because to do so would be too computationally expensive.

There are also reasons to believe that the improvement in this model would not be as large as might be hoped. Including flow in the conditioning process does not change the fact that the process only acts on fractures that intersect the tunnel and leaves other fractures alone. The fractures in the final model that do not intersect the tunnels and pilot boreholes will not match the fractures in the real site, whose size and extent will never be completely known. As a result, there is no guarantee that even a perfect match from the library will provide a better match to observed flow found in the final conditioned realisation.

Instead, the improvement from flow-based conditioning arises because high-flow-bearing fractures in the library are likely to have different properties to low-flow-bearing fractures. Most significantly, there is normally a correlation between observed flow and fracture size in the library. This correlation can thus be used to infer fracture size in models where it is relatively unknown.

The models used for this work contain thousands of deposition holes. Direct fracture connections between pilot boreholes and deposition tunnels are assumed to be known. As a result, in most cases fracture size can already be partially inferred based on where the fracture intersects (or does not intersect) the deposition tunnels and pilot boreholes. In many cases, flow-based conditioning will add little significant additional information to this.

However, this only applies because of the way this model has been calculated, with geometric data available for all deposition hole positions at once. In practice, most of this information will be unknown, particularly during the early stages of repository construction. As a result, fracture sizes will not be so easy to infer from geometry, and flow-based conditioning will be more useful.

4.2 Flow measures

The correlations from Sections 3.2 and 3.3 (i.e. the correlations between flow measures) can be calculated for the conditioned models in the same way as for unconditioned models. This section documents the results from these correlations and compares them with the unconditioned results from Chapter 3.

4.2.1 Open repository conditions

The most useful correlation in open repository conditions is the comparison between the specific capacity and deposition hole inflow. For the conditioned calculations in this work, specific capacity derives from calculations based on PFL testing rather than injection testing. This is because the PFL testing proved more numerically stable and the final calculated specific capacities were the same (as demonstrated in Figure 2-2).

The specific capacity and deposition hole inflow are compared in Figure 4-2 (a repeat of Figure 3-6, the equivalent unconditioned result) and Figure 4-3 (the conditioned result). The two plots are broadly similar, but the most noticeable difference is that the conditioning has somewhat disrupted the correlation between deposition hole inflow and specific capacity at higher values of specific capacity and inflow. This appears to arise simply because the larger specific capacities do not appear in the synthetic reality, and so conditioning does not create the requisite fractures.

It is also noticeable that the higher specific capacities are separated from the main body of points. There are notably few pilot boreholes with calculated specific capacities between about 4×10^{-8} m^2/s and about 8×10^{-8} m^2/s in Figure 4-3.

The aim of the conditioning is to alter the DFN near the repository openings so that it closely matches the geometry in the synthetic reality. For example, if a pilot borehole is close to a deformation zone but is not intersected by any fractures, the conditioned model will not connect it to the deformation zone

in any realisation, and there will be no measurable flow in any realisation. In the unconditioned model, the ten realisations will be independent of one another and will likely include some versions with connectivity to the deformation zone. It is likely that this is the explanation for the gaps in the specific capacities and for the reduced number of pilot boreholes and deposition holes with high flows.

The overall effect of these differences is to make the correlation appear somewhat worse in the conditioned case than in the unconditioned case. The reason for this seems to be that the conditioning reduces the amount of variability between deposition hole positions. The variability is reduced because, while the results of the ten unconditioned realisations are independent of one another, the ten conditioned realisations each have fractures that are constrained to approximately match the traces found in the synthetic reality. While the fractures created in each deposition hole position may vary significantly between unconditioned realisations, in the conditioned realisations they should be similar in all realisations.

One might reasonably expect that reduced variability would push the data toward the correlation line, but this does not appear to happen. The results with specific capacity between about 10^{-12} m^2/s and 10^{-8} m^2/s are quite similar between the two realisations. However, the best correlation in the unconditioned case in Figure 4-2 is at the top end of the distribution. This correlation is not found to the same degree in Figure 4-3, and this may be caused by the fact that the conditioned model has relatively few deposition hole positions with very high deposition hole inflow and pilot borehole specific capacity. In addition, the correlation between the specific capacity in the conditioned model and the specific capacity in the synthetic reality is relatively poor, as discussed in Subsection 4.3.1.

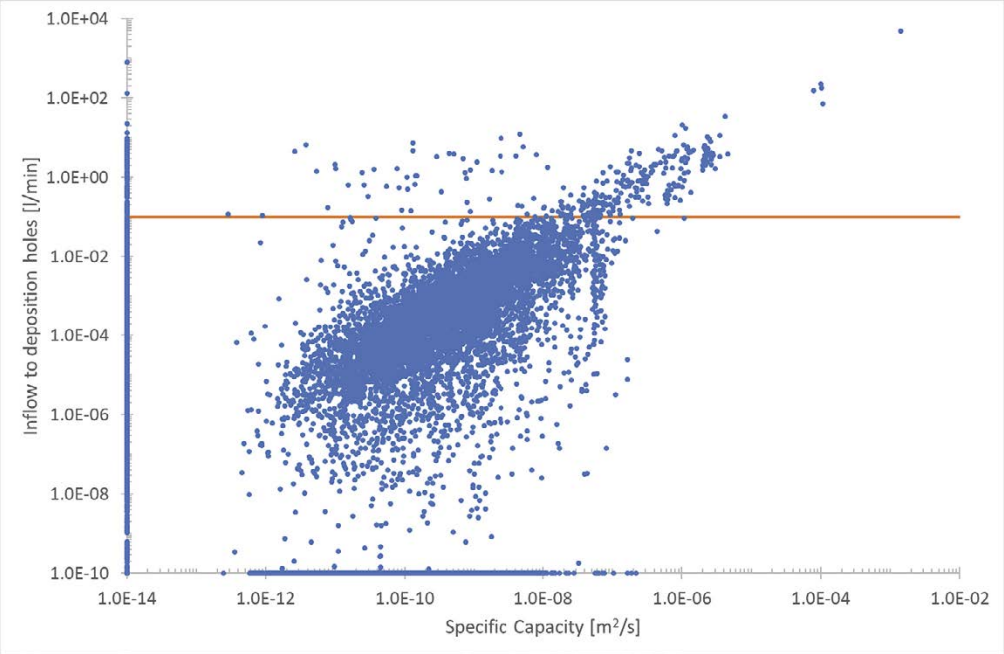

Figure 4-2. *Repeat of Figure 3-6. Comparison between inflow into deposition holes and specific capacity from injection tests in pilot boreholes over 10 unconditioned realisations (blue dots). Negligible inflows are represented as 10^{-10} l/min, and negligible specific capacities are represented as 10^{-14} m^2/s. The orange line indicates the existing hydraulic rejection criterion for flow into deposition holes (0.1 l/min).*

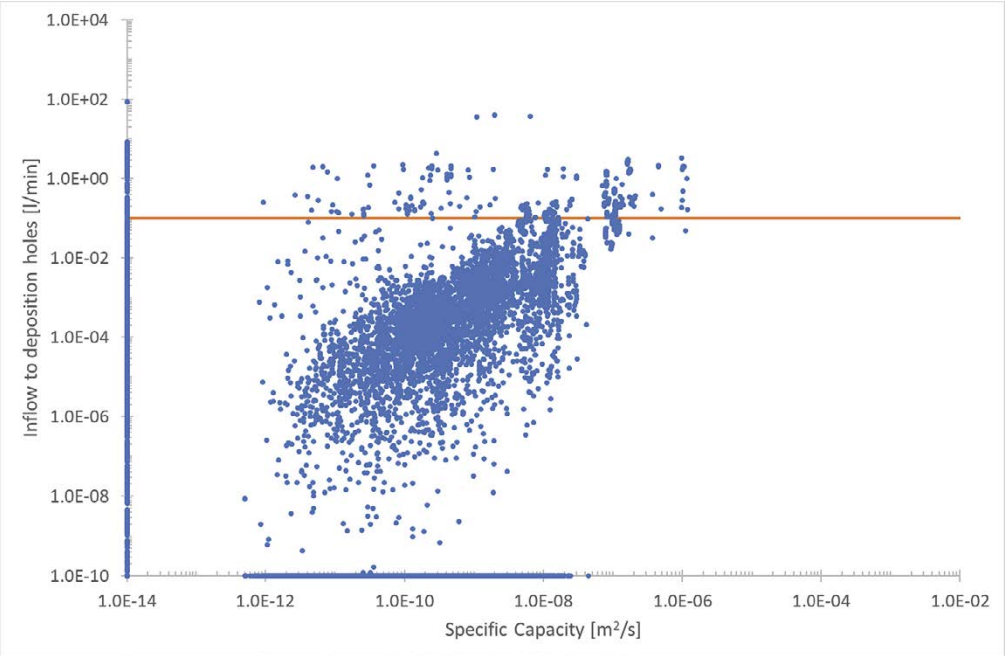

Figure 4-3. *Comparison between inflow into deposition holes and specific capacity from PFL tests in pilot boreholes over 10 conditioned realisations (blue dots). Negligible inflows are represented as 10^{-10} l/min, and negligible specific capacities are represented as 10^{-14} m^2/s. The orange line indicates the existing hydraulic rejection criterion for flow into deposition holes (0.1 l/min).*

4.2.2 Correlations with post-closure performance measures

Similar conclusions to Section 4.2.1 may be reached when comparing specific capacity and deposition hole inflow with the post-closure performance measures U_0 and F.

The correlations between specific capacity and U_0 are found in Figure 4-4 (a repeat of Figure 3-7) for unconditioned data, and Figure 4-5 for conditioned data. The correlations between specific capacity and F are Figure 4-6 (repeating Figure 3-8) and Figure 4-7, for unconditioned and conditioned data respectively. In these correlations, the basic patterns found are that both distributions in the conditioned results are cut off at high specific capacity compared with the unconditioned results. This is the same pattern as found when comparing specific capacity and deposition holes inflow in Section 4.2.1. The effect is that the overall correlation is not as strong as in the unconditioned model.

The correlations between deposition hole inflow and U_0 and F are also presented here. Correlations between deposition hole inflow and U_0 are shown in Figure 4-8 (which repeats Figure 3-9) for unconditioned data, and Figure 4-9 for conditioned data. Correlations between deposition hole inflow and F are shown in Figure 4-10 (which repeats Figure 3-10) and Figure 4-11 for unconditioned and conditioned data respectively. Similar conclusions apply for these correlations as for the correlations with specific capacity, though to a much lesser extent. As a result, other than the relatively lack of points at high inflow and high U_0, the correlations appear to be broadly similar to those found in the unconditioned case. They are neither significantly better nor significantly worse. This may suggest that the variation in other measures with respect to specific capacity is the cause of the poorer correlations with those measures.

As the correlations with unconditioned realisations are generally better than with conditioned realisations, this section does not proceed to infer limits from the conditioned calculations.

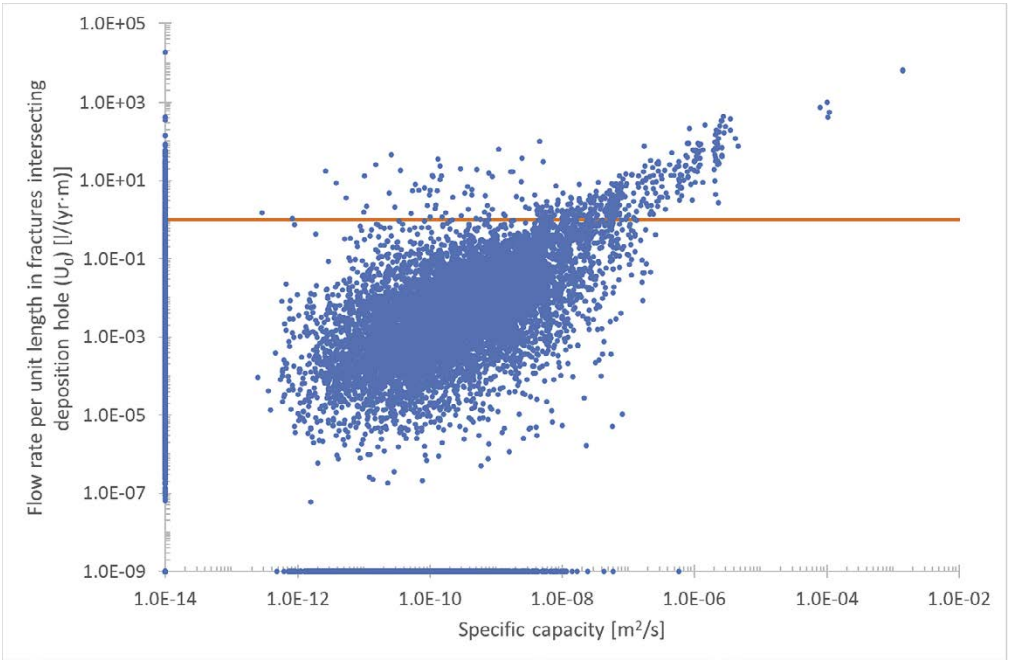

Figure 4-4. *Repeat of Figure 3-7. Comparison between pilot borehole specific capacity and U_0 over 10 unconditioned realisations (blue dots). Negligible values of U_0 are included as 10^{-9} l/(yr·m), and negligible specific capacities are represented as 10^{-14} m^2/s. The orange line indicates the post-closure performance target for U_0 of 1 l/(yr·m).*

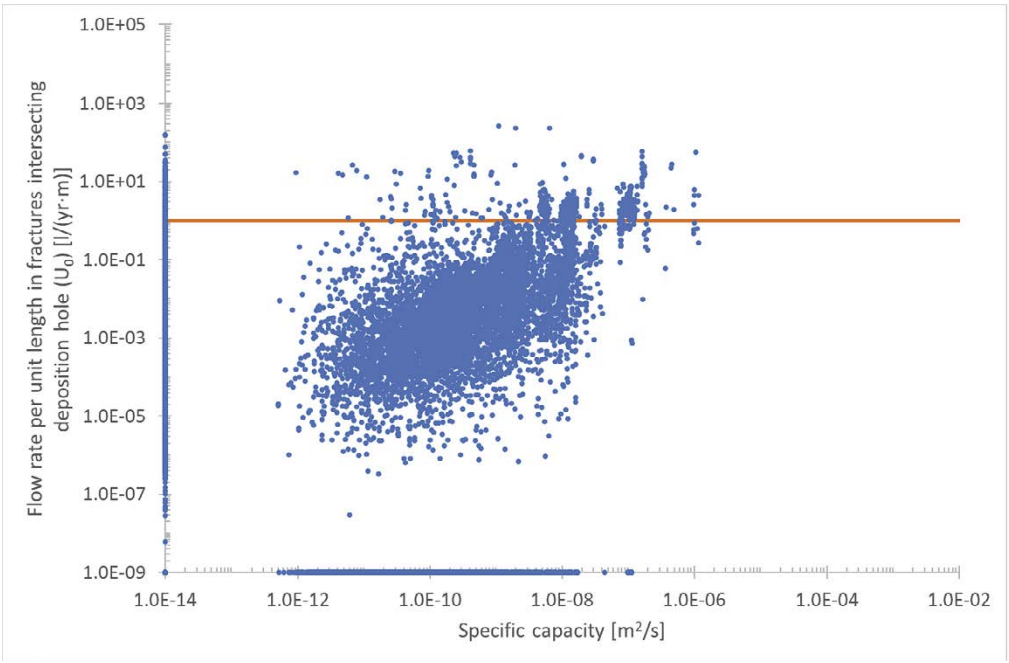

Figure 4-5. *Comparison between pilot borehole specific capacity and U_0 over 10 conditioned realisations (blue dots). Negligible values of U_0 are included as 10^{-9} l/(yr·m), and negligible specific capacities are represented as 10^{-14} m^2/s. The orange line indicates the post-closure performance target for U_0 of 1 l/(yr·m).*

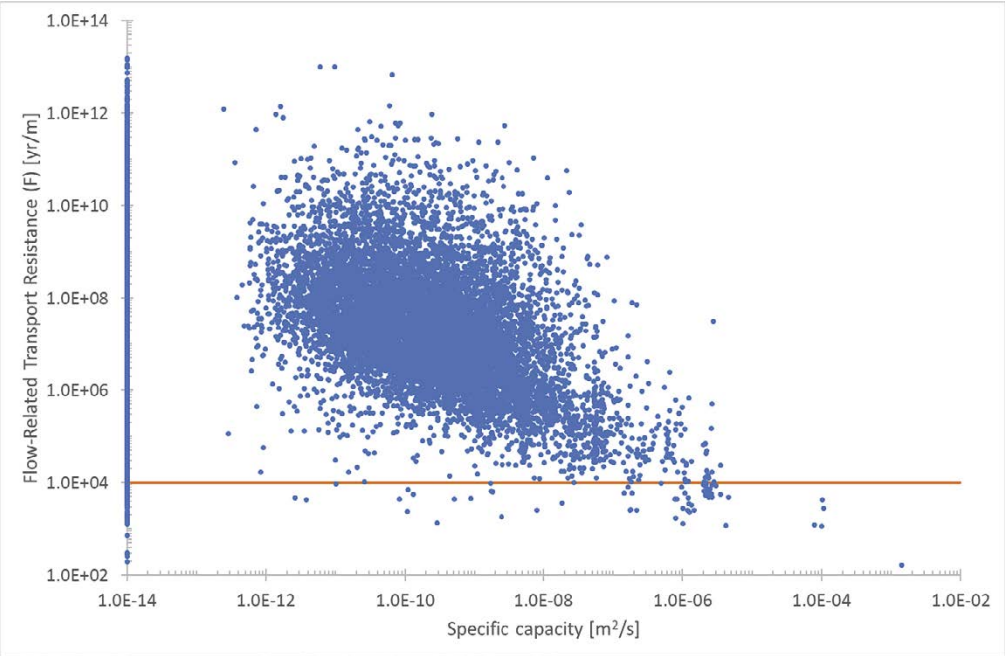

Figure 4-6. *Repeat of Figure 3-8. Comparison between pilot borehole specific capacity and F over 10 unconditioned realisations (blue dots). Negligible specific capacities are represented as 10^{-14} m^2/s. The orange line indicates the post-closure performance target for F of 10^4 yr/m.*

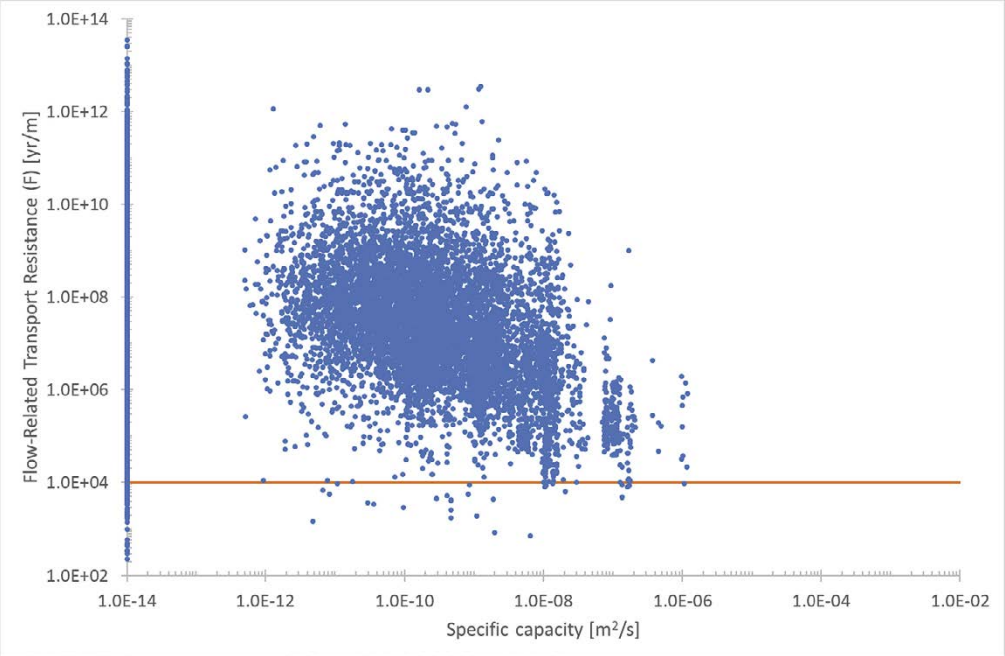

Figure 4-7. *Comparison between pilot borehole specific capacity and F over 10 conditioned realisations (blue dots). Negligible specific capacities are represented as 10^{-14} m^2/s. The orange line indicates the post-closure performance target for F of 10^4 yr/m.*

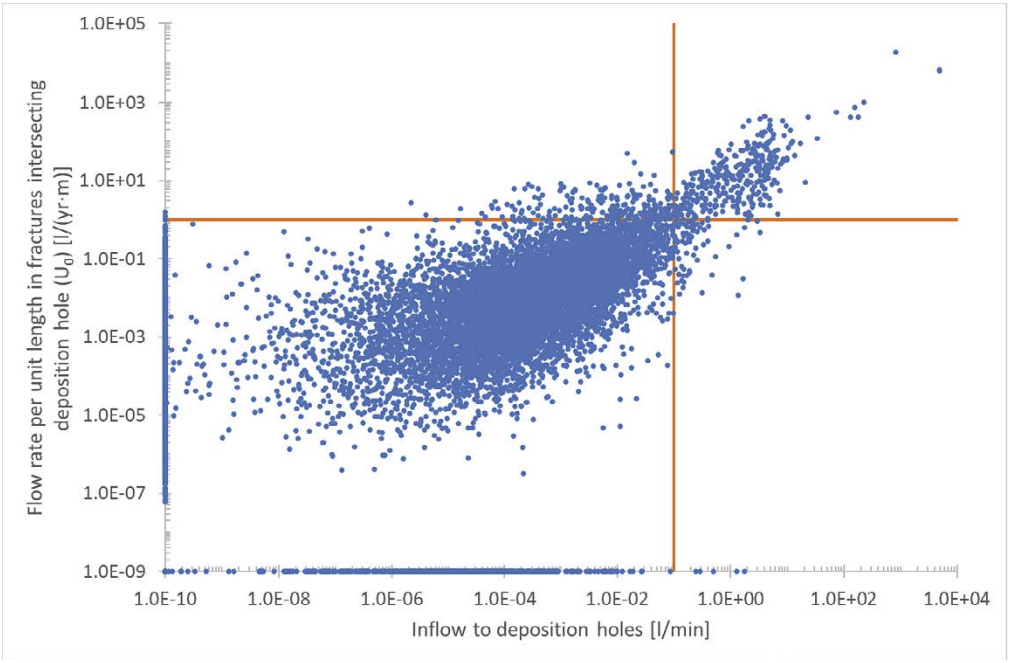

Figure 4-8. *Repeat of Figure 3-9. Comparison between deposition hole inflow and U_0 over 10 unconditioned realisations (blue dots). Negligible values of U_0 are represented as 10^{-9} l/(yr·m), and negligible inflows are represented as 10^{-10} l/min. The horizontal orange line indicates the post-closure performance target of 1 l/(yr·m); the vertical orange line indicates the existing hydraulic rejection criterion of inflow 0.1 l/min.*

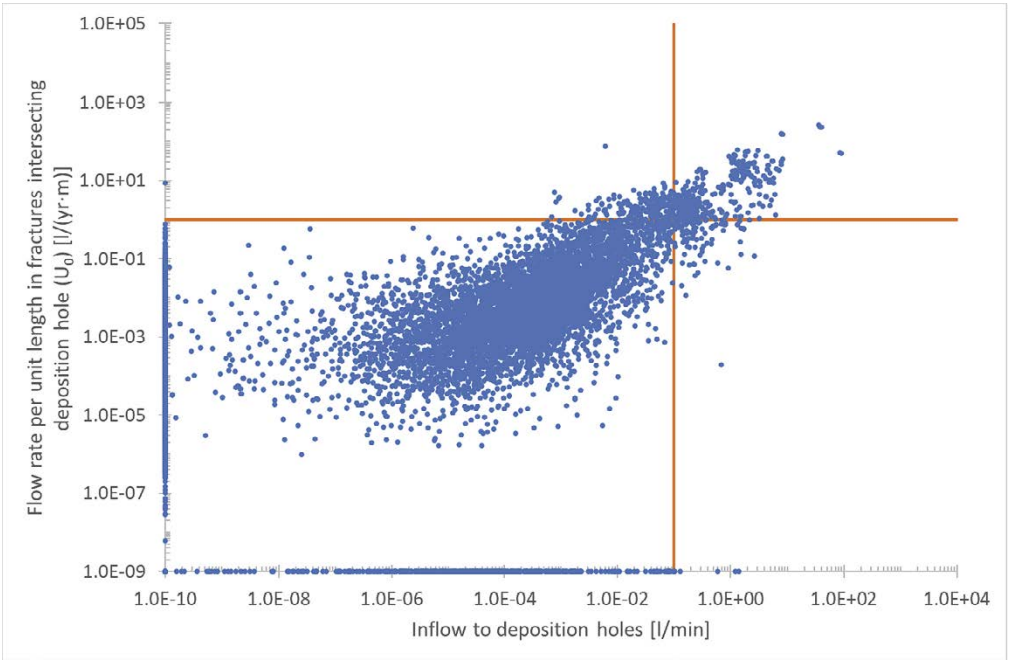

Figure 4-9. *Comparison between deposition hole inflow and U_0 over 10 conditioned realisations (blue dots). Negligible values of U_0 are represented as 10^{-9} l/(yr·m), and negligible inflows are represented as 10^{-10} l/min. The horizontal orange line indicates the post-closure performance target of 1 l/(yr·m); the vertical orange line indicates the existing hydraulic rejection criterion of inflow 0.1 l/min.*

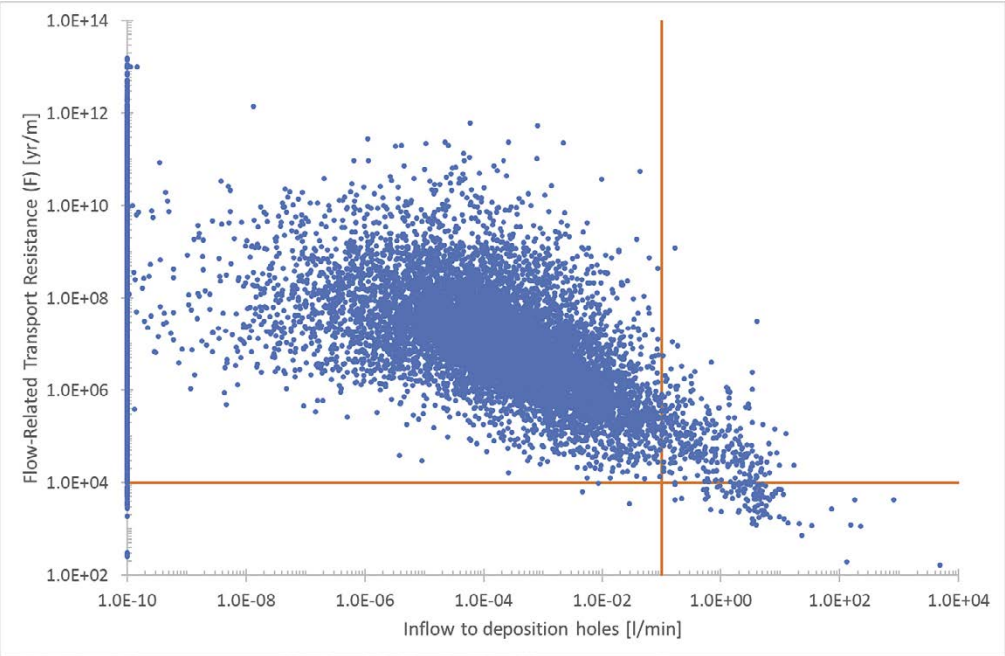

Figure 4-10. *Repeat of Figure 3-10. Comparison between deposition hole inflow and F over 10 unconditioned realisations (blue dots). Negligible inflows are included as 10^{-10} l/min. The horizontal orange line indicates the post-closure performance target of 10^4 yr/m; the vertical orange line indicates the existing hydraulic rejection criterion of inflow 0.1 l/min.*

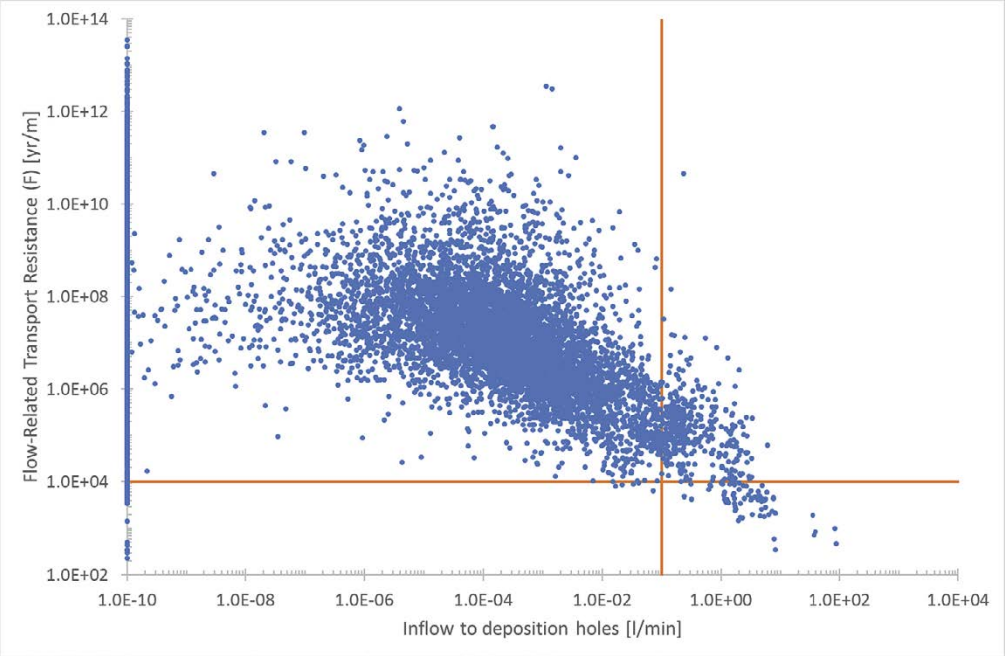

Figure 4-11. *Comparison between deposition hole inflow and F over 10 conditioned realisations (blue dots). Negligible inflows are included as 10^{-10} l/min. The horizontal orange line indicates the post-closure performance target of 10^4 yr/m; the vertical orange line indicates the existing hydraulic rejection criterion of inflow 0.1 l/min.*

4.3 Comparing with synthetic reality

While conditioning affects the fractures connected to a specific pilot borehole, comparing pilot borehole and deposition hole inflows (or other flow measures) as described above continues to make predictions for an ensemble of deposition hole positions in the same way as for unconditioned models. For example, a pilot borehole with a given inflow is likely to have a similar or greater inflow when it is excavated to a deposition hole.

In general, the goal of conditioning is to make predictions for specific deposition hole positions. It is thus useful to compare the flow measures predicted for individual deposition hole positions with the flow in those deposition hole positions in the synthetic reality. In the unconditioned case, there should be no significant correlation between the two, but in the conditioned case there should be at least some correlation.

As before, this section begins by comparing data from quantities that can be measured in open repository conditions (i.e. inflow and specific capacity) and moves on to post-closure performance measures U_0 and F. In the third subsection, the conditioned results are combined in different ways. Combining the conditioned realisations potentially allows predictions to be made for specific deposition hole positions based solely on the conditioned calculations.

4.3.1 Open repository conditions

In comparing conditioned data with the synthetic reality, the results for open repository conditions are predicting measurable data. The aim is to infer flow from the geometry of intersections of fractures found in a pilot borehole, and to compare that flow with the flow observed in the same deposition hole position in the synthetic reality. This comparison may be useful as a means of improving confidence in later predictions of post-closure flow quantities that cannot be measured directly.

The comparison between calculated pilot borehole inflows and those observed in the synthetic reality are given Figure 4-13. For calculated deposition hole inflow, comparisons are given by Figure 4-15. For calculated specific capacity, comparisons are given by Figure 4-17.

There is no reason why flows from an unconditioned calculation will be correlated at all with the observed flows from the synthetic reality for individual deposition holes. However, it is useful to confirm this result to demonstrate that the conditioning adds value. Unconditioned results for these three calculations are given in Figure 4-12 (pilot borehole inflows), Figure 4-14 (deposition hole inflows) and Figure 4-16 (specific capacity).

Each result for a deposition hole position in the synthetic reality is compared with ten calculated results. When plotted, the results from a given position will be arranged as a vertical line, as all ten results will be associated with the same measurement in the synthetic reality. In practice, it is likely that some results will be found on the x-axis (meaning that the predicted flow was insignificant but the flow in the synthetic reality was significant), or the y-axis (meaning that the flow in the synthetic reality was insignificant but the predicted flow was significant) because of the differences in the unconditioned background fracture network.

As in Chapter 3, the minimum inflow on these plots that is considered significant is 10^{-10} l/min, equivalent to 1 millilitre of flow every 19 years. This limit is set to allow almost all flows to be included in the analysis, though it is far lower than could be realistically measured in a pilot borehole or deposition hole in a repository.

As anticipated, the unconditioned plots (Figure 4-12, Figure 4-14 and Figure 4-16) do not show any significant correlation between the calculated flows and the flows from the synthetic reality. The only real exception is that there is a cluster of four deposition holes in the top right of Figure 4-14. The main source of flow to these four deposition holes is a nearby deterministic deformation zone rather than the random fracture network. Since the deterministic deformation zone is present in all unconditioned realisations, similar behaviour is observed in each realisation for those deposition holes that are close to it.

The conditioned inflow plots (Figure 4-13 and Figure 4-15) do show a significant correlation between the predicted inflows and the inflows from the synthetic reality. For specific capacity, the correlation on Figure 4-17 is better than Figure 4-16 but is still relatively marginal. This is a useful result partly

because correlations are still found in the equivalent comparisons for deposition hole inflow in Figure 4-15 and for U_0 Subsection 4.3.2. The result implies that a set of relatively unsuccessful predictions for specific capacity does not mean that predictions for deposition hole inflow or for U_0 will be similarly unsuccessful.

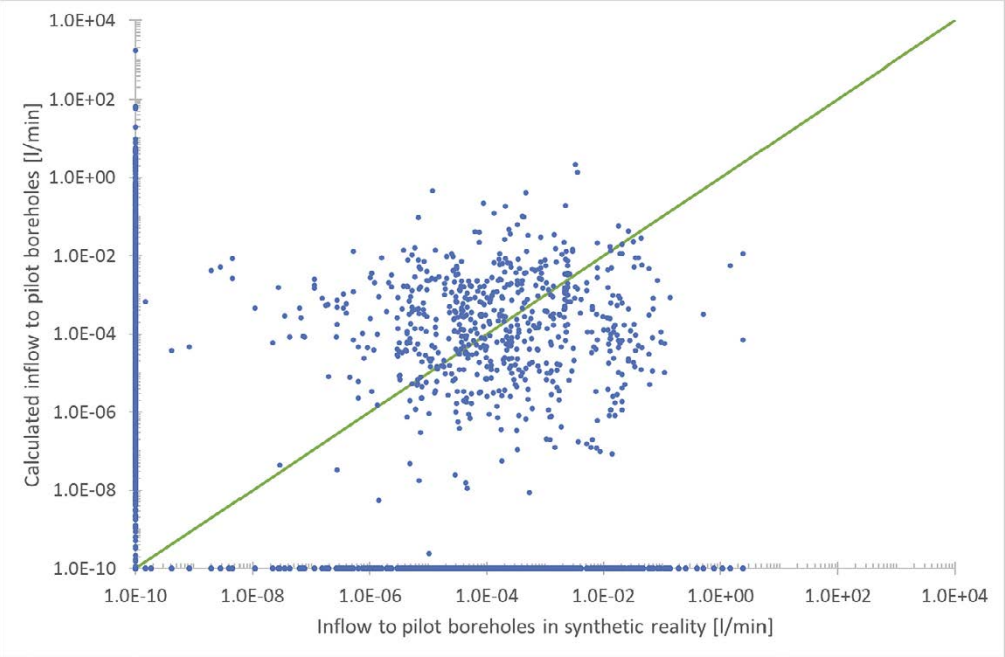

Figure 4-12. *Comparison between pilot borehole inflows from the synthetic reality and from 10 unconditioned realisations (blue dots). Negligible inflows are represented as 10^{-10} l/min. The green line is where the inflow is equivalent in the two cases.*

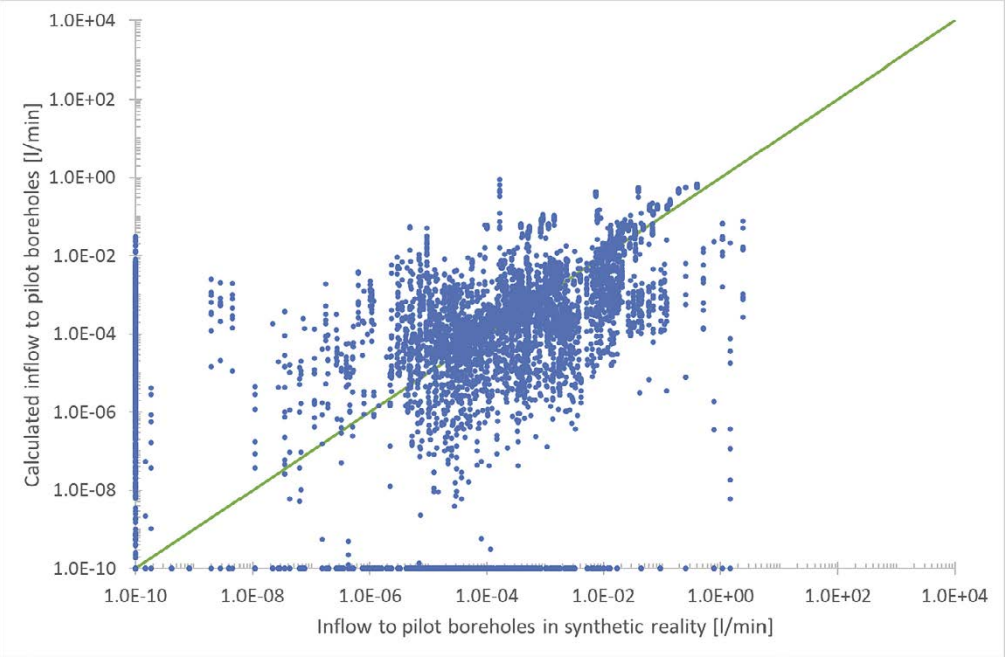

Figure 4-13. *Comparison between pilot borehole inflows from the synthetic reality and from 10 conditioned realisations (blue dots). Negligible inflows are represented as 10^{-10} l/min. The green line is where the inflow is equivalent in the two cases.*

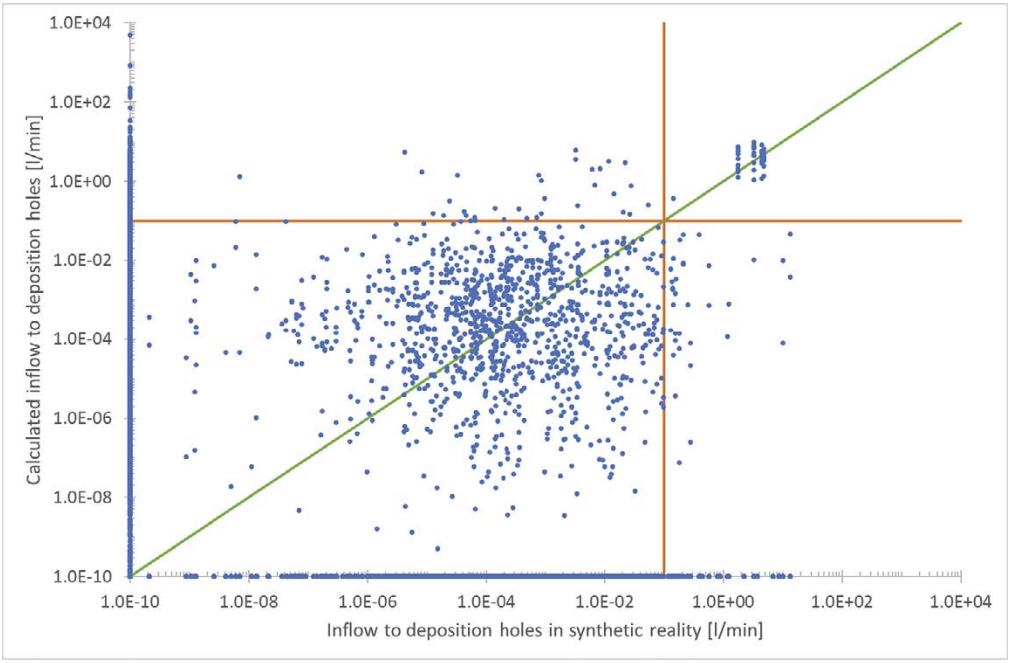

Figure 4-14. *Comparison between deposition hole inflows from the synthetic reality and from 10 unconditioned realisations (blue dots). Negligible inflows are represented as 10^{-10} l/min. The green line is where the inflow is equivalent in the two cases. The orange lines show the existing hydraulic rejection criterion of inflow to a deposition hole of 0.1 l/min, included for context.*

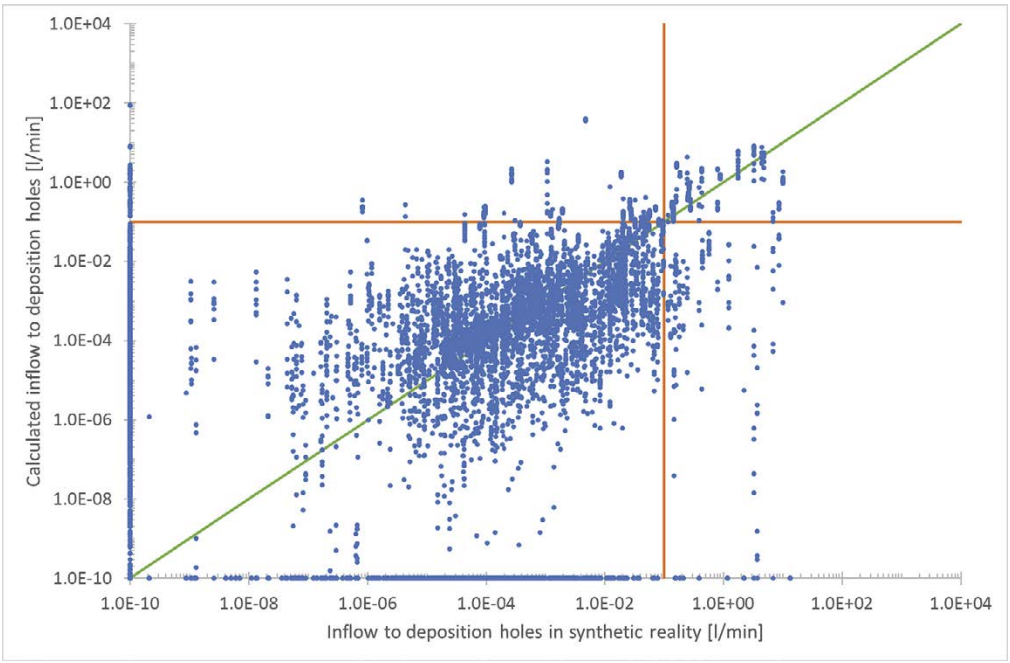

Figure 4-15. *Comparison between deposition hole inflows from the synthetic reality and from 10 conditioned realisations (blue dots). Negligible inflows are represented as 10^{-10} l/min. The green line is where the inflow is equivalent in the two cases. The orange lines show the existing hydraulic rejection criterion of inflow to a deposition hole of 0.1 l/min, included for context.*

This relatively poor correlation in Figure 4-17 may be the source of the relatively poor correlations with specific capacity found in Section 4.2. In that section, it was noted that the correlations between specific capacity and post-closure performance measures was worse for conditioned models than for unconditioned models. The equivalent correlations between deposition hole inflows and post-closure performance measures in conditioned models were broadly similar to those in unconditioned models. If the specific capacity is not well predicted by the conditioning, then it may be unsurprising that correlations reliant on that prediction are also less successful.

All three plots based on conditioned data are also are significantly denser in terms of number of visible points. This is not because there are any more deposition hole positions considered, but because the conditioned case is considerably more successful at predicting whether any flow will be detected. The equivalent points on the plots with unconditioned data are found on the x- and y-axes.

The improvement in detection rate can be quantified in terms of number of deposition hole positions that non-negligible calculated flow that are associated with holes from the synthetic reality with non-negligible flow. For example, there are 841 deposition holes with significant inflows in the synthetic reality, and thus 8 410 measurements, to compare (because there are ten realisations of the calculated model per deposition hole position). Of these, 1 225 (14.6 %) have significant inflow according to the unconditioned calculation. A further 8 438 deposition holes also have significant inflow according to the calculation, that does not exist in the synthetic reality.

In the conditioned case, 5 270 (68.0 %) of these 8 410 measurements have significant inflow according to the calculation. There are an additional 2 140 deposition holes with significant inflow according to the calculation, but no significant inflow in the synthetic reality. These numbers obviously represent a significant improvement upon the unconditioned case.

4.3.2 Correlations with post-closure performance measures

It is useful to progress from the predictions for open repository conditions to predictions of post-closure performance targets U_0 and F, based on the calculated values from conditioned models. The aim is to use conditioned models to predict the performance measures in the synthetic reality. As the only information from the synthetic reality that is used in the conditioning is the geometry of the intersections between fractures and tunnels and pilot boreholes, predictions made do not rely on any attempt at measuring flow in any pilot borehole, or on any measurement from a deposition hole.

The correlation between U_0 from the conditioned calculation and from the synthetic reality is given by Figure 4-19. The equivalent plot based on the unconditioned calculation is Figure 4-18. Figure 4-19 demonstrates that there is a significant correlation between calculated values of U_0 and values from the synthetic reality. The correlation is not as good as that found, for example, between the deposition hole inflows and U_0 in Figure 3-9 and Figure 4-9, but any flow-based measure clearly relies on an accurate and reliable measurement of the flow in the pilot borehole or deposition hole, which is not necessarily easy to achieve in the field.

In terms of the number of predictions made, of 440 deposition holes with U_0 greater than 1 l/(yr·m) in the synthetic reality, 149 (33.9 %) also have U_0 greater than 1 l/(yr·m) in the conditioned realisations. An additional 370 deposition holes also have U_0 greater than 1 l/(yr·m) in the conditioned realisations that do not have high U_0 in the synthetic reality.

The plot based on the unconditioned calculation in Figure 4-18 shows no obvious correlation, and thus demonstrates the improvement made by the conditioned calculation. In this case, only 38 (8.6 %) of the 440 deposition holes with U_0 greater than 1 l/(yr·m) in the synthetic reality are predicted by the calculation. Of these, 35 come from the four deposition holes highlighted in Subsection 4.3.1, whose flow is significantly affected by a nearby deformation zone. There are also 529 deposition holes whose flow in the calculated realisation is greater than 1 l/(yr·m), but that do not have a similarly high flow in the synthetic reality.

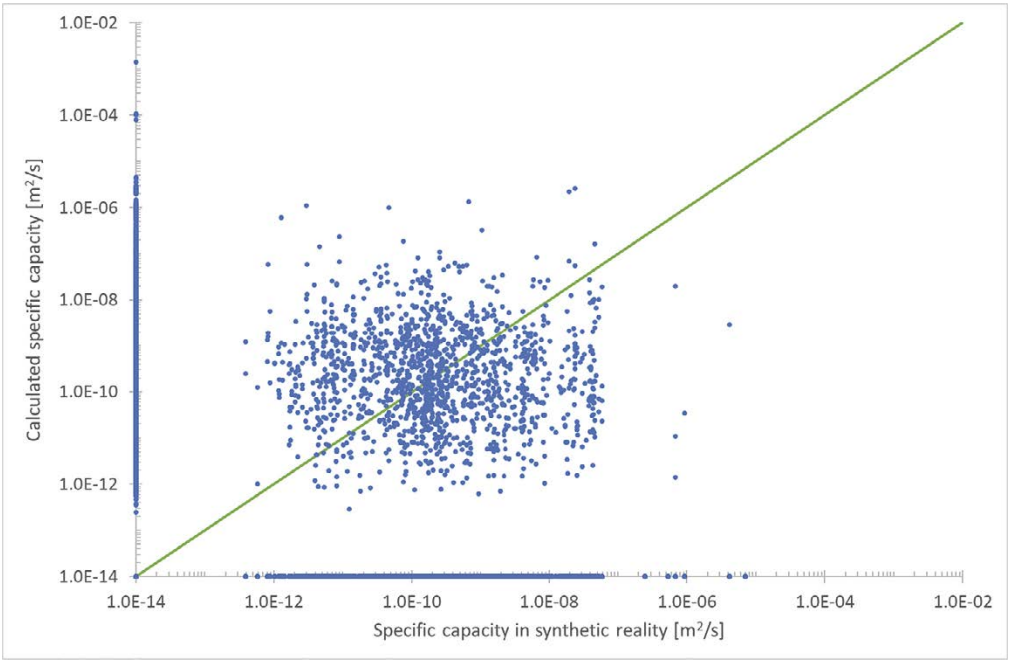

Figure 4-16. *Comparison between specific capacities from the synthetic reality and from 10 unconditioned realisations (blue dots). Negligible specific capacities are represented as 10^{-14} m^2/s. The green line is where the specific capacity is equivalent in the two cases.*

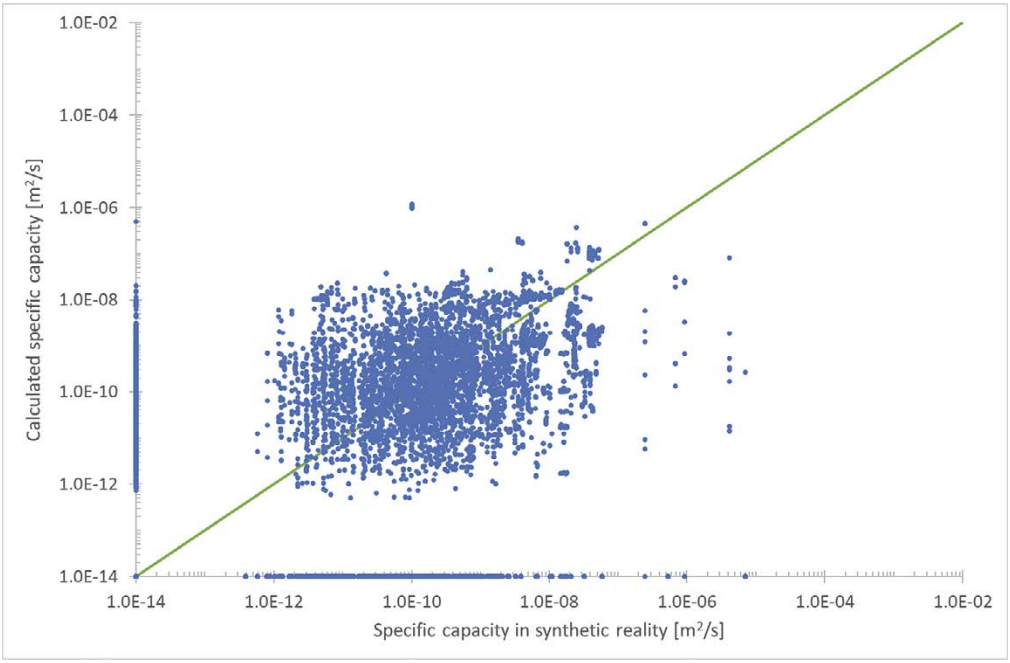

Figure 4-17. *Comparison between specific capacities from the synthetic reality and from 10 unconditioned realisations (blue dots). Negligible specific capacities are represented as 10^{-14} m^2/s. The green line is where the specific capacity is equivalent in the two cases.*

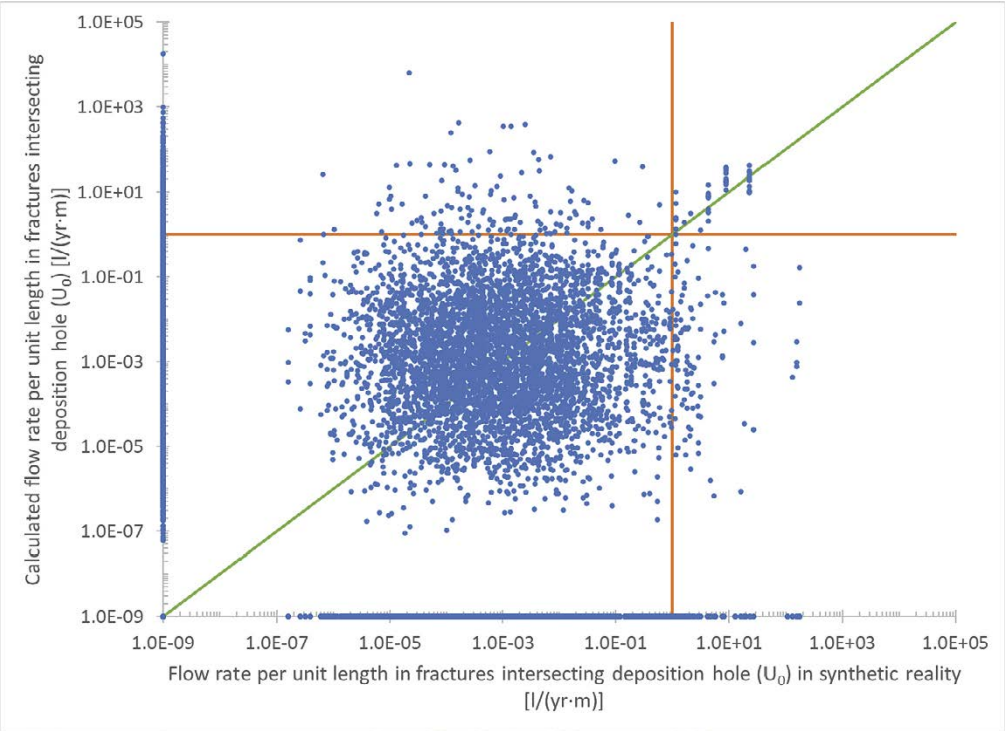

Figure 4-18. *Comparison between U_0 from the synthetic reality and from 10 unconditioned realisations (blue dots). Negligible values of U_0 are represented as 10^{-9} l/(yr·m). The green line is where U_0 is equivalent in the two cases. The orange lines show the post-closure performance target for U_0 of 1 l/(yr·m).*

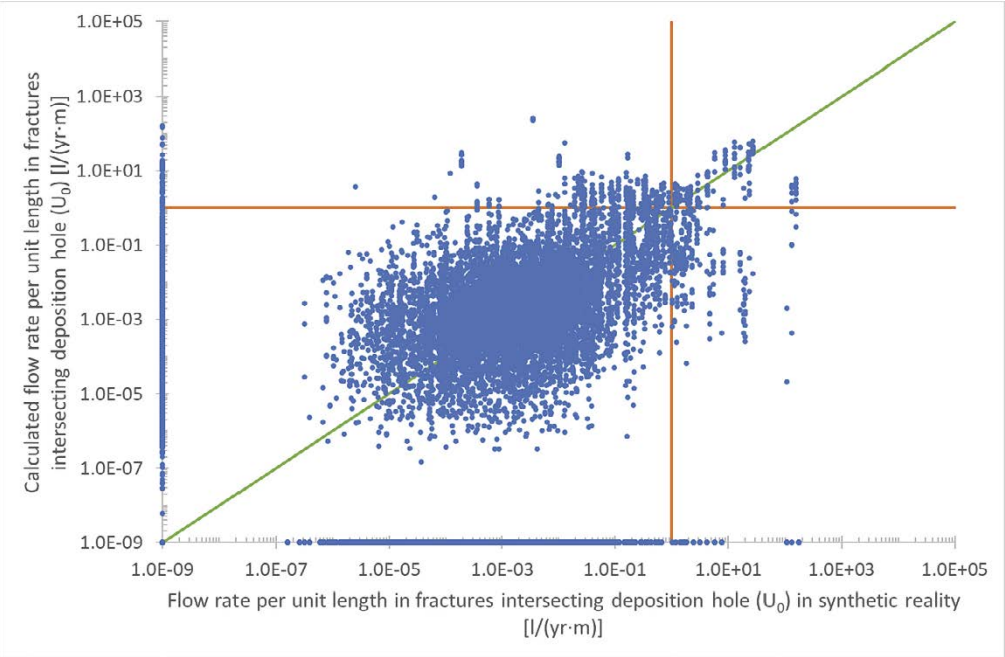

Figure 4-19. *Comparison between U_0 from the synthetic reality and from 10 conditioned realisations (blue dots). Negligible values of U_0 are represented as 10^{-9} l/(yr·m). The green line is where U_0 is equivalent in the two cases. The orange lines show the post-closure performance target for U_0 of 1 l/(yr·m).*

The correlation for the conditioned calculation of F is given by Figure 4-21. The equivalent correlation without conditioning is Figure 4-20. There is clearly no correlation visible at all in the unconditioned case, and there is some improvement in the conditioned case. However, the correlation is still relatively poor even in the conditioned case, and so it is difficult to see that predictions based on this calculation will be useful. This probably occurs because the conditioning acts only on the fractures that directly intersect the tunnel or pilot borehole for the deposition hole, while the F depends on all the fractures between the engineered openings and the discharge location.

Perhaps unsurprisingly, there is little significant change in the number of deposition holes where F is successfully predicted in the conditioned results. In the conditioned case, 43 out of 200 results (21.5 %) associated with deposition holes with low F in the synthetic reality are also associated with deposition holes with low F in the calculated results. In the unconditioned case, this value is 42 out of 200 (21.0 %). In the conditioned case there are 75 deposition holes with calculated low F that do not have low F in the synthetic reality. In the unconditioned case this number is 92.

One might argue that conditioning that includes flow data from the synthetic reality might improve the correlations found for F. However, as discussed in Subsection 4.1.1, adding a flow measure does not change the fact that conditioning only acts on the fracture directly intersecting the deposition hole. While there will likely be some improvement from a better prediction of fracture size, the improvement is likely not to be as large as might be hoped.

In most circumstances, it is unlikely to be useful to compare the calculated values from one measure with the data for a different measure from the synthetic reality, because the results would be needlessly indirect. For example, there is no need to infer U_0 from realisations of calculated deposition hole inflows when U_0 can be calculated directly in those same realisations. However, given the relatively poor correlations for F seen in Figure 4-20 and Figure 4-21, it is potentially useful to investigate how well values of F from the synthetic reality are predicted by calculated values of U_0. These comparisons are shown in Figure 4-22 (unconditioned case) and Figure 4-23 (conditioned case). To help with comparison, the comparison between U_0 and F for the synthetic reality is overlaid on these plots in Figure 4-24 (unconditioned case) and Figure 4-25 (conditioned case). As would be anticipated, in the unconditioned case there is little correlation. What predictive power does exist can be attributed to the four deposition holes close to the deformation zone. In the conditioned case the correlation is clearly improved. In fact, it does not seem unreasonable to suggest that the calculated U_0 in a conditioned model is a better predictor of F than the calculated F is.

The numerical results bear this out. Of the 200 results associated with deposition holes with low F in conditioned models, 71 (35.5 %) are calculated to have U_0 greater than 1 l/(yr·m). While a further 448 deposition holes without low F also have U_0 greater than 1 l/(yr·m), a significant number of these deposition holes will still need to be screened out because they are associated with deposition holes with high U_0 in the synthetic reality.

4.3.3 Combining calculated results

A problem with the correlations listed in Subsections 4.3.1 and 4.3.2 is that, even where there is a useful correlation between the conditioned data and data from the synthetic reality, they do not necessarily clearly predict which deposition holes have problematic post-closure flow characteristics. The most obvious way to resolve this would be to say that if all the conditioned realisations indicate that a deposition hole position should not be used then it should not be used. However, this leaves it unclear how to handle cases where some conditioned realisations suggest that the deposition hole position should not be used and others indicate that there is no problem. As such, a more nuanced method is required.

In some ways having a range of results for each deposition hole position is a good thing, because it gives an idea of the uncertainty of the prediction. However, it is probably useful to combine the results for each deposition hole position into a single measure that can be used to give a clear answer as to whether that deposition hole position should be accepted or rejected.

There are a few other obvious methods for combining the results. One might, for example, consider the median or a ranked value from the ten calculated values for the deposition holes, or one might consider the arithmetic, geometric or harmonic mean value.

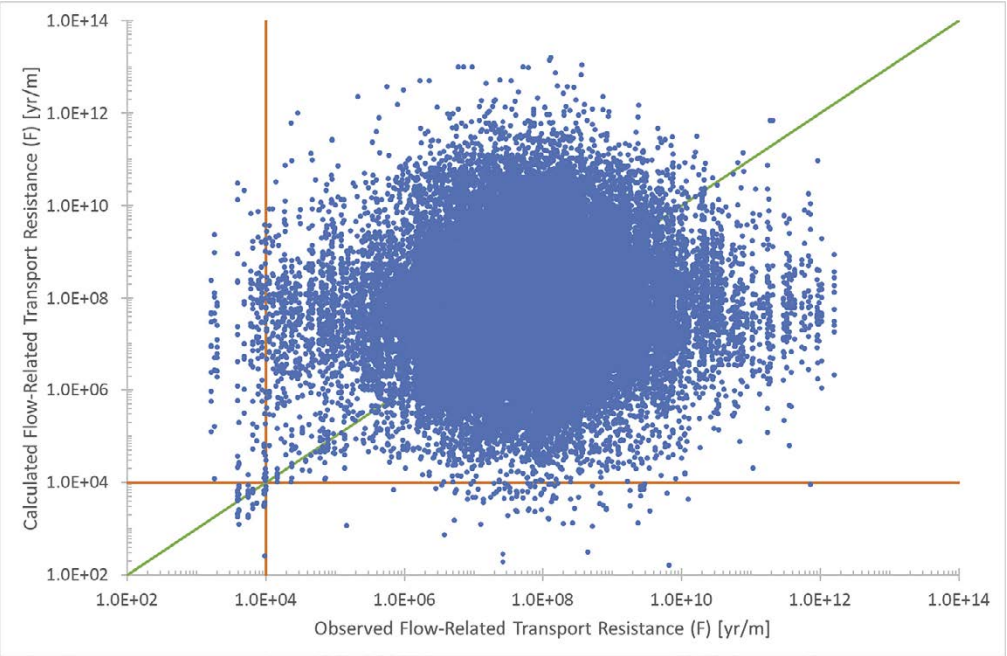

Figure 4-20. *Comparison between F from the synthetic reality and from 10 unconditioned realisations (blue dots). The green line is where F is equivalent in the two cases. The orange lines show the post-closure performance target for F of 10^4 yr/m.*

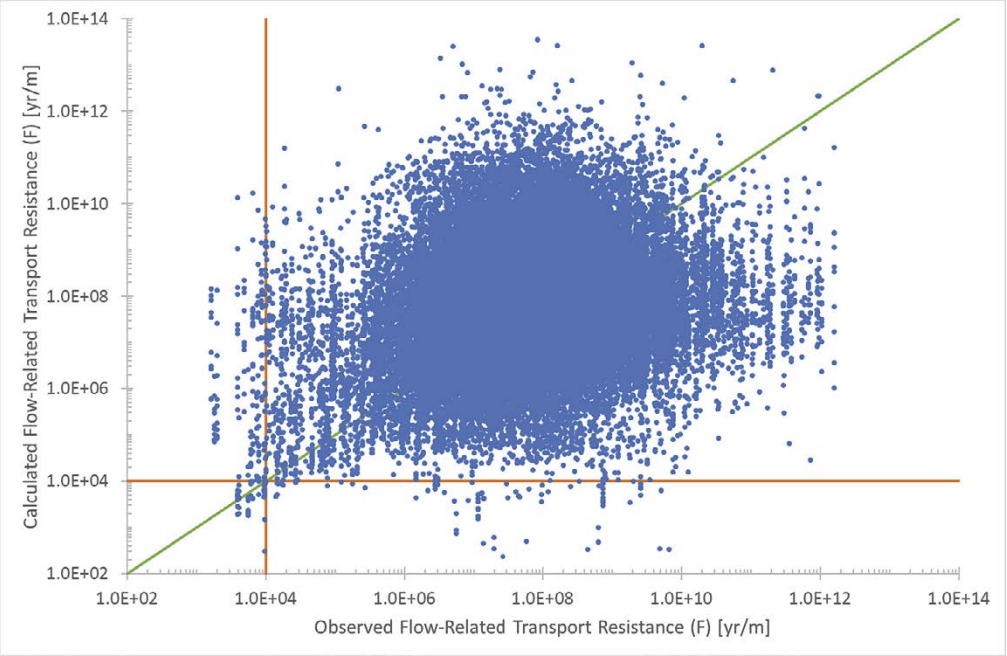

Figure 4-21. *Comparison between F from the synthetic reality and from 10 conditioned realisations (blue dots). The green line is where F is equivalent in the two cases. The orange lines show the post-closure performance target for F of 10^4 yr/m.*

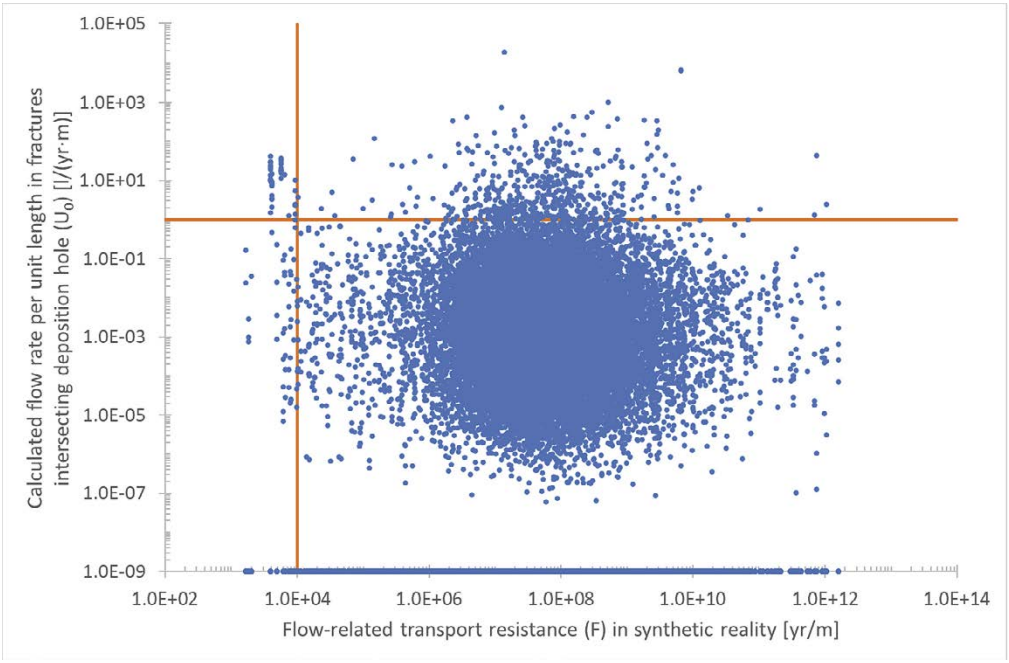

Figure 4-22. *Comparison between F from the synthetic reality and U_0 calculated from 10 unconditioned realisations (blue dots). The vertical orange line shows the post-closure performance target for F of 10^4 yr/m, and the horizontal orange line shows the post-closure performance target for U_0 of 1 l/(yr·m).*

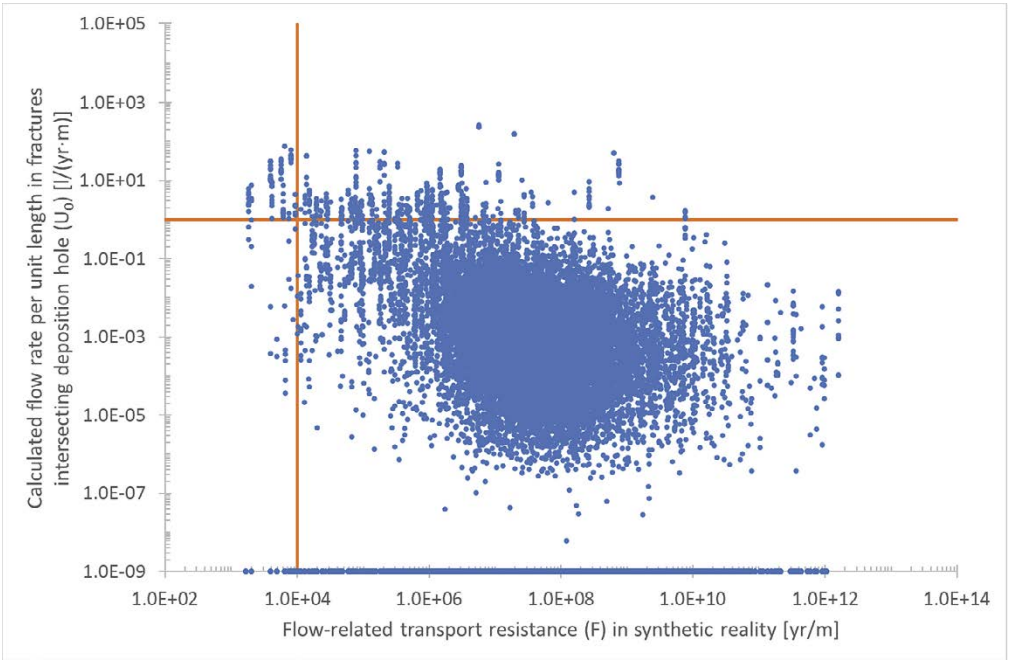

Figure 4-23. *Comparison between F from the synthetic reality and U_0 calculated from 10 conditioned realisations (blue dots). The vertical orange line shows the post-closure performance target for F of 10^4 yr/m, and the horizontal orange line shows the post-closure performance target for U_0 of 1 l/(yr·m).*

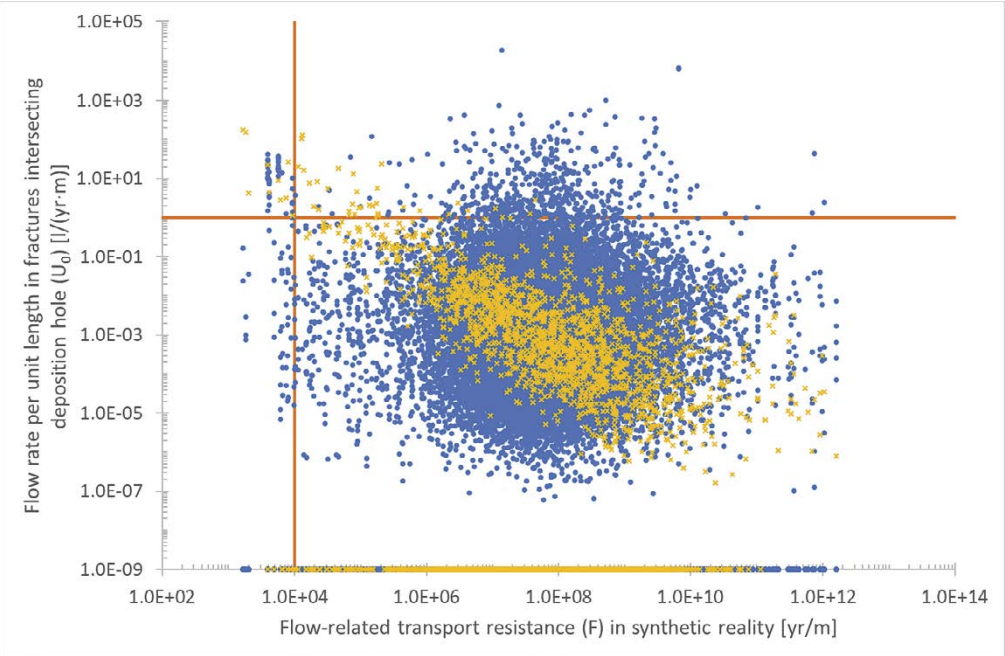

Figure 4-24. *Comparison between F from the synthetic reality and U_0 calculated from 10 unconditioned realisations (blue dots) and from the synthetic reality (yellow dots). The vertical orange line shows the post-closure performance target for F of 10^4 yr/m, and the horizontal orange line shows the post-closure performance target for U_0 of 1 l/(yr·m).*

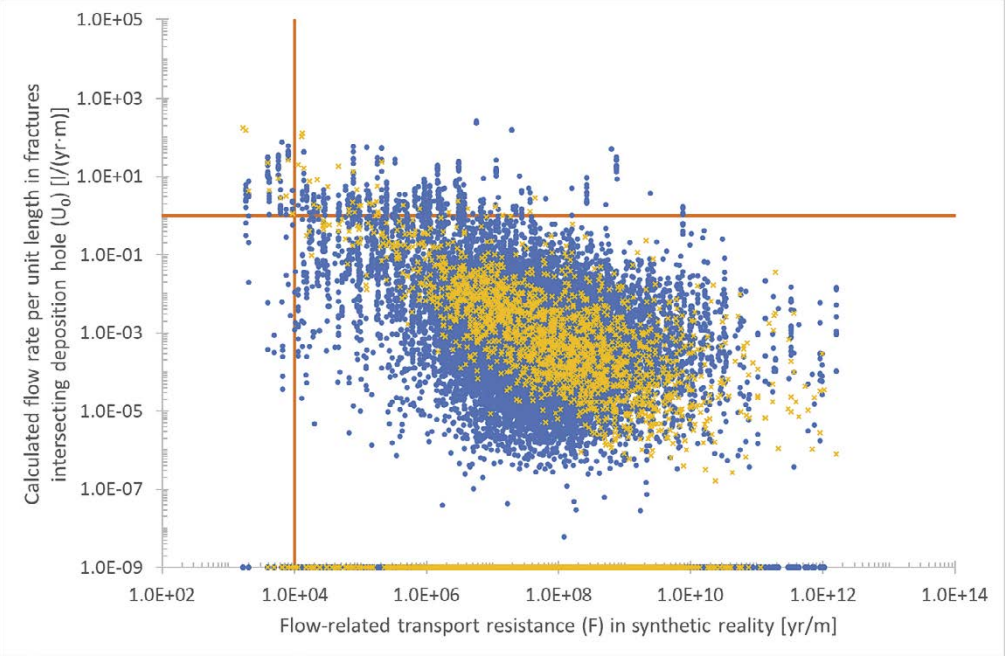

Figure 4-25. *Comparison between F from the synthetic reality and U_0 calculated from 10 conditioned realisations (blue dots) and from the synthetic reality (yellow dots). The vertical orange line shows the post-closure performance target for F of 10^4 yr/m, and the horizontal orange line shows the post-closure performance target for U_0 of 1 l/(yr·m).*

The correlations between the U_0 in the synthetic reality and the U_0 determined from each of three possible metrics are shown in Figure 4-26, Figure 4-27 and Figure 4-28. The first metric is based on the median value of the ten realisations, shown in Figure 4-26. Secondly, the correlation based on the highest calculated U_0 from the ten realisations is shown in Figure 4-27. Thirdly, the correlation based on the arithmetic mean U_0 is shown in Figure 4-28.

The largest value of U_0 is used because it is more likely to correctly predict significant flow potential than a lower-ranked realisation such as the median. However, this method is also the least likely of the three to have the same characteristics when the number of realisations calculated is altered. It is also somewhat arbitrary in that deposition holes ranked in other places in the list could have been chosen.

The arithmetic mean was chosen over the geometric mean for U_0 to reduce the influence of negligible results. The choice to assign negligible U_0 a value of 10^{-9} l/(yr·m) makes very little difference to the arithmetic mean compared with alternative choices such as zero. However, the precise handling of negligible results makes a significant difference to the geometric mean value in cases where some realisations give negligible results and others non-negligible results for the same deposition hole. This is undesirable because, by definition, negligible results are not significantly different to one another or to zero.

All three plots show a clear correlation with the U_0 from the synthetic reality. Figure 4-27 (highest value) and Figure 4-28 (arithmetic mean) generally overpredict the U_0 in the synthetic reality, while Figure 4-26 (median) is closer to the centre line. This is not surprising. Both Figure 4-27 and Figure 4-28 use metrics that give significantly greater weight to higher calculated values than to lower calculated values.

Of the three metrics described, the arithmetic mean value and highest value are equally likely to successfully predict which deposition holes have non-negligible U_0. Of the 1 780 deposition holes in the synthetic reality where non-negligible flow is detected, 1 560 (87.6 %) are predicted by this method. This is not surprising. If there is non-negligible flow in any one of the ten realisations, then the flow in that realisation will be the highest of the ten, and it will cause the arithmetic mean flow to be non-negligible. If the number of realisations were increased, there would eventually be a non-negligible U_0 recorded by these measures in every deposition hole in the model. It is thus also not surprising that there is a large number of deposition holes (2 937) predicted to have non-negligible flow according to the arithmetic mean, that have negligible flow in the synthetic reality.

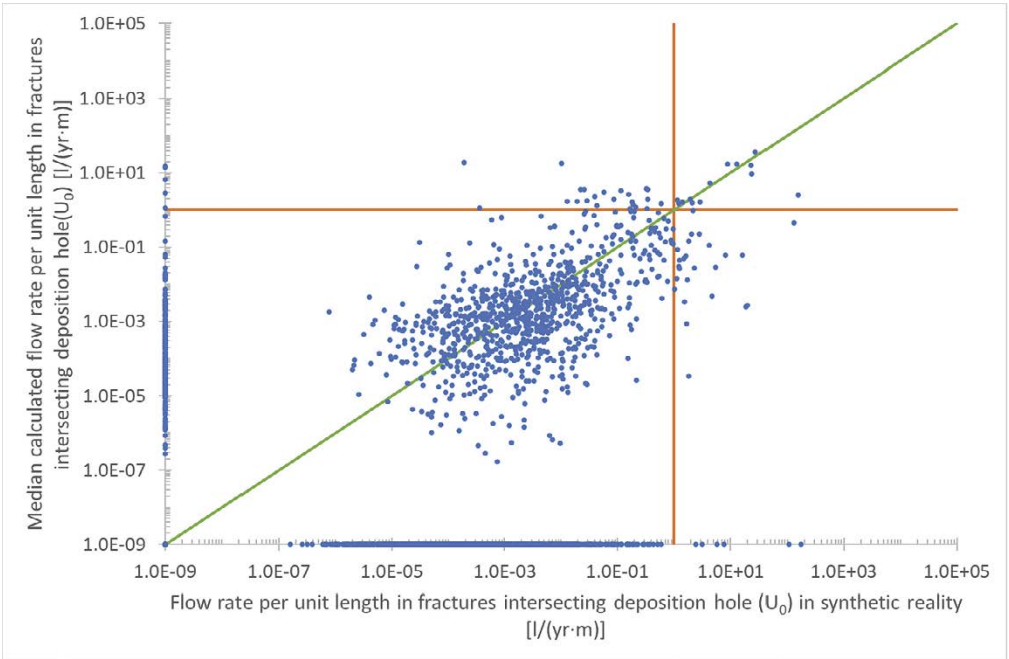

Figure 4-26. *Comparison between U_0 from the synthetic reality and median U_0 (blue dots) for a given deposition hole calculated from 10 conditioned realisations. Negligible values of U_0 are represented as 10^{-9} l/(yr·m). The green line is where the inflow is equivalent in the two cases. The orange lines show the post-closure performance target for U_0 of 1 l/(yr·m).*

Using the median predicts 947 (53.2 %) of the deposition holes with non-negligible flow, but in this case there are only an additional 200 deposition holes incorrectly predicted to have non-negligible flow in the synthetic reality.

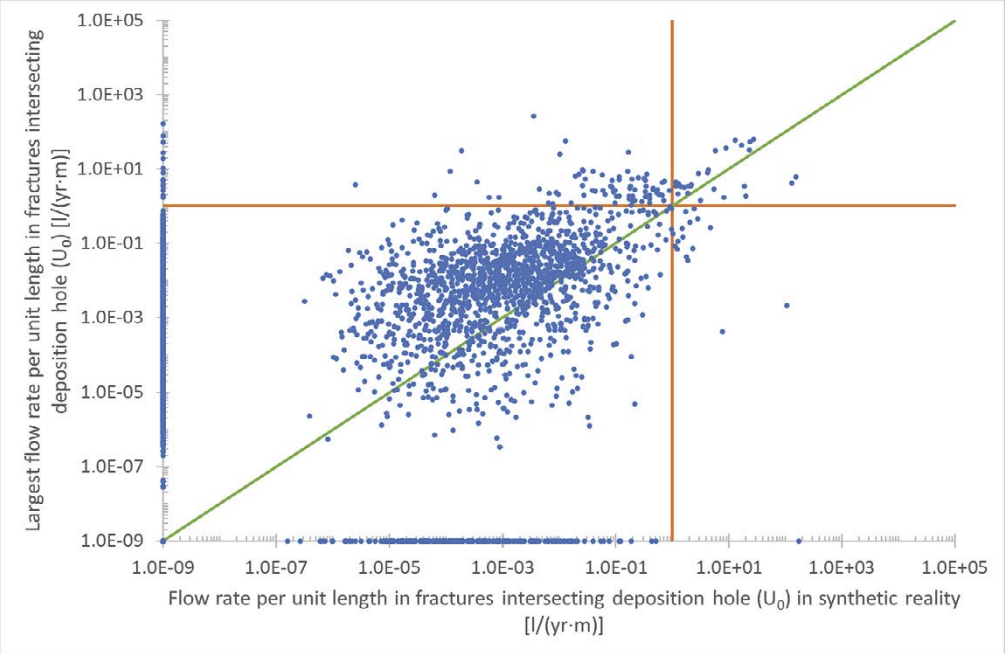

Figure 4-27. *Comparison between U_0 from the synthetic reality and the largest U_0 (blue dots) for a given deposition hole calculated from 10 conditioned realisations. Negligible values of U_0 are represented as 10^{-9} l/(yr·m). The green line is where the inflow is equivalent in the two cases. The orange lines show the post-closure performance target for U_0 of 1 l/(yr·m).*

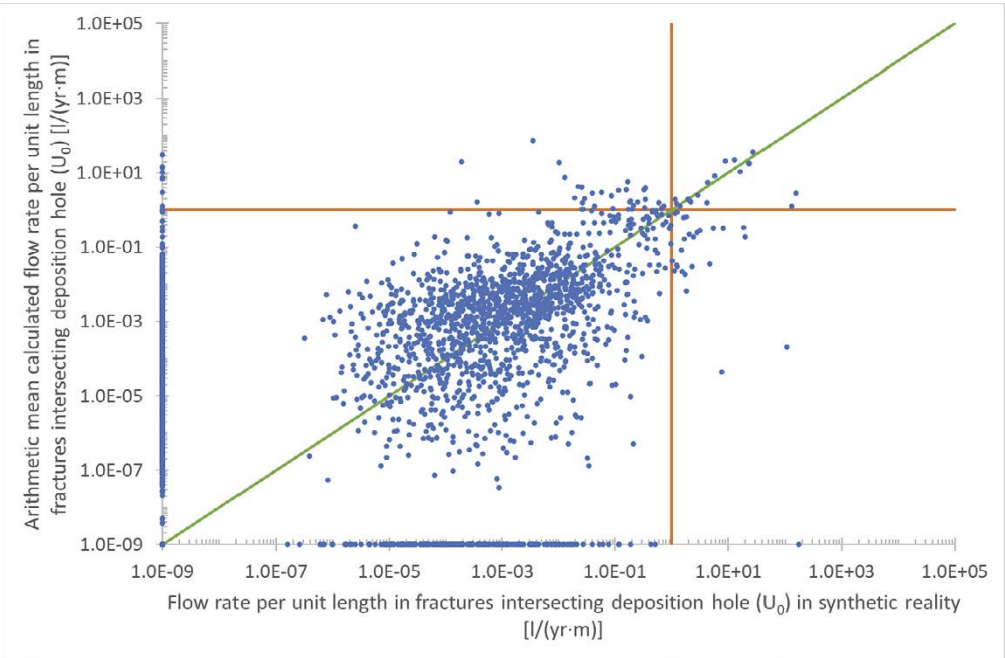

Figure 4-28. *Comparison between U_0 from the synthetic reality and the arithmetic mean U_0 (blue dots) for a given deposition hole calculated from 10 conditioned realisations. Negligible values of U_0 are represented as 10^{-9} l/(yr·m). The green line is where the inflow is equivalent in the two cases. The orange lines show the post-closure performance target for U_0 of 1 l/(yr·m).*

However, the fact that there is non-negligible U_0 predicted in a deposition hole by some metric does not mean that that U_0 is significant to repository safety. The limit at which U_0 is considered non-negligible in this calculation is 10^{-9} l/(yr·m), which is far smaller than the post-closure performance target of 1 l/(yr·m). It is thus also natural to use these plots to attempt to predict whether a given deposition hole will have a U_0 greater than the post-closure performance target. While Subsection 4.3.4 will infer limits from correlation lines obtained from the plots as in Section 3.4, it is interesting initially to reject those deposition holes whose combined calculated U_0 is greater than the post-closure performance target.

Based on this standard, the metric that finds the most deposition holes with high U_0 is the largest value from the ten. Of the 44 deposition holes in the synthetic reality that have U_0 greater than the post-closure performance target, 27 are predicted to have high U_0 by this method. A further 92 deposition holes are predicted to have an unacceptable U_0 but actually have U_0 less than the performance target in the synthetic reality. Looking at only those deposition holes that are rejected by the conditioned calculation (i.e. above the horizontal orange line), it is not necessarily possible to predict which of the rejected deposition hole positions will be associated with deposition holes that have U_0 greater than the post-closure performance target.

When predictions for 10 realisations are combined using the arithmetic mean, 18 deposition holes (out of 44) are correctly predicted to have U_0 greater than the post-closure performance target in the synthetic reality. An additional 43 deposition holes are predicted to have an unacceptable U_0 that do not have an unacceptable U_0 in the synthetic reality. The final metric, using the median value, predicts 13 of the 44 deposition holes whose U_0 is greater than the performance target, and 28 deposition holes predicted to have an unacceptable U_0 whose U_0 in the synthetic reality is less than the performance target.

If, instead of the largest calculated value of U_0, the second largest had been used, this would show a smaller number of deposition holes correctly rejected (24, instead of 27, out of 44). However, only 65 deposition holes (instead of 92) would be rejected by this measure despite being suitable based on the post-closure performance measure in the synthetic reality. This is as would be expected, as (by definition) changing the metric in this way results in a smaller or equal calculated value of U_0 being chosen for every deposition hole.

Equivalent results for F are shown in Figure 4-29 (median value) Figure 4-30 (smallest value) and Figure 4-31 (harmonic mean). The harmonic mean was preferred for F over of the arithmetic and geometric mean because the most important values of F are the smaller ones. The arithmetic mean would be dominated by large values of F representing high-resistance transport paths, and the important low-resistance paths would be relatively ignored. Compared with the geometric mean, the harmonic mean emphasises the smaller values at the expense of the larger ones.

It is clear from the three plots that the correlation between the combined calculated result and the result from the synthetic reality is relatively poor, and as a result most deposition holes that have low F are not predicted to have low F. With the lowest value of F, 10 out of 20 deposition holes whose F is less than the post-closure performance target in the synthetic reality are successfully predicted, but 47 deposition holes predicted to have unacceptable F have F greater than the post-closure performance target in the synthetic reality.

The other two metrics give far fewer deposition holes with F less than the post-closure performance target. Using the harmonic mean, only five of the 20 deposition holes whose F is less than the post-closure performance target in the synthetic reality are successfully predicted. Using the median F, the equivalent number is four. There are an additional 11 deposition holes whose calculated harmonic mean F is less than the performance target, but the equivalent deposition hole in the synthetic reality has an acceptable F. The equivalent value based on the median F is two.

If instead of the lowest value, the second-lowest values were used, 17 deposition holes would be predicted to have F less than the post-closure performance target, of which 8 would be associated with deposition holes that actually have F less than the performance target in the synthetic reality. Of the results found here, this one arguably gives the best balance between finding problematic deposition holes, without rejecting large numbers of acceptable deposition hole positions.

It is also obvious from these three figures, however, that the line $y = x$ is not the best-fit correlation line when all data points are considered. Attempts to derive better results from different correlation lines are given in Subsection 4.3.4.

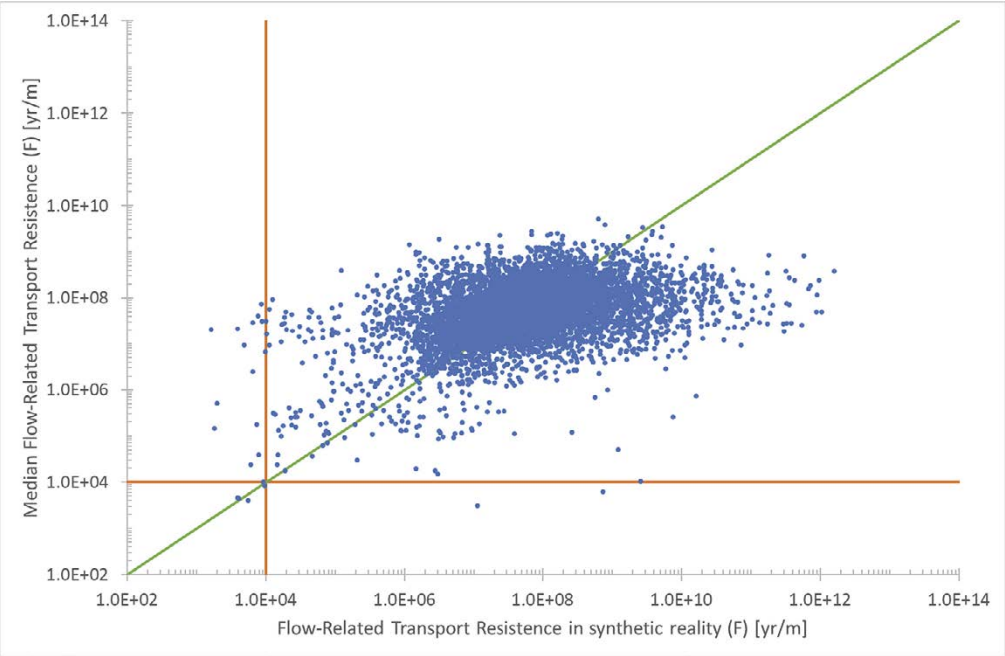

Figure 4-29. *Comparison between F from the synthetic reality and median F (blue dots) for a given deposition hole calculated from 10 conditioned realisations. The green line is where the F is equivalent in the two cases. The orange lines show the post-closure performance target for F of 10^4 yr/m.*

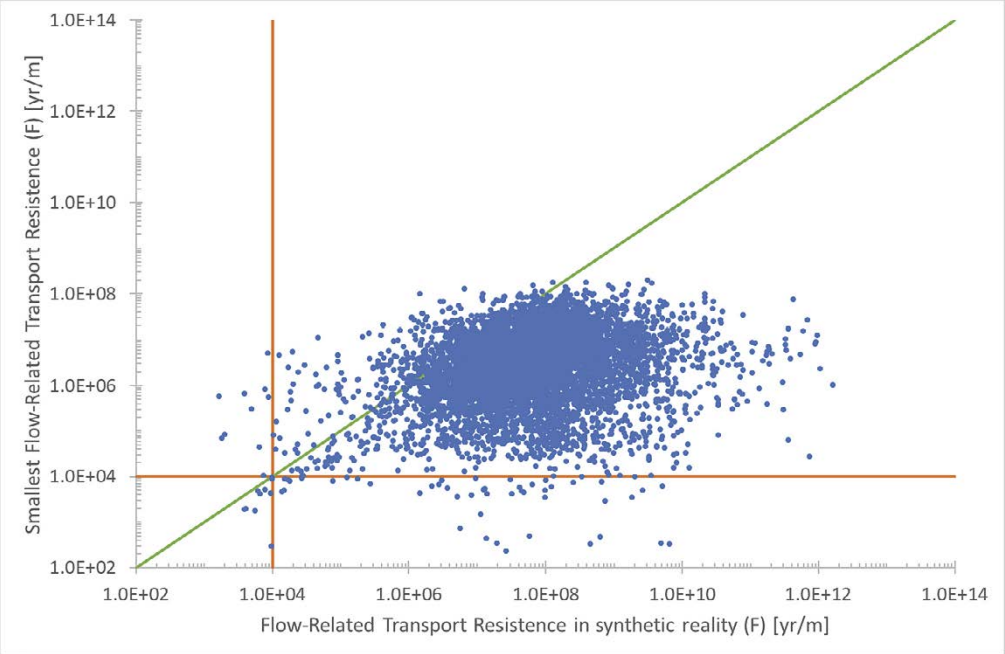

Figure 4-30. *Comparison between F from the synthetic reality and the smallest F (blue dots) for a given deposition hole calculated from 10 conditioned realisations. The green line is where the F is equivalent in the two cases. The orange lines show the post-closure performance target for F of 10^4 yr/m.*

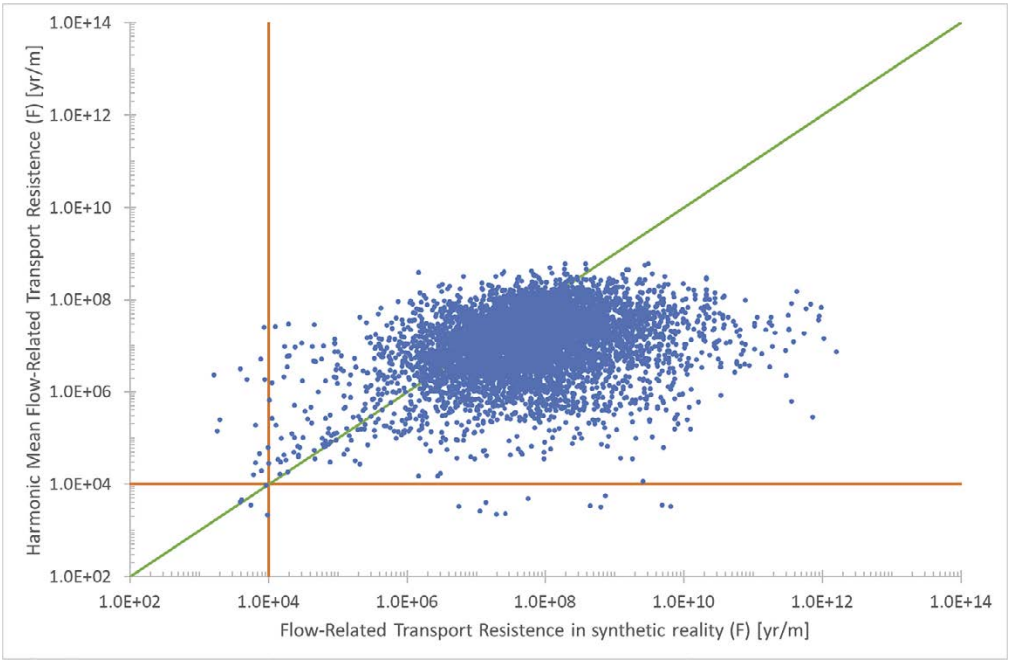

Figure 4-31. *Comparison between F from the synthetic reality and the harmonic mean F (blue dots) for a given deposition hole calculated from 10 conditioned realisations. The green line is where the F is equivalent in the two cases. The orange lines show the post-closure performance target for F of 10^4 yr/m.*

There is an important caveat with all these results, that the conditioning calculation assumes knowledge of all intersections with deposition tunnels and pilot boreholes in the tunnel. In a real scenario, these intersections will not all be known at the same time. On the contrary, it is likely that at the time the initial deposition holes are used, only a small proportion of the repository will have been constructed and mapped.

The advantage of having a large number of intersections available is that the knowledge of intersections in one pilot borehole effectively constrains the size of fractures that are possible in nearby pilot boreholes. If it is known that a fracture intersects one pilot borehole and not a neighbouring pilot borehole, this provides significant information to the conditioning algorithm. However, with fewer pilot boreholes in existence, this information is not available to the same extent, and hence the predictive power of the conditioned models is likely to be weaker. This may imply that flow-based conditioning may be more useful in the earlier phases of construction, as discussed in Subsection 4.1.1.

4.3.4 Limits inferred from combined conditioned data

Just as potential rejection limits were inferred from the correlations between measures in Section 3.4, one might also infer limits from the correlations between post-closure performance measures from the synthetic reality and the calculated metrics in Subsection 4.3.3.

Based on the plots from Subsection 4.3.3, there is potentially some value in using the correlation between the predicted U_0 from ten conditioned realisations and the U_0 from the synthetic reality to infer limits. However, given that the correlations for F are relatively weak, it seems less likely that any limits inferred for F will be meaningful.

The three correlations for U_0 from Subsection 4.3.3 are shown again in Figure 4-32 (median calculated U_0), Figure 4-33 (largest calculated U_0) and Figure 4-34 (arithmetic mean calculated U_0). Unlike in Subsection 4.3.3, however, these plots also include the correlation lines and rejection limits inferred from those correlations, where the calculated value is approximately equivalent to the value from the synthetic reality. The resulting inferred U_0 limits for each of these plots are given by Table 4-2, and the correlation line equations are given in Appendix.

Table 4-2. Inferred limit of U_0 based on correlations between the predicted U_0 from ten conditioned realisations and the U_0 from the synthetic reality.

	Inferred limit for U_0 [l/(yr·m)]
Median from 10 realisations	1.106
Highest value from 10 realisations	2.848
Arithmetic mean from 10 realisations	0.547

Of the 44 deposition holes with U_0 greater than the performance target in the synthetic reality, 13 have U_0 greater than the post-closure performance target according to the inferred limit based on the median value from the ten realisations. This is the same result as was found in Subsection 4.3.3 using a limit of 1 l/(yr·m), which is unsurprising because the inferred limit is close to 1 l/(yr·m). There are also 26 deposition holes with median values greater than the inferred limit, that do not have U_0 greater than the performance target in the synthetic reality. The equivalent number reported with a limit of 1 l/(yr·m) was 28.

The inferred limit based on the highest value of U_0 is substantially larger. As a result, the number of deposition holes successfully predicted as having U_0 greater than the post-closure performance target is reduced from 27 to 22 (out of 44). An additional 47 deposition holes have a highest U_0 value greater than the inferred limit but do not have high U_0 in the synthetic reality. Previously there were 92.

The inferred limit based on the arithmetic mean of the calculated values is about half that based on the median. The result, unsurprisingly, is that this increases the proportion of deposition holes that are correctly identified as having a U_0 that exceeds the post-closure performance target (from 18 to 22), and also increases the number that are predicted to have U_0 greater than the performance target but that actually have U_0 less than the performance target (from 43 to 66).

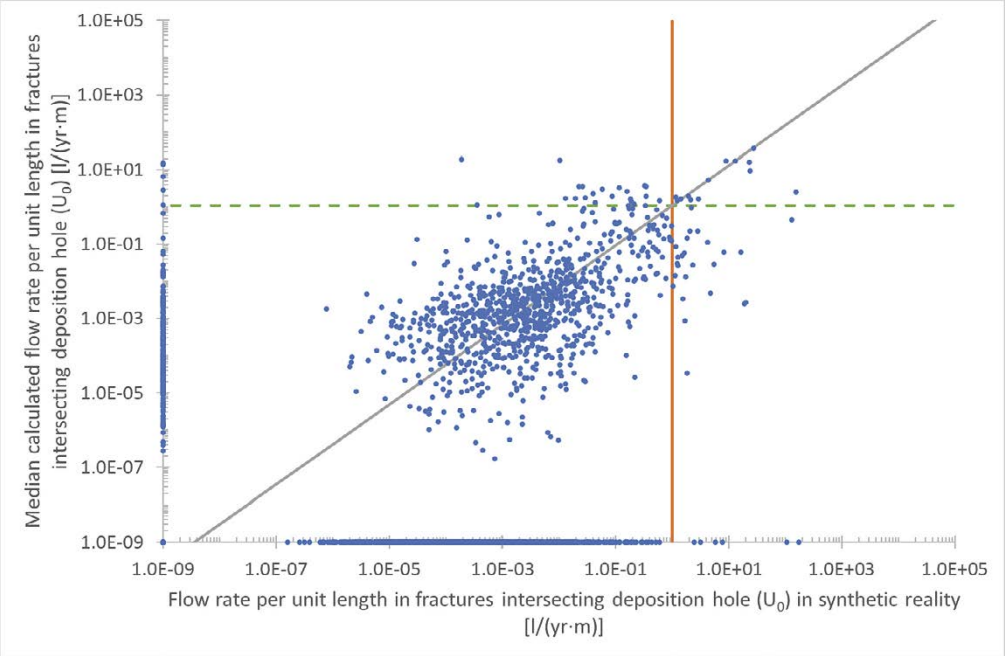

Figure 4-32. *Comparison between U_0 from the synthetic reality and the median U_0 (blue dots) calculated from 10 conditioned realisations for the same deposition hole. Negligible values of U_0 are represented as 10^{-9} l/(yr·m). The orange line shows the performance target of 1 l/(yr·m), the grey line is a correlation line, and the green dashed line where they meet gives the inferred U_0 limit.*

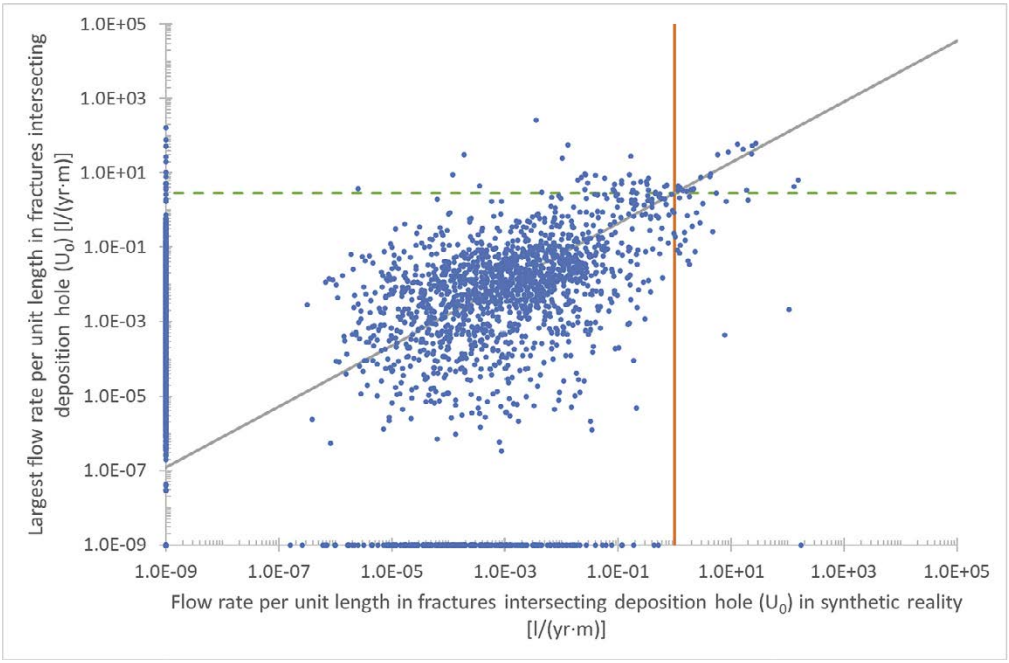

Figure 4-33. *Comparison between U_0 from the synthetic reality and the largest U_0 (blue dots) calculated from 10 conditioned realisations for the same deposition hole. Negligible values of U_0 are represented as 10^{-9} l/(yr·m). The orange line shows the performance target of 1 l/(yr·m), the grey line is a correlation line, and the green dashed line where they meet gives the inferred U_0 limit.*

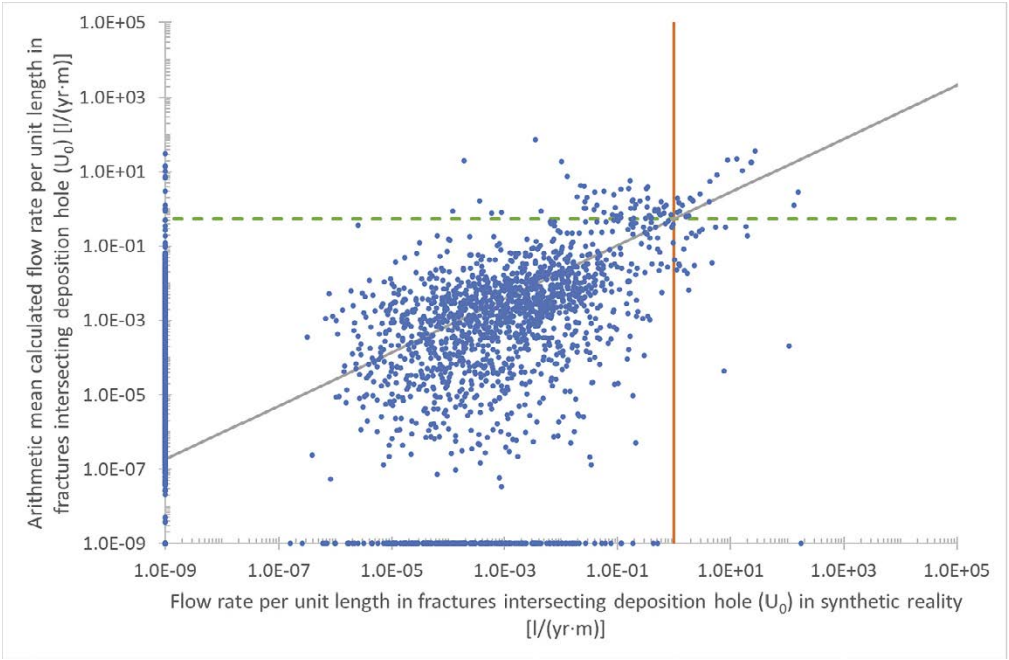

Figure 4-34. *Comparison between U_0 from the synthetic reality and the arithmetic mean U_0 (blue dots) calculated from 10 conditioned realisations for the same deposition hole. Negligible values of U_0 are represented as 10^{-9} l/(yr·m). The orange line shows the performance target of 1 l/(yr·m), the grey line is a correlation line, and the green dashed line where they meet gives the inferred U_0 limit.*

In the case of F, the most obvious correlation lines that might be drawn on plots such as Figure 4-29, Figure 4-30 and Figure 4-31 are very shallow. The inferred limits for F based on these correlation lines would be more than 10^6 yr/m. These limits are too high to be useful. A significant proportion of deposition holes have calculated F less than the inferred limits, and almost all of these have F greater than 10^4 yr/m in the synthetic reality.

There appears to be some correlation between calculated measures and measures from the synthetic reality in deposition holes with low-valued F. This might allow some limits to be developed, that would be significantly lower (of the order 10^4 yr/m), and so are potentially more useful as a means of predicting which deposition holes have low F in the synthetic reality.

Some inferred correlation lines are shown in Figure 4-35, Figure 4-36 and Figure 4-37, based on the median calculated F, the lowest value of F and the harmonic mean value of F respectively. The inferred limits are given in Table 4-3.

Table 4-3. Inferred limit of F based on correlations between the calculated F across ten realisations and the F from the synthetic reality.

	Inferred limit for F [yr/m]
Median from 10 realisations	4.04×10^4
Lowest value from 10 realisations	6.20×10^3
Harmonic mean from 10 realisations	2.50×10^4

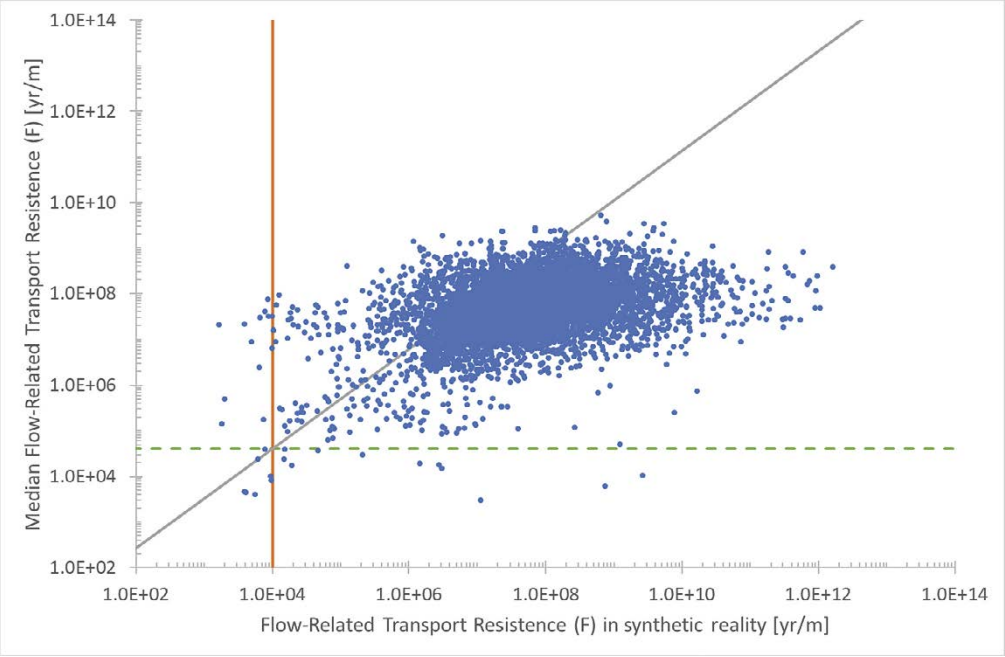

Figure 4-35. *Comparison between F from the synthetic reality and the median F (blue dots) calculated from 10 conditioned realisations for the same deposition hole. The orange line shows the performance target of 1 l/(yr·m), the grey line is a correlation line, and the green dashed line where they meet gives the inferred U_0 limit.*

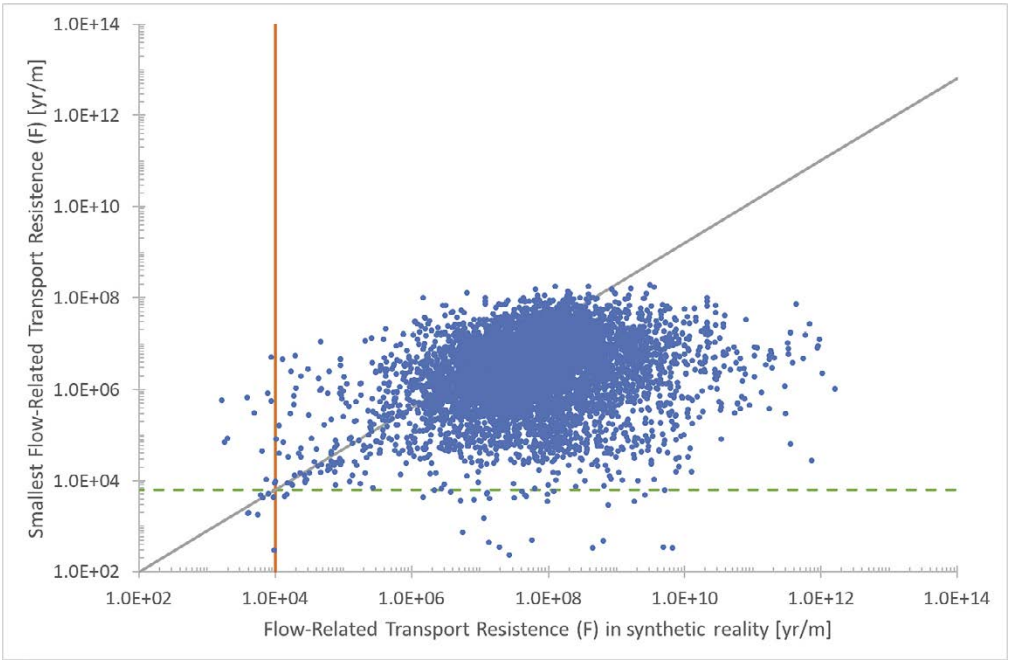

Figure 4-36. *Comparison between F from the synthetic reality and the smallest F (blue dots) calculated from 10 conditioned realisations for the same deposition hole. The orange line shows the performance target of 1 l/(yr·m), the grey line is a correlation line, and the green dashed line where they meet gives the inferred U_0 limit.*

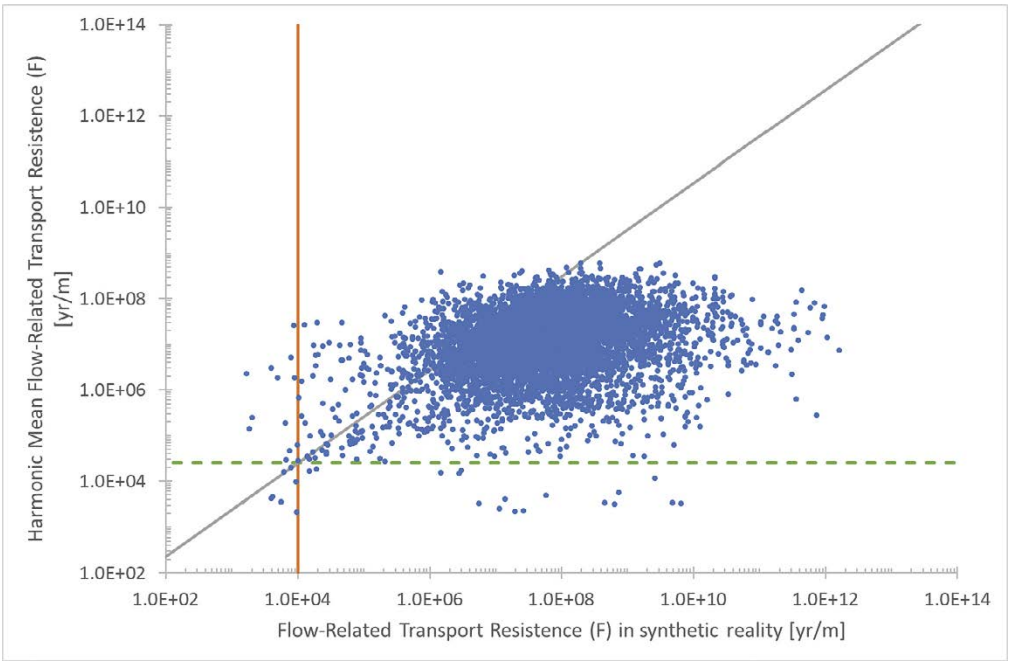

Figure 4-37. *Comparison between F from the synthetic reality and the harmonic mean F (blue dots) calculated from 10 conditioned realisations for the same deposition hole. The orange line shows the performance target of 1 l/(yr·m), the grey line is a correlation line, and the green dashed line where they meet gives the inferred U_0 limit.*

The inferred limits based on the median and harmonic mean increase the number of deposition holes successfully predicted to have low F. There are twenty deposition holes with F less than the post-closure performance target in the synthetic reality. Of these twenty, the number of correctly screened deposition holes rises from 4 and 5 to 7 and 7 (using limits for the median calculated value and harmonic mean calculated value, respectively). Because the limits for calculated F are greater than the post-closure performance target of 10^4 yr/m, this result is probably unsurprising. However, for the same reason, in both cases there are a few more deposition holes incorrectly predicted to have low F. Using 10^4 yr/m there were an additional 2 and 11 deposition holes predicted to have low F using limits for the median calculated value and harmonic mean calculated value, respectively. Using the inferred limits, the new numbers are 11 and 17 deposition holes.

As the inferred limit for the lowest value of F is somewhat smaller than the post-closure performance target, the opposite occurs. The number of deposition holes that are correctly screened remains the same (8 out of 20). However, instead of finding an additional 47 deposition holes with low F, this limit finds 29 such deposition holes.

These results are moderately successful, particularly given that the correlations are based on a relatively small number of deposition holes. The proportion of deposition holes rejected that actually have F less than the post-closure performance target is significantly higher than would be expected if the choice were purely random. However, the correlation lines drawn here are more open to interpretation than other correlation lines in this report, and the number of deposition holes with F less than 10^4 yr/m is small. This method is thus probably not useful in a real-world setting.

In practice, several of the deposition holes that have low F in the synthetic reality will be very difficult to predict from the values of F in the calculated realisations, without also finding a large number of deposition holes with high F in the synthetic reality.

5 Conclusions

The results reported here demonstrate the degree of correlation between simulated measures of inflow, specific capacity, and post-closure performance for a model of the Forsmark site. Specifically, results of tests performed in pilot boreholes (i.e. inflows and specific capacities) are compared with deposition hole inflows. Quantities that can be measured in open repository conditions (pilot borehole specific capacity and deposition hole inflow) are then compared with simulated post-closure performance measures (flow rate per unit length in the fractures intersecting each deposition hole, U_0, and flow-related transport resistance, F).

Ten realisations of the SR-Site model for Forsmark were run in two phases. In the first phase, the realisations were purely stochastic. In the second phase fractures intersecting deposition holes and tunnels were conditioned to match the fractures found in those deposition holes and tunnels in a synthetic reality (created from an additional realisation of the model).

5.1 Unconditioned models

The first objective for the unconditioned models is to assess the correlations between measures from pilot boreholes and deposition holes, in open repository conditions. The second objective is to assess the correlations between measures in open repository conditions and the post-closure performance measures, U_0 and F.

For deposition holes in open repository conditions, the aim is to find those with inflow greater than 0.1 l/min, which is the existing hydraulic rejection criterion based on the properties of the buffer. Between the ten realisations and hence 69 160 deposition holes studied, there are 407 deposition holes that exceed this criterion, which is about 0.6 % of the total.

The best correlation found is, perhaps unsurprisingly, between inflows to pilot boreholes and inflows to deposition holes. Each of the 183 pilot boreholes with an inflow greater than 0.1 l/min was associated with a deposition hole with an inflow greater than 0.1 l/min. However, inflows to pilot boreholes are not necessarily easy to measure in the field.

Using hydraulic testing, the correlation between the resultant specific capacity and the deposition hole inflow is significantly weaker. Nonetheless, 161 of the 179 pilot boreholes with hydraulic tests that give a specific capacity greater than 10^{-7} m^2/s are associated with deposition hole inflows greater than 0.1 l/min.

For post-closure performance measures, the aim is to find the 567 deposition holes (out of the ten realisations) that have U_0 greater than 1 l/(yr·m) and the 134 deposition holes that have F less than 10^4 yr/m. It is found that values of U_0 and F correlate reasonably well with specific capacity, and this correlation improves at higher flow rates. The correlations with deposition hole inflow are stronger, including at higher flow rates. Of the 567 deposition holes that have U_0 greater than the post-closure performance target, a total of 327 (57.7 %) also have deposition hole inflows greater than 0.1 l/min. For F, this number is 100 out of 134 (74.6 %).

The correlations between U_0 and F, specific capacity and deposition hole inflow can be used to infer new hydraulic rejection criteria from the post-closure performance targets for U_0 and F. The limits inferred from the performance target for U_0 are a specific capacity of 4.10×10^{-8} m^2/s, and a deposition hole inflow of 0.118 l/min (inferred from the specific capacity limit) or 0.0736 l/min (inferred directly). These are similar to the existing hydraulic rejection criterion of 0.1 l/min and appear to predict a reasonable proportion of deposition holes whose post-closure flow is greater than the U_0 target without filtering out too many deposition holes that should not be rejected.

The limits inferred from F are a specific capacity of 4.77×10^{-6} m^2/s, and a deposition hole inflow of 26.54 l/min (inferred from specific capacity) or 9.79 l/min (inferred directly). These are very large values. When they are used to screen deposition holes out, most deposition holes that exceed the U_0 performance target are not found, while most deposition holes with a value of F less than the

performance target are found using the inferred U_0 limits. This suggests that the limits based on U_0 are of greater use in screening out unsuitable deposition holes, and – as the newly-inferred rejection criteria for U_0 are close to the existing rejection criterion of 0.1 l/min – that the existing rejection criterion itself is a reasonable limit for screening out deposition holes with unsuitable post-closure flow properties.

5.2 Conditioned models

Conditioned models differ from unconditioned models in that intersections between fractures and engineered openings (tunnels and pilot boreholes) in conditioned models are selected from a library with the aim that the intersections in the tunnels and pilot boreholes will match those found in reality. In this case, the ten realisations used for unconditioned calculations were conditioned using the intersections taken from a separate realisation, used as a synthetic reality.

The conditioning process used in these calculations relied on the geometry of intersections in the synthetic reality, without taking account of flow conditions. While it would be possible to also take account of flows measured in the pilot boreholes and deposition tunnels, the calculation time required to generate libraries would be prohibitive.

Conditioning was conducted on the basis that the correct connectivity between pilot boreholes is more important than a precise geometrical match to observed fracture intersections. This choice ensures that flow paths between pilot boreholes are maintained to the maximum degree practical.

As a rule, the correlations between flow metrics from conditioned calculations were broadly similar to, or somewhat less successful than, those from unconditioned calculations. In particular, many of the conditioned calculations had a less-well defined high-flow tail of the distribution, and some had no significant tail at all. This was likely because the fractures that led to these pilot boreholes and deposition holes being associated with high flows were not present in the synthetic reality and so were removed from the conditioned models. In a more general sense, there is an assumption inherent in these kinds of correlation calculations that the result from each deposition hole position will be independent and that any deposition hole position can be replaced with any other deposition hole position. Models with conditioning conform less well to this assumption than those without because in conditioned models, each pilot borehole is conditioned in roughly the same way in all ten realisations. There is thus less variability between realisations, leading to greater sampling bias.

Perhaps, however, the area where conditioning adds more benefit is in predicting the flow for an individual deposition hole position based on the calculated flows for that same deposition hole position. Such prediction does not work in the unconditioned case. There is no reason why an ensemble of ten independent realisations will successfully predict the flow in a specific deposition hole position in an eleventh realisation (the synthetic reality) that is independent of the original ten. In conditioned realisations, because the fractures intersecting any given deposition hole position will be based on the fractures found in the synthetic reality, it is possible for them to predict the flows in the synthetic reality from the ensemble of ten calculated realisations. This predictive power is beneficial, particularly because – unlike the correlations found in unconditioned models – this measure does not require any physical measurement of the flow in any of the deposition holes or pilot boreholes. As a result, predictions can be made before flow measurements are complete, and can be also made in cases where flow measurement results have large associated error margins.

The synthetic reality had a total of 40 deposition holes whose inflow was greater than the existing hydraulic rejection criterion of 0.1 l/min, 44 deposition holes where the flow rate per unit length in intersecting fractures (U_0) was greater than the post-closure performance target of 1 l/(yr·m), and 20 deposition holes whose transport-related flow resistance was less than the post-closure performance target of 10^4 yr/m.

It was found that there was a clear correlation between inflows calculated for conditioned realisations and those observed in the synthetic reality. It was also found that there was no significant correlation in unconditioned models. It was particularly noticeable that the conditioned calculations were far better than unconditioned calculations at predicting whether flow would be observed or not in a given deposition hole in the synthetic reality. This may be a good test of the predictive methods given that U_0 and F are not measurable.

A similar calculation using U_0 showed, in the conditioned models, a similarly significant correlation between the calculated data and the synthetic reality. However, in the case of F, while the correlation did improve from unconditioned to conditioned models, it did not improve to a point where it could be used to make useful predictions.

The fact that these calculations provide ten answers (one from each realisation) is of some benefit as it gives information about the uncertainty of the result. However, it is not necessarily obvious how to infer from those ten answers whether a deposition hole position should be screened out or not. A measure that combines the calculated flows from the ten realisations can be more useful in that it allows a single conclusion for each deposition hole position, that takes account of all the data available.

Thus, as an illustration, three metrics were chosen for the calculated post-closure performance measures. First, the median value; second, the largest value of U_0 (out of ten) or smallest for F; and third, the arithmetic mean value of U_0 or harmonic mean value of F.

As a rule, these measures correlated well with the values of U_0 from the synthetic reality but did not correlate usefully well with values of F from the synthetic reality. The difficulty when calculating F is likely due to the contribution of fractures other than the fractures directly intersecting the tunnel. These fractures remain stochastic and there is likely too much variation to make a good prediction.

Looking more particularly at U_0, the limits predicted for the first three measures were a median U_0 of 1.106 l/(yr·m), a largest U_0 of 2.848 l/(yr·m) and an arithmetic mean U_0 of 0.547 l/(yr·m). These are all somewhat similar to the post-closure performance target of 1 l/(yr·m).

5.3 Results summary table

For ease of reference, a table summary of results obtained in this report is provided in Table 5-1.

Table 5-1. Summary of correlations found from the calculations in this report. Rows are the starting data used for prediction; columns are the data predicted. Cell colouring indicates the degree of correlation (green – yellow – orange – red indicates high to low predictive capability).

	To predict inflow to open deposition holes	**Flow rate per unit length in fractures intersecting deposition holes in backfilled repository (U_0)**	**Flow-related transport resistance in paths from deposition holes in backfilled repository (F)**
Unconditioned pilot borehole measures	Good correlation with unconditioned pilot borehole inflows, significant correlation with specific capacities	Significant correlation with specific capacities	Moderate correlation with specific capacities
Unconditioned deposition hole inflows		Significant correlation with deposition hole inflows	Significant correlation with deposition hole inflows
Conditioned pilot borehole measures	Good correlation with unconditioned pilot borehole inflows, significant correlation with specific capacities	Moderate correlation with specific capacities	Moderate correlation with specific capacities
Conditioned deposition hole inflows		Significant correlation with deposition hole inflows	Significant correlation with deposition hole inflows
Unconditioned calculated data for the same hole	No significant correlation with calculated deposition hole inflows	No significant correlation with calculated U_0	No significant correlation with calculated F
Conditioned calculated data for the same hole	Moderate correlation with calculated deposition hole inflows	Moderate correlation with calculated U_0	No significant correlation with calculated F

6 Recommendations

The basic correlations between flow measures presented in this report provide useful information about the relationships between the measurable/calculated flows in an open repository and the unmeasurable post-closure performance measures. These results can be used to recommend new hydraulic rejection criteria for use in the repository.

6.1 Rejection criteria from measured flow

Both specific capacity and deposition hole inflow provide reasonable predictions of both the post-closure U_0 and the post-closure F (Section 3.3). It is thus possible to provide threshold values for specific capacity, and for deposition hole inflow, that approximately correspond to the post-closure performance targets for U_0 and F. This means that there are potentially two specific capacity limits and two deposition hole limits.

These limits should be based on unconditioned calculations because the unconditioned calculations were better correlated than the conditioned calculations.

In the interests of long-term safety, it is preferable to choose the lower of the two limits. This lower limit will exclude more deposition hole positions where post-closure flow characteristics are unacceptable according to the performance targets, but a higher proportion of the deposition hole positions that are excluded would have been acceptable according to the performance targets. However, choosing the higher limit is likely to lead to acceptance of many deposition hole positions whose flow characteristics are not acceptable. In all cases discussed in this report, the lower limit is the limit based on the post-closure limit for U_0.

It is therefore recommended that inferred hydraulic rejection criteria be based on the requirement that U_0 be less than the performance target of 1 l/(yr·m).

As to the values for the hydraulic rejection criteria, these must be based on an assessment of the requirement for conservatism and caution, balanced with the requirement that some deposition hole positions be allowed. No limit will successfully detect every deposition hole where the post-closure U_0 exceeds 1 l/(yr·m), and there is no point in constructing a repository in which all deposition hole positions will be rejected.

For specific capacity, Subsection 3.4.2 proposes a limit of 4.10×10^{-8} m^2/s. This limit finds 260 out of 567 deposition holes (45.8 %) whose U_0 exceeds 1 l/(yr·m). There are also another 93 deposition holes that are rejected but whose U_0 does not exceed 1 l/(yr·m). That means that 73.6 % of deposition holes rejected by this limit have U_0 greater than 1 l/(yr·m).

This value can be mapped across to approximately 0.118 l/min for deposition hole inflow, slightly greater than the existing hydraulic rejection criterion for deposition holes (Subsection 3.4.3). This is significant because it is highly undesirable to excavate deposition holes that have inflows greater than the existing hydraulic rejection criterion of 0.1 l/min. Since the calculated specific capacity equivalent to 0.1 l/min is 3.54×10^{-8} m^2/s, it seems sensible to suggest that the specific capacity limit be no higher than this. In addition, there is some value in choosing a limit that is based on a round number, for ease of use.

The requirement for conservatism suggests that a smaller limit may be preferable. Thus, Subsection 3.4.2 also considers the implications of a limit of 1×10^{-8} m^2/s. In this case, 334 of the 567 deposition holes whose U_0 exceeds 1 l/(yr·m) are found. This is equivalent to 58.9 % of all those deposition holes. However, another 443 deposition holes are rejected where U_0 does not exceed 1 l/(yr·m). Only 42.9 % of deposition holes that are rejected have U_0 greater than 1 l/(yr·m).

Based on these results, it is recommended that a new hydraulic rejection criterion should be applied based on the specific capacity in the pilot borehole. The pilot borehole should be rejected if its specific capacity is greater than a given limit that is between 1×10^{-8} m^2/s and 3×10^{-8} m^2/s. From this range, a limit of 1×10^{-8} m^2/s is most conservative and thus might be the most appropriate.

In Subsection 3.4.4, limits based on inflows to deposition holes are also considered. It is preferable to screen out deposition hole positions before the deposition holes are excavated due to the cost of excavation. However, there is only so much information that can be inferred using only specific capacities calculated from pilot boreholes. It is highly likely that some deposition holes will intersect fractures that do not intersect the corresponding pilot boreholes. It is thus important to investigate the deposition holes before using them.

The proposed limit for deposition hole inflow from Subsection 3.4.4 is 7.36×10^{-2} l/min, slightly lower than the existing hydraulic rejection criterion based of 0.1 l/min. With this limit, a total of 351 out of 567 deposition holes (61.9 %) where U_0 exceeds 1 l/(yr·m) are found, and an additional 114 deposition holes are rejected with a U_0 less than 1 l/(yr·m). While 7.36×10^{-2} l/min is similar to the existing hydraulic rejection criterion based of 0.1 l/min, it is lower than that limit, and it would not seem conservative to round it up.

As with specific capacity, the implications of an inflow limit of 1×10^{-2} l/min are also examined in Subsection 3.4.4. In this case, an additional 93 deposition holes are found where U_0 exceeds 1 l/(yr·m), at the expense of 690 deposition holes that are rejected that have a U_0 less than 1 l/(yr·m). However, many of these deposition holes will be in positions that were rejected at the pilot borehole stage, and thus will not have been excavated.

Based on these calculations, it is recommended that the hydraulic rejection criterion for deposition hole inflow be reduced to a value between 1×10^{-2} l/min and 7×10^{-2} l/min. As with the specific capacity limit, the principle of conservatism in long term safety would argue for a lower limit in this range.

It is known that deposition hole inflow is normally greater than or approximately equal to the pilot borehole inflow (Subsection 3.2.1), and it is desirable to avoid excavating holes that are going to be rejected. It is thus recommended that pilot boreholes whose inflow is greater than the hydraulic rejection criterion for deposition holes should be rejected without excavation.

Using the lower bounds of both hydraulic rejection criteria proposed (inflow 1×10^{-2} l/min and specific capacity 1×10^{-8} m^2/s), a total of 519 of the 567 deposition hole positions (91.5 %) where U_0 exceeds 1 l/(yr·m) are rejected. Of these, 370 are rejected prior to excavation of the deposition hole. An additional 916 deposition hole positions are rejected that have a U_0 that is less than 1 l/(yr·m). Of these, 583 are rejected at the pilot borehole stage.

Using these limits across the entire repository, 1.4 % of pilot boreholes are rejected before the corresponding boreholes are excavated. Of those deposition holes that are excavated, 0.7 % are rejected.

While specific hydraulic rejection criteria have been recommended by this report, they are not necessarily the final word on the matter. It may be useful to perform sensitivity calculations to determine whether different assumed properties of the site give different results. This would allow greater understanding of the sensitivity of the results of this calculation to the precise model used. It would also be useful to repeat this exercise on updated versions of the model of the site at Forsmark when they are produced, in order to ensure that the limits proposed remain valid.

6.2 Rejection criteria from conditioned results

The conditioning methodology provides a second means of generating inferred hydraulic rejection criteria. According to this method, models are conditioned based on the traces observed in pilot boreholes. The post-closure performance measures in the conditioned models can then be calculated for several realisations, combined, and compared with a new hydraulic rejection criterion to determine whether the deposition hole position should be rejected.

A benefit of these calculations is that they can be performed without any physical measurement of flow. This is most useful if flow measurements are incomplete, or in cases where the flow measurements have significant uncertainties.

However, these calculations have the drawback that they are based on knowledge of fractures inferred from the observed traces in the repository. All results in this section were generated starting from a completed repository, with a fully mapped pilot borehole for every deposition hole. In a real repository this information will not all be available at the same time. If there is less information available, then it is reasonable to assume that the calculated results from the conditioning may be less reliable. The effect of this is that conditioning is likely to become more useful as the repository is developed and more of the repository is known.

For the information from early construction phases to be useful in later stages of construction, however, it must have been collected before the early holes and tunnels are backfilled. It is thus recommended that detailed mapping of fracture intersections be performed in all pilot boreholes that are drilled, and all deposition tunnels and deposition holes that are excavated, including those that are rejected for other reasons. This recommendation applies even if conditioning is not being used to reject deposition hole positions initially.

The issue with conditioning during early phases of repository construction may be partially mitigated using flow-based conditioning as discussed in Subsection 4.1.1. However, use of flow-based conditioning would need to be the subject of a separate study. The remainder of this section will deal with the case studied here, where information for all pilot boreholes is available.

As with the hydraulic rejection criteria proposed in Subsection 6.1, while results have been calculated for both U_0 and F, it is the limits proposed that are based on U_0 that are likely to be the most useful. There are two major reasons for this. Firstly, there is little correlation between the calculated metrics for F and the F in the synthetic reality. Secondly, the fact that there are relatively few deposition holes in the synthetic reality where F is less than the post-closure performance target of 10^4 yr/m means that the differences between the three calculated metrics are not statistically meaningful.

Any one of the three metrics proposed for U_0 could be used as the basis for a new rejection criterion. However, if a criterion based on the highest (or second highest) calculated value of U_0 were chosen, some additional work may be required. This is because the limit based on this metric is likely to vary with the number of realisations used. The highest value of U_0 from a hundred realisations is likely to be higher than the highest value from ten realisations, for example. For this reason, this discussion will focus on the median and arithmetic mean calculated U_0. The question of number of realisations to be used will be addressed later in this section.

The limits calculated in Subsection 4.3.4 for the median and mean calculated U_0 were 1.106 l/(yr·m) and 0.547 l/(yr·m) respectively. These compare with the post-closure performance target of 1 l/(yr·m). Using these metrics, 22 deposition holes are found out of the 44 deposition holes with U_0 greater than the post-closure performance target in the synthetic reality. An additional 66 deposition holes are incorrectly rejected when they have U_0 less than the post-closure performance target in the synthetic reality.

As with the flow measures, a conservative approach would be to choose a lower limit. A lower rejection criterion would detect more deposition holes that are likely to have high U_0 but would also reject more deposition holes that do not have high U_0. For example, one might reduce the two limits so that all deposition holes with a median or mean calculated U_0 greater than 0.1 l/(yr·m) are rejected. As a result, 31 out of 44 deposition holes with U_0 greater than the post-closure performance target in the synthetic reality are rejected. An additional 130 deposition holes are incorrectly rejected with U_0 less than the post-closure performance target in the synthetic reality.

It is possible to go further. However, as the limits are reduced, fewer additional deposition holes are found with high U_0 in the synthetic reality, and many more deposition holes are rejected unnecessarily. For example, with limits of 0.01 l/(yr·m), 40 deposition holes with high U_0 in the synthetic reality are found and 462 other deposition holes are also rejected. This is about 6.7 % of deposition holes in the entire repository.

It is thus recommended, that if this method is used, that any deposition hole whose calculated median or mean U_0 is greater than 0.1 l/(yr·m) should be rejected.

A significant proportion of the deposition holes with U_0 greater than the performance target are not found by these methods. Thus, it is also recommended that they only be used in conjunction with the flow-based limits proposed in Subsection 6.1. Of the two methods, the calculation based on measured flows should be considered the more reliable.

These limits are based on models conditioned on a single synthetic reality using a single DFN recipe. They have not been checked with other possible synthetic realities or other possible DFN recipes. There is no reason to assume that results in other models are likely to be significantly different, as the conditioning methodology is not tailored to this model. However, it would be of benefit to test this assumption by applying the model to other synthetic realities and other models.

As a final point, it is useful to consider the number of conditioned realisations to calculate. The optimum number of conditioned realisations to be used is as many as practically possible, given the time and resources required to calculate them. It was found in this work that it can be very time-consuming to condition models that have a large number of observed fracture intersections. In addition, these calculations required significant computer memory because of the size of the libraries. This meant that multiple realisations could not easily be run in parallel. Using current computer technology and the current calculation methodology, it is likely to be impractical to condition more than about ten realisations of the Forsmark model in a reasonable timeframe. If limits based on conditioned models are to be used on such large models, it would be worthwhile to study ways of further streamlining the conditioning calculations.

An initial option for streamlining of the conditioning calculations would be to reduce the large amount of memory required for the libraries. At present, the entire library is stored in memory as a series of linked lists. This is implemented for speed. It is far quicker to access the data in memory than to repeatedly search the stored library files. However, it would be possible to store the data more on disk in a way that could be more efficiently searched. For example, the library could be reimplemented as a database, or using temporary files based on the internal linked list structure.

Other performance gains may be implemented by more efficient use of parallelisation and through introducing simplifying assumptions. There may be places in the conditioning algorithm where searches continue even though there is no realistic prospect of finding a successful match. It would be of benefit to find these places and to prevent unnecessary searches.

However, the main reason why individual conditioning calculations take a long time is the presence of very large fractures that create a large number of intersections with tunnels and pilot boreholes. This is slow, as discussed in Section 4.1, because these fractures are statistically rare and because the fracture from the library must match the fracture from the synthetic reality very precisely. A more deterministic method for conditioning these very large fractures would significantly reduce calculation times.

References

SKB's (Svensk Kärnbränslehantering AB) publications can be found at www.skb.com/publications. Posiva's publications can be found at https://www.posiva.fi/en/index/media/reports.html.

Appleyard P, Jackson P, Joyce S, Hartley L, 2018. Conditioning discrete fracture networks models on intersection, connectivity and flow data. SKB R-17-11, Svensk Kärnbränslehantering AB.

Baxter S, Appleyard P, Hartley L, Hoek J, Williams T, 2018. Exploring conditioned simulations of discrete fracture networks in support of hydraulic acceptance of deposition holes. Application to ONKALO demonstration area. Posiva SKB Report 07, Posiva Oy, Svensk Kärnbränslehantering AB.

Cordes C, Kinzelbach W, 1992. Continuous groundwater velocity fields and path lines in linear, bilinear and trilinear finite elements. Water Resources Research 28, 2903–2911.

Follin S, Ludvigson J-E, Levén J, 2011. A comparison between standard well test evaluation methods used in SKB's site investigations and the generalised radial flow concept. SKB P-06-54, Svensk Kärnbränslehantering AB.

Hjerne C, Komulainen J, Aro S, Winberg A, 2016. Development of hydraulic test strategies in support of acceptance criteria for deposition hole positions – Results of hydraulic injection tests in ONKALO DT2 pilot holes for experimental deposition holes. Posiva Working Report 2016-06, Posiva Oy, Finland.

Jacobs, 2008. ConnectFlow, version 9.6. Jacobs Clean Energy Limited (published as Serco).

Jacobs, 2018a. ConnectFlow, version 12.0. Jacobs Clean Energy Limited (published as Wood).

Jacobs, 2018b. ConnectFlow Technical Summary, Release 12.0. Jacobs Clean Energy Limited (published as Wood).

Joyce S, Simpson T, Hartley L, Applegate D, Hoek J, Jackson P, Swan D, Marsic N, Follin S, 2010. Groundwater flow modelling of periods with temperate climate conditions – Forsmark. SKB R-09-20, Svensk Kärnbränslehantering AB.

Joyce S, Swan D, Hartley L, 2013. Calculation of open repository inflows for Forsmark. SKB R-13-21, Svensk Kärnbränslehantering AB.

Posiva SKB, 2017. Safety functions, performance targets and technical design requirements for a KBS-3V repository. Conclusions and recommendations from a joint SKB and Posiva working group. Posiva SKB Report 01, Posiva Oy, Svensk Kärnbränslehantering AB.

SKB, 2010. Design, construction and initial state of the underground openings. SKB TR-10-18, Svensk Kärnbränslehantering AB.

Appendix

Correlation lines

The correlation lines inferred from a plot in this report are simple straight lines. In each case, two points are chosen from the distribution, one at each end of the line. The correlation line is the line drawn between these points. As the coordinates of the two points are known, it is simple to calculate the equation of the line drawn.

Because plots in this report have logarithmic scales on both axes, all straight correlation lines are of the form $y = ax^b$.

Correlation lines are given in Table A-1.

Table A-1. List of correlation lines inferred from plots in this report.

Figure	Page Number	X-axis	Y-axis	Correlation Line
Figure 3-12	27	Specific capacity (unconditioned)	U_0 (unconditioned)	$y = 1.31 \times 10^8 x^{1.10}$
Figure 3-13	28	Specific capacity (unconditioned)	F (unconditioned)	$y = 0.460 x^{-0.815}$
Figure 3-16	30	Specific capacity (unconditioned)	Deposition hole inflow (unconditioned)	$y = 3.01 \times 10^7 x^{1.14}$
Figure 3-17	31	Deposition hole inflow (unconditioned)	U_0 (unconditioned)	$y = 10.0 x^{0.883}$
Figure 3-18	32	Deposition hole inflow (unconditioned)	F (unconditioned)	$y = 4.47 \times 10^4 x^{-0.656}$
Figure 4-32	59	U_0 in synthetic reality	Median conditioned U_0	$y = 1.11 x^{1.07}$
Figure 4-33	60	U_0 in synthetic reality	Largest conditioned U_0	$y = 2.85 x^{0.820}$
Figure 4-34	60	U_0 in synthetic reality	Arithmetic mean conditioned U_0	$y = 0.547 x^{0.720}$
Figure 4-35	61	F in synthetic reality	Median conditioned F	$y = 1.79 x^{1.09}$
Figure 4-36	62	F in synthetic reality	Smallest conditioned F	$y = 1.53 x^{0.902}$
Figure 4-37	62	F in synthetic reality	Harmonic conditioned F	$y = 2.06 x^{1.02}$

Arkitektkopia AB, Bromma, 2021

A CO-OPERATION REPORT BETWEEN SVENSK KÄRNBRÄNSLEHANTERING AB AND POSIVA OY

SKB's and Posiva's programmes both aim at the disposal of spent nuclear fuel based on the KBS-3 concept. Formal cooperation between the companies has been in effect since 2001. In 2014 the companies agreed on extended cooperation where SKB and Posiva share the vision "Operating optimised facilities in 2030". To further enhance the cooperation, Posiva and SKB started a series of joint reports in 2016, which includes this report.